Green tea extract and epigallocatechin gallate decrease muscle pathology and NF-κB immunostaining in regenerating muscle fibers of *mdx* mice

Nicholas Paul Evans

Dissertation submitted to the faculty of the Virginia Polytechnic Institute and State University in partial fulfillment of the requirements for the degree of

Doctor of Philosophy
In
Human Nutrition Foods and Exercise

Dr. Robert W. Grange, chair
Dr. Young H. Ju
Dr. Josep Bassaganya-Riera
Dr. John L. Robertson
Dr. Jim G. Tidball

September 25, 2009
Blacksburg, VA

Keywords: *mdx* mice, green tea extract, epigallocatechin gallate, NF-κB, muscle regeneration

Green tea extract and epigallocatechin gallate decreases muscle pathology and NF-κB immunostaining in regenerating muscle fibers of *mdx* mice

Nicholas Paul Evans

Abstract

Duchenne muscular dystrophy is a debilitating genetic disorder characterized by severe muscle wasting and early death in affected boys. The primary cause of this disease is mutations in the dystrophin gene resulting in the loss of the dystrophin protein from the plasma membrane of muscle fibers. In the absence of dystrophin, muscles undergo massive muscle degeneration and inflammation. Inflammation is believed to contribute substantially to dystrophic muscle pathology. The transcription factor NF-κB regulates inflammatory gene expression and provides a logical target for therapeutic treatments. Green tea extract and its primary polyphenol, epigallocatechin gallate, have been shown to have anti-inflammatory properties and to improve dystrophic muscle pathology. The purpose of these studies was to determine if dietary treatment with green tea extract or epigallocatechin gallate administered prior to disease onset could reduce dystrophic muscle pathology during the early disease time course and identify potential mechanisms through which NF-κB may be involved.

Green tea extract has been shown to decrease muscle pathology and increase muscle function in *mdx* mice, a dystrophic mouse model. These changes have been attributed to the antioxidant potential of epigallocatechin gallate; however, other mechanisms such as suppression of the inflammatory response have not been evaluated. In the studies reported herein, both green tea extract and epigallocatechin gallate significantly decreased muscle pathology in *mdx* mice when provided in their diets prior to disease onset. In green tea extract (0.25% and 0.5%) treated *mdx* mice, serum creatine kinase, a systemic marker of muscle damage, was decreased by 85% at age 42 days. Normal fiber morphology in the tibialis anterior muscle was increased by 32% at this age ($P \leq 0.05$). The primary histopathological change was a 21% decrease in regenerating fibers ($P \leq 0.05$). NF-κB staining in central nuclei of regenerating fibers was decreased by 34% ($P \leq 0.05$). In epigallocatechin gallate (0.1%) treated *mdx* mice, serum creatine kinase was unchanged; however, normal fiber morphology in the tibialis anterior was increased by 20% at ages 28 and 42 days ($P \leq 0.05$). At age 42 days, the primary histopathological change was a 21% decrease in regenerating fibers ($P \leq 0.05$). NF-κB staining in central nuclei of regenerating muscle fibers was decreased by 21% at this age ($P \leq 0.05$). Epigallocatechin gallate appears to be the primary polyphenol of green tea extract responsible for many of the beneficial changes in dystrophic muscle. These data suggest that both green tea extract and epigallocatechin gallate decrease NF-κB activity in regenerating fibers resulting in reduced muscle pathology.

Complimentary and alternative medicine approaches, including the use of green tea, provide important therapeutic options for ameliorating Duchenne muscular dystrophy. Green tea extract and epigallocatechin gallate are effective at decreasing muscle pathology potentially by reducing NF-κB activity in regenerating fibers in *mdx* mice. Use of these botanicals appears to elicit a beneficial response in dystrophic muscle that may ultimately lead to effective therapies for patients with this incurable disease.

Acknowledgments

Proverbs 25:2

It is the glory of God to conceal a matter; to search out a matter is the glory of kings.

I would like to thank my committee members for their excellent encouragement and support throughout my training. Dr. Grange generously provided the resources and questions that motivated my research. Both Dr. Ju and Dr. Tidball contributed their expertise and advice for refining the details of my studies. Dr. Bassaganya-Riera provided exceptional direction for my study designs and statistical analyses. I have a great deal of appreciation for my mentor, Dr. Robertson, who provided me with perspective and the drive to continue when times were tough. Thanks to all of you for your time and consideration during this process.

My lab mates, both past and present, have been a huge influence over my research and have contributed to my drive to succeed. Andy Wolff and Kevin Voelker are some of the best guys I know and are also excellent scientists. Sarah Misyak helped me piece together many of the aberrant signaling pathways in dystrophic muscle. Jarrod Call first initiated research with green tea extract in our lab and put in place many of the necessary components for my research. Mary Pat Meany provided her humorous stories and was also there to share in the burdens of lab life. Thanks everyone for your help, understanding, and friendship. I look forwarding to seeing where your careers take you.

My parents have been the strongest supporters of my life goals. They have given me direction when I had none and support when I needed it the most. You both have made things possible for me that I could not have achieved on my own. My achievement is, in many ways, as much yours as it is mine. Thanks Mom and Dad.

Most importantly, to my wife Brandi, thanks for keeping me motivated and happy. Without you I would have given up many times. I know you have made sacrifices and I thank you for your support. I also want to thank you for helping me to meet my goals when they seemed out of reach. You are my closest friend and I hope I can provide the same support to you in reaching your goals. I am very blessed to have you in my life and I am excited to begin a new stage in our lives together.

Attribution

Several colleagues and coworkers contributed to the writing and research incorporated in the chapters of this dissertation. A brief description of their background and contributions are included here.

Dr. Robert W. Grange – PhD (Department of Human Nutrition Foods and Exercise, Virginia Tech) was my primary Advisor and Committee Chair. Dr. Grange provided his guidance in study design and aided in revisions of all manuscripts (Chapters 3-6). Furthermore, he supplied funding, lab facilities, and supplies for the green tea extract and epigallocatechin gallate research projects (Chapters 5 and 6).

Dr. Josep Bassaganya-Riera – DVM, PhD (Virginia Bioinformatics Institute, Virginia Tech) provided expertise in immunology that was imperative to developing novel pathways involved in inflammatory lesion development in dystrophic muscles of DMD patients and *mdx* mice (Chapters 3 and 4). He was also instrumental in the experimental design and statistical analysis for all research projects (Chapters 5 and 6)

Dr. John L. Robertson – VMD, PhD (Department of Biomedical Sciences and Pathobiology, Virginia Tech) provided critical feedback for the literature reviews (Chapters 3 and 4) and aided in the development of histopathological quantification techniques (Chapters 5 and 6)

Sarah A. Misyak – MS (Department of Biomedical Sciences and Pathobiology, Virginia Tech) was responsible for developing pathways involved in the dystrophic muscle disease time course and contributed to revisions of the literature reviews (Chapters 3 and 4).

Jarrod A. Call - MS (Department of Physical Medicine and Rehabilitation, University of Minnesota) initiated and designed the experimental protocol for dietary supplementation with green tea extract and contributed to manuscript development (Chapters 5 and 6).

Table of Contents

Glossary and Abbreviations

ANOVA: analysis of variance

AP-1: activator protein-1

CAM: complementary and alternative medicine

CK: creatine kinase

DGC: dystrophin glycoprotein complex

DMD: Duchenne muscular dystrophy

ECM: extracellular matrix

EGCG: epigallocatechin gallate

GTE: green tea extract

H&E: hematoxylin and eosin

IκB: inhibitor of kappa B

IKK: IκB kinase

MCP-1: monocyte chemoattractant protein-1

Mdx: X-linked muscular dystrophy mouse model

NFAT: nuclear factor of activated T cells

NF-κB: nuclear factor kappa B

ROS: reactive oxygen species

TA: Tibialis anterior

TNFα: Tumor necrosis factor alpha

TGF-β: transforming growth factor beta

List of Figures

List of Tables

Chapter 1 Introduction

1.1 Motivation

Duchenne muscular dystrophy (DMD) is a debilitating muscle wasting disease that affects approximately one in 3500 new born boys and typically results in their death by age 30 years. This disease results from mutations in the dystrophin gene located on the X-chromosome. These mutations lead to an absence of the dystrophin protein and the proteins that compose the dystrophin glycoprotein complex (DGC) in the sarcolemma of muscle fibers. The DGC is believed to provide both mechanical stability to the sarcolemma and act as a scaffold for cell signaling proteins that regulate cell viability. Although the primary cause of this disease is known the mechanisms that trigger the devastating muscle wasting have not been fully characterized and beneficial treatment options are limited.

Green tea extract (GTE) and its major polyphenol, epigallocatechin gallate (EGCG), have recently received much attention due to their perceived health benefits. GTE and EGCG are strong antioxidants that have anti-inflammatory properties which may act through the regulation of the NF-κB cell signaling pathway. Elevated NF-κB activation resulting from the loss of the DGC has been indicated as a possible mechanism regulating dystrophic muscle wasting. Both GTE and EGCG have shown promise as treatments for improving dystrophic muscle pathology. A further understanding of how GTE and EGCG can improve dystrophic muscle pathology and alter NF-κB activation will provide valuable insight into the disease process. Exploring these possibilities may lead to the development of viable treatment options for DMD patients.

1.2 Specific Aims

DMD is characterized by progressive muscle weakness and muscle lesions. While a key defect in the disease is the absence of the protein dystrophin, the role of inflammatory signaling mechanisms in the initiation of dystrophic muscle wasting has not been well defined. Initial disease onset, characterized by elevated serum creatine kinase levels and massive muscle degeneration in *mdx* mice at age 21 days, is preceded by immune cell infiltration of muscle tissue. Inflammation and elevated NF-κB activity represent major elements of dystrophic disease progression, and therefore may provide insight into potential therapeutic targets. The goals of this project are to determine the efficacies of GTE and one of its derivatives, EGCG, to reduce muscle pathology by altering the immune response and NF-κB activity when administered prior to initial disease onset in *mdx* mice.

1.2.1 Specific Aim 1

Test the overarching hypothesis that GTE decreases muscle pathology and inflammation in *mdx* mice by decreasing NF-κB activation. A detailed time course of tibialis anterior (TA) muscle histopathology will be assessed in *mdx* mice to determine the disease profile during the initial disease onset stage. GTE growth diets will be fed to *mdx* breeder pairs and pups. At age 21 days, pups will be weaned and placed on a GTE maintenance diet. Serum creatine kinase (CK) will be assessed as a systemic indicator of muscle damage. Additionally, muscle histopathology, macrophage infiltration, and NF-κB localization will be characterized in GTE treated *mdx* muscles and compared to age-matched *mdx* and C57BL/6J mice at ages 28 and 42 days.

1.2.2 Specific Aim 2

Test the overarching hypothesis that EGCG derived from green tea extract improves muscle pathology and inflammation in *mdx* mice by decreasing NF-κB activation. EGCG will be fed to weaned pups beginning at age 18 days. Serum CK will be assessed as a systemic indicator of muscle damage to determine if EGCG treatments reduce muscle pathology. TA muscle histopathology, macrophage infiltration, and NF-κB immunolocalization will be characterized in EGCG treated *mdx* muscles and compared to age matched *mdx* and C57BL/6J mice at ages 28 and 42 days.

1.2.3 Rationale

DMD is caused by mutations in the dystrophin gene, which results in absence of the dystrophin protein in muscle tissue. The absence of this protein is believed to contribute to muscle membrane permeability and mechanical injury. However, changes in membrane permeability and mechanical integrity do not account for all of the abnormalities observed in dystrophic muscle. The inflammation triggered by elevated NF-κB activity in dystrophic muscle may be a significant contributor to the initial disease onset. Therapies targeted at suppressing inflammation and NF-κB activity may be the most beneficial treatments for DMD when initiated before disease onset. The proposed studies will provide a detailed time course of muscle pathology and the immune/inflammatory response during initial disease onset, and determine the benefits of treating *mdx* mice with GTE or EGCG during this early disease stage.

1.3 Specific Hypotheses

1.3.1 Specific Aim 1

H_1: Normal fiber morphology will be decreased in *mdx* mice compared to C57BL/6J mice from ages 21 to 42 days.

H_2: The histopathological features: regenerating fibers, immune cell infiltration, necrotic fibers, and degenerating fibers will be increased in *mdx* mice compared to C57BL/6J mice from ages 21 to 42 days.

H_3: Serum CK will be decreased in GTE treated *mdx* mice compared to control *mdx* mice at ages 28 and 42 days.

H_4: Normal fiber morphology will be increased in GTE treated *mdx* mice compared to control *mdx* mice at ages 28 and 42 days.

H_5: The histopathological features: regenerating fibers, immune cell infiltration, necrotic fibers, and degenerating fibers will be decreased in GTE treated *mdx* mice compared to control *mdx* mice at ages 28 to 42 days.

H_6: Macrophage infiltration will be decreased in GTE treated *mdx* mice compared to control *mdx* mice at age 42 days.

H_7: Necrotic fibers with NF-κB staining will be decreased in GTE treated *mdx* mice compared to control *mdx* mice at age 42 days.

H_8: Centralized nuclei of regenerating fibers with NF-κB staining will be decreased in GTE treated *mdx* mice compared to control *mdx* mice at age 42 days.

1.3.2 Specific Aim 2

H_1: Serum CK will be decreased in EGCG treated *mdx* mice compared to control *mdx* mice at ages 28 and 42 days.

H_2: Normal fiber morphology will be increased in EGCG treated *mdx* mice compared to control *mdx* mice at ages 28 and 42 days.

H_3: The histopathological features: regenerating fibers, immune cell infiltration, necrotic fibers, and degenerating fibers will be decreased in EGCG treated *mdx* mice compared to control *mdx* mice at ages 28 to 42 days.

H_4: Macrophage infiltration will be decreased in EGCG treated *mdx* mice compared to control *mdx* mice at ages 28 and 42 days.

H_5: Necrotic fibers with NF-κB staining will be decreased in EGCG treated *mdx* mice compared to control *mdx* mice at ages 28 and 42 days.

H_6: Centralized nuclei of regenerating fibers with NF-κB staining will be decreased in GTE treated *mdx* mice compared to control *mdx* mice at ages 28 and 42 days.

1.4 Research Design

1.4.1 Specific Aim 1

A detailed time course (age 14, 21, 28, 35, and 42 days) of TA muscle histopathology will be characterized for *mdx* and C57BL/6 mice to determine the disease profile during the initial disease onset stage. Muscle histopathology, serum CK activity, macrophage infiltration, and NF-κB immunolocalization will be characterized in GTE treated *mdx* mice at ages 28 and 42 days (± 1 day) **(Figure 1.1)**. Because early intervention may have beneficial effects, *mdx* breeder pairs will be fed a growth diet containing either 0% GTE (control diet), 0.25 % GTE, or 0.5% GTE (w/w). C57BL/6J and *mdx* pups will be weaned at age 21 days and fed a maintenance diet containing the same percent GTE as the breeder pairs from which they originated **(Figure 1.2)**. A sample size of 4-5 mice will be collected for each genotype, treatment, and age group. Body mass will be recorded weekly for each mouse.

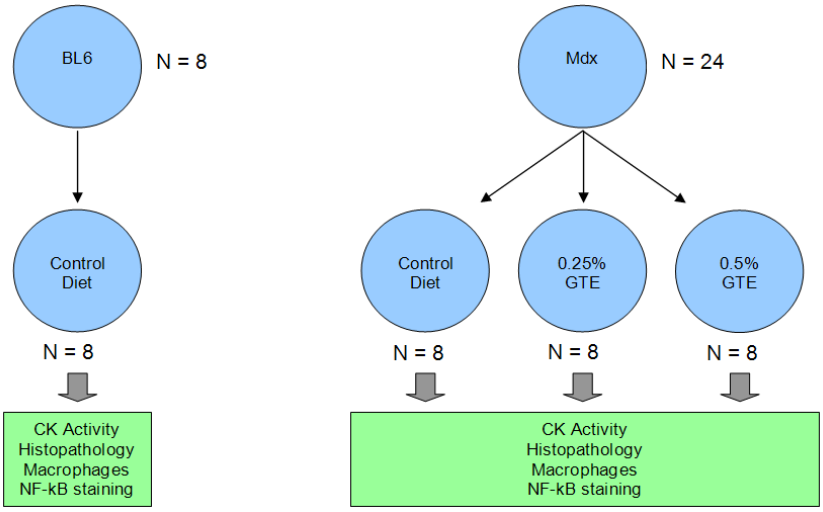

Figure 1.1 – C57BL/6J mice will be fed the control diet only. *Mdx* will be divided into three diet treatment groups and assessed for differences in serum creatine kinase, histopathology, macrophage infiltration, and NF-κB staining.

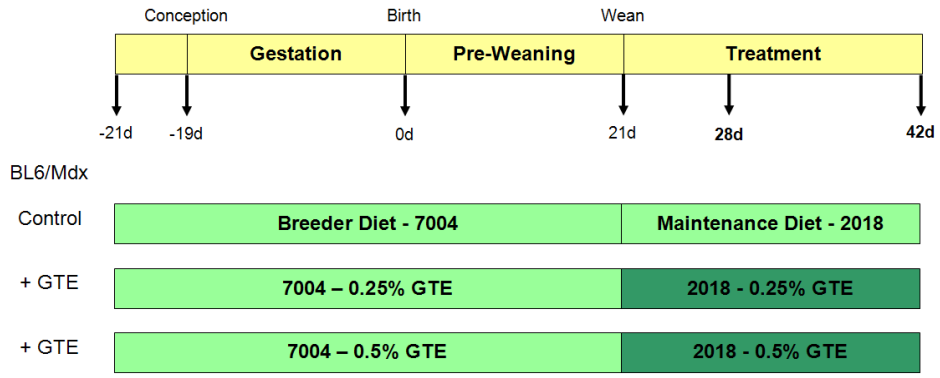

Figure 1.2 – *Mdx* and C57BL/6 breeder pairs and pups will be provided with pelleted diet (7004 Harlan Teklad). At age 21 days pups will be weaned and placed on a maintenance diet (2018 Harlan Teklad) with either 0%, 0.25%, or 0.5% GTE diet. Mice will be sacrificed at ages 28 and 42 days.

1.4.2 Specific Aim 2

A detailed time course of TA muscle histopathology, serum CK, macrophage infiltration and NF-κB immunolocalization will be characterized in EGCG treated and untreated age-matched *mdx* and C57BL/6J mice at ages 28 and 42 days (± 1 day) **(Figure 1.3)**. C57BL/6J and *mdx* mice will be divided into two diet treatment groups beginning at age 18 days which will be fed either the control diet (i.e., AIN-93G Harlan Teklad), or 0.1% EGCG diet (w/w) **(Figure 1.4)**. Only weaned mice were provide with the EGCG diet to eliminate variation associated with the breeder's care of their pups. To ensure the mice have reached adequate maturation, only mice age 18 days with a body mass greater than 8 grams will be weaned. A sample size of five to ten mice will be collected for each genotype at each age. Body mass and food consumption will be recorded weekly for each mouse.

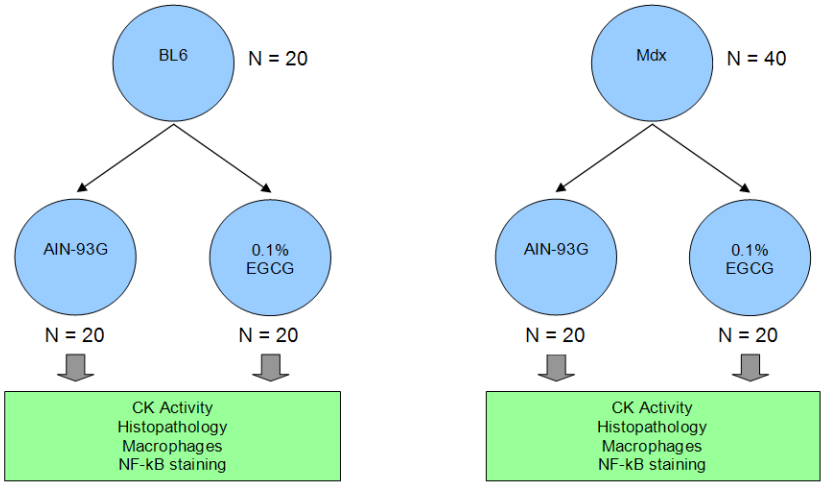

Figure 1.3 – C57BL/6J and *mdx* will be divided into control of EGCG diet treatment groups and assessed for differences in serum creatine kinase, histopathology, macrophage infiltration, and NF-κB staining.

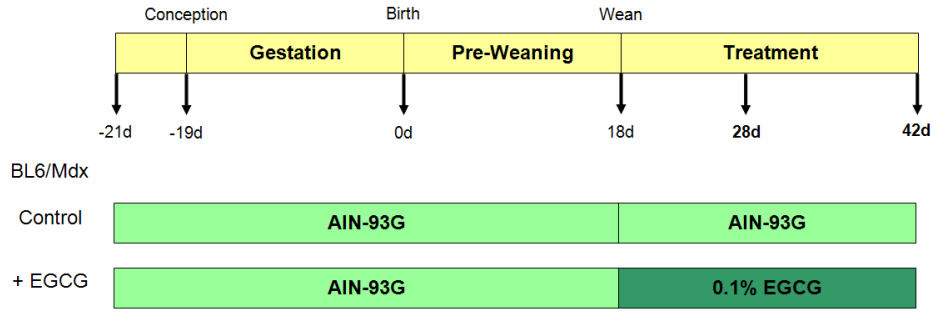

Figure 1.4 – Breeder pairs and pups will be provided with pelleted AIN-93G diet. At age 18 days pups will be weaned and placed on either a control diet, or 0.1% EGCG diet. Mice will be sacrificed at ages 28 and 42 days.

Chapter 2 Background

2.1 Duchenne muscular dystrophy

Duchenne muscular dystrophy (DMD) is a lethal muscle wasting disease affecting approximately one in 3,500 boys [19,197]. Patients appear clinically normal at birth with the exception of elevated serum creatine kinase levels. The onset of DMD begins in early childhood with the first observed symptoms between two and five years of age. The first symptoms usually include a delay in walking, a waddling gait, difficulty climbing stairs and difficulty running. Soon after the onset of the disease, pseudohypertrophy of the calf muscles appears. Then, weakness in the proximal limb muscles is seen; affected boys use Gowers' maneuver (using the hands and arms to push off the floor in order to raise the posterior and then pushing or climbing up the legs to erect the torso) to stand. DMD patients typically require the use of a wheelchair by age 12 due to the loss of lower limb muscle strength. Progressive weakness of the arms and legs, along with kyphoscoliosis continue through late disease progression. Many patients die in their late teens or early twenties due to respiratory or cardiac complications. Death is often a result of respiratory infection, intercostal muscle weakness or cardiomyopathy [19,64]. A common end of life scenario is a case of pneumonia compounded by cardiac involvement [64]. Currently there are no effective means of therapy or treatment for DMD.

2.1.1 Etiology of DMD

Duchenne muscular dystrophy is caused by mutations in the dystrophin gene which is located on chromosome Xp21. This gene encodes various promoters and isoforms of

dystrophin [19,27]. The dystrophin gene, at ~2.6 million base pairs, is the largest in the human genome [138]. The 427-kDa isoform of dystrophin is a cytoskeletal protein expressed in muscle and brain tissue, but is absent in DMD patients [27]. In normal muscle cells, dystrophin is a component of the dystrophin-glycoprotein complex (DGC) localized in the sarcolemma, which acts as a link between the extracellular matrix and the cytoskeleton [192]. The DGC may serve to protect muscle cells from contraction-induced injury and preserve cell viability [19,139]. In the absence of dystrophin, there is a loss of associated DGC proteins, which likely leads to muscle fragility, contraction-induced damage, necrosis and imbalance of calcium homeostasis [181]. Increased levels of intracellular calcium, along with increased calcium-dependent protease activity have been observed in dystrophic muscle [19,182,183]. Activation of calcium-dependent proteases (calpains) causes widespread myofibrillar protein degradation, thus exacerbating the dystrophic condition [182,183]. The DGC has also been shown to play an important role in signal transduction and may regulate cellular functions including cell growth, differentiation, cytoskeletal organization and secretion [60,139].

2.1.2 Pathophysiology

Repeated cycles of degeneration followed by regeneration in dystrophic muscle fibers is believed to eventually deplete satellite replacement cells [17,55,202]. Depletion of satellite cells results in the loss of the muscle's ability to regenerate. Muscle tissue is progressively replaced with adipose and fibrous connective tissue [41]. The morphological characteristics of both muscle degeneration and regeneration have been described in detail [55,148]. However, the mechanisms that initiate and perpetuate the cycles of degeneration and regeneration are not clearly defined.

Dystrophin deficiency does not always produce muscle degeneration at all life stages, in all muscle phenotypes, or in all animal models [155]. In dystrophin-deficient skeletal muscle, for example, mechanical injury and proteolysis may be important factors but do not fully explain DMD pathogenesis. Mechanisms such as the immune/inflammatory response to injury appear to contribute substantially to muscle pathophysiology. Observations of activated immune cell infiltrates in dystrophic muscle suggest that the immune/inflammatory response may play a role in exacerbating the disease [154,155,184,187,210].

2.1.3 *Mdx* mouse model

In 1984, Bulfield *et al.* identified a spontaneous mutation in C57BL/10ScSn inbred mice that exhibited a disease state similar to human DMD. The X-chromosome-linked mutation produced mice with high serum levels of muscle enzymes and with histological lesions comparable to those seen in human muscular dystrophy. This research group named the mutation "X-linked muscular dystrophy" or "*mdx*" [24]. This mutation in the murine dystrophin gene caused an absence of dystrophin in skeletal muscle and this key defect validated the *mdx* mouse as a suitable DMD model [41,60].

Histological examination of distal limb muscles, diaphragm and the heart of *mdx* mice has shown that no lesions are observable before 2 weeks of age, but by 3 weeks of age noticeable lesions are seen. These lesions are characterized by marked atrophy, variation in fiber size, centralized nuclei and infiltrations of degenerating tissue with phagocytic cells [24]. Periods of cyclical degeneration/regeneration plateau between 3-4 weeks of age. Mild progressive pathology, including fibrosis, continues for the duration of the animal's life [28,45].

Compared to DMD, the *mdx* mouse presents a mild phenotype and may not satisfactorily model the human disease [41]. Greater than 90% of DMD patients develop cardiomyopathies, but *mdx* mice rarely develop these complications [82]. DMD patients show progressive physical impairment leading to death, while mature *mdx* mice are capable of substantial muscle regeneration, exhibit little physical impairment and have a normal life span [82]. Utrophin, a homolog for dystrophin, can replace dystrophin in the DGC [52,60,82]. Compensation for the lack of dystrophin by upregulation of utrophin gene activity may effectively reduce the associated pathology and be responsible for the mild phenotype and normal life span of *mdx* mice compared to DMD patients. Interestingly, not all muscles in *mdx* mice present with the same pathology; for example, the diaphragm and limb muscles are severely affected, but the extraocular muscles are spared [154]. Although there is considerable variation observed in muscles of the *mdx* mouse, the tibialis anterior muscle has been studied extensively and is believed to be representative of the severe muscle wasting observed in DMD patients [53,76,85,111].

2.1.4 Inflammatory mechanisms in dystrophic muscle

Inflammatory-mediated mechanisms, which result in muscle cell death or lead to fibrosis, may be important initiators of lesions in dystrophin-deficient muscle. Large populations of lymphocytes, macrophages and neutrophils are present in DMD muscle tissue [187]. T-cells and macrophages are classically thought to be responsible for triggering and orchestrating the immune response, inducing target cell death, recognizing immune stimuli and removing cellular debris. NF-κB, an inflammatory transcription factor, has been indicated as a potential mechanism in the regulation of these cells and the dystrophic inflammatory process [2,57,105,127,130,214]. Immunosuppressive therapy, such as treatment with

glucocorticoids, improves muscle strength and prolongs ambulation in DMD patients, but these treatments do not prevent disease progression [64,154]. Therefore, new treatment options for suppressing disease progression, like treatments targeted for decreasing NF-κB activation, are needed to improve disease prognosis of DMD patients.

Mdx mice have been used as immune models of DMD because their muscle immune cell populations resemble that of DMD muscle. Although, *mdx* skeletal muscle pathology resolves soon after onset, immune cell infiltration during early disease stages is considered representative of DMD [184]. Primarily, elevated concentrations of macrophages (> 80,000 cells/mm^3, normal ~1000 cells/mm^3) and activated CD8+ and CD4+ T-cells (>1200 cells/mm^3, normal ~100 cells/mm^3) have been observed in 4-8 week *mdx* mouse muscle, but rapidly decrease by age 12-14 weeks [184,186,210]. Both macrophages and T-cells are believed to be key contributors to dystrophic muscle wasting. Antibody-mediated depletion of these cells results in significant reductions in muscle pathology (macrophage, >75%; CD8+, ~75%; CD4+, ~61%), suggesting an important role of these cells in the development of lesions [186,210].

NF-κB is known to regulate expression for a plethora of inflammatory genes [94,96,144]. In its inactive form, NF-κB is sequestered in the cytoplasm of cells; however, multiple stimuli can activate NF-κB allowing it to enter the nucleus and induce transcription of cytokines, chemokines, adhesion molecules and enzymes that produce secondary inflammatory mediators [96]. In *mdx* mice, NF-κB activation is elevated prior to the initial disease onset [105]. Activation of this signaling molecule is believed to suppress muscle regeneration and induce pro-inflammatory macrophage activity in dystrophic muscle [2].

Treatments, including green tea extract and epigallocatechin gallate, that specifically alter NF-κB activity are promising options for the amelioration of DMD.

2.2 Green tea extract and epigallocatechin gallate

Complementary and alternative medicine (CAM) approaches are being perused in the amelioration of a wide variety of incurable inflammatory diseases [34,117,135,141]. In DMD patients, the available conventional treatment options are non-curative and are associated with many side effects [9,162]. Consequently, CAM therapies are gaining recognition as potential treatment options for this disease [162,172]. Treatments that reduce free radical production or can alter NF-κB activity are shown to be highly effective in *mdx* mice [126,127,145,180,214]. Both green tea extract and epigallocatechin gallate have shown promise as treatments for improving muscle pathology in *mdx* mice; however, the mechanism by which this occurs has not been fully identified.

2.2.1 Extracts and polyphenols derived from the green tea plant

Green tea is a beverage consumed throughout the world for its many health benefits, which are primarily attributed to its anti-oxidant and anti-inflammatory properties [36,204]. Green tea extract (GTE) is derived from the hot water-soluble portion of unfermented *Camellia sinensis* leaves. GTE is mainly composed of the polyphenolic catechins: gallocatechin (GC), epigallocatechin (EGC), epicatechin (EC), and epigallocatechin gallate (EGCG) [71,204]. Due to the ability of these catechins to stabilize free radicals under physiological conditions, they are believed to be ideal therapeutic candidates for quenching reactive oxygen species (ROS) *in vivo* [71]. In GTE, ~30-50% of the total polyphenols are

comprised of EGCG which is believed to provide the majority of the beneficial effects attributed to green tea consumption [58].

2.2.2 GTE and EGCG treatments in *mdx* mice

The antioxidant potential of GTE may be beneficial in treating dystrophic muscle, because oxidative stress is believed to contribute substantially to muscle pathology [164,213]. Evidence suggests that oxidative stress is involved in early disease stages and occurs before initial disease onset in *mdx* mice [56]. Buetler et al. first showed that *mdx* mice fed diets supplemented with GTE (0.01% or 0.05%, w/w) from birth had significant reductions in areas of necrosis and regeneration of extensor digitorum longus (EDL) muscles at age 28 days [23]. In a follow up study, they showed *mdx* mice treated with either GTE (0.05% or 0.25%) or EGCG (0.1%) for one to five weeks after weaning had increased antioxidant capacity, improved contractile properties, and decreased muscle pathology [58].

More recently, *mdx* mice treated with GTE and who performed voluntary wheel running for three weeks demonstrated increased endurance capacity. GTE treated *mdx* mice ran 128% more than untreated *mdx* counterparts after three weeks of voluntary wheel running. Independent of wheel running serum creatine kinase, lipid peroxidation, and serum antioxidant potential were also decreased in GTE treated *mdx* mice [26]. Subcutaneous injections of EGCG in *mdx* mice for eight weeks after birth significantly decreased markers of oxidative stress and pathophysiology. Serum creatine kinase was reduced to nearly normal levels in these mice. In severely affected diaphragm muscles, lipofuscin granules, a marker of oxidative stress, were significantly reduced by 53%. Normal fiber morphology was increased by two fold with connective tissue and necrosis reduced by 41% and 93%,

respectively. Additionally, expression of utrophin was increased by 17% [136]. These studies indicate the GTE and EGCG may provide beneficial treatment options for reducing oxidative stress and improving dystrophic muscle pathology; however, further research is required to gain mechanistic insight into the role they play in cell viability of dystrophic muscle.

2.2.3 Potential mechanism for GTE and EGCG in dystrophic muscle

Reducing oxidative stress in dystrophic muscle may be one way in which GTE improves dystrophic muscle pathology; however, another possibility is that the components of GTE are capable of interacting with signaling cascades that regulate cell viability and inflammation in dystrophic muscle. For example, EGCG is believed to modulate the activity of ERK1/2, PI-3K/Akt, and IKK signaling, all of which are involved in NF-κB regulation [36,110,160,170,175,220,223]. These pathways have been identified as key regulators in the pathophysiology of dystrophic muscle [2,57,105,106,151]. Although EGCG is recognized as a modulator of NF-κB activity [36,220], the role GTE or EGCG plays in altering dystrophic muscle wasting is unknown. Since NF-κB has been indicated as a regulator of the pro-inflammatory response and muscle regeneration in dystrophic muscle [2,57,105], these extracts may play a key role in altering this disease process.

2.3 Summary

DMD is a severe muscle wasting disease that results in immobilization of affected patients by age 12 and death by age 20-30. Current treatment options do not provide an appreciable improvement in disease prognosis or life span. Until treatments are available that can reverse the genetic cause of this disease, CAM approaches that can greatly enhance

muscle function by altering inflammation and muscle regeneration may provide significant improvements in the lives of DMD patients.

Infiltrating immune cells are key contributors in dystrophic muscle pathology. However, their role in the regulation of muscle pathology has not been thoroughly investigated, particularly during the early disease stages. Specifically, macrophages have been shown to be key modulators of muscle damage and regeneration. NF-κB appears to be a critical component in macrophage activation and muscle regeneration. GTE and EGCG improve muscle pathology and function; potentially, these changes result from the ability of these extracts to alter NF-κB activity.

In the following chapters, an initial literature review establishes the absence of the DGC as an important factor contributing to dysregulated signaling cascades and inflammatory gene expression. Alterations in these pathways occur prior to disease onset indicating their role in the initiation of muscle wasting (see Chapter 3) [69]. In the subsequent literature review, NF-κB activation is identified as a key contributor to dystrophic muscle wasting through the expression of inflammatory genes and immune cell regulation (see Chapter 4) [68]. Therapeutic approaches, including the use of GTE and EGCG, for treating these inflammatory processes in dystrophic muscle are also discussed (see Chapter 3 and 4) [68,69]. The results of studies conducted to determine the efficacies of using GTE (Specific Aim 1; see Chapter 5) and EGCG (Specific Aim 2; see Chapter 6) to modulate muscle pathology and NF-κB in dystrophic muscle are reported. Finally, a summary of the major findings is presented and future research directions are identified (see Chapter 7).

Chapter 3 Dysregulated intracellular signaling and inflammatory gene expression during initial disease onset in Duchenne muscular dystrophy

Nicholas P. Evans BS[a*], Sarah A. Misyak MS[a], John L. Robertson VMD, PhD[b], Josep Bassaganya-Riera DVM, PhD[c], and Robert W. Grange PhD[a]

[a] Department of Human Nutrition, Foods and Exercise, Virginia Polytechnic Institute and State University, Blacksburg, Virginia 24061, USA

[b] Department of Biomedical Sciences and Pathobiology, Virginia Polytechnic Institute and State University, Blacksburg, Virginia 24061, USA

[c] Virginia Bioinformatics Institute, Virginia Polytechnic Institute and State University, Blacksburg, Virginia 24061, USA

[*]Correspondence to Nicholas P. Evans, Department of Human Nutrition, Foods and Exercise, Virginia Polytechnic Institute and State University, 338 Wallace Hall, Blacksburg, Virginia 24061, USA, Tel: 540-231-9048, Fax: 540-231-3916, Email: nievans@vt.edu

Supported by NIH RO1AR049881 (RWG)

Reprinted with permission: Dysregulated intracellular signaling and inflammatory gene expression during initial disease onset in Duchenne muscular dystrophy. Evans NP, Misyak SA, Robertson JL, Bassaganya-Riera J, Grange RW.

Am J Phys Med Rehabil. 2009 Jun;88(6):502-22.

Abstract

Duchenne muscular dystrophy (DMD) is a debilitating genetic disorder characterized by severe muscle wasting and early death in affected boys. The primary cause of this disease is mutations in the dystrophin gene that result in the absence of the protein dystrophin and the associated dystrophin-glycoprotein complex in the plasma membrane of muscle fibers. In normal muscle, this complex forms a link between the extracellular matrix and the cytoskeleton that is thought to protect muscle fibers from contraction-induced membrane lesions and to regulate cell signaling cascades. Although the primary defect is known, the mechanisms that initiate disease onset have not been characterized. Data collected during early maturation suggest that inflammatory and immune responses are key contributors to disease pathogenesis and may be initiated by aberrant signaling in dystrophic muscle. However, detailed time course studies of the inflammatory and immune processes are incomplete and need to be further characterized to understand the disease progression. The purposes of this review are to examine the possibility that initial disease onset in dystrophin-deficient muscle results from aberrant inflammatory signaling pathways and to highlight the potential clinical relevance of targeting these pathways to treat DMD.

3.1 Introduction

The purposes of this review are to discuss potential mechanisms of initiation and progression of dystrophic muscle lesions in both Duchenne muscular dystrophy (DMD) patients and *mdx* mice and to highlight the potential clinical relevance of targeting these mechanisms to treat DMD. Disregulated inflammatory signaling processes have been recognized in the pathogenesis of dystrophic muscle wasting and the identification of an appropriate immunosuppressive therapy from these studies may drastically improve disease prognosis. However, a major limitation to understanding the role of the immune response in DMD and *mdx* muscle pathology is the absence of detailed time course studies of disease before, during, and after the onset of lesion development in muscle of affected animals/humans. Review of existing studies is important to understand the role of the immune response in the onset and progression of the disease and to identify specific immune targets and time points at which therapeutic interventions will be most effective. Ultimately, additional detailed time course studies will be suggested to determine the clinical efficacy of these interventions to treat DMD.

DMD is a lethal, human muscle wasting disease that affects approximately one in 3500 boys. DMD is caused by mutations in the dystrophin gene that result in the loss of the dystrophin protein [19,197]. In normal muscle cells, the dystrophin protein is a component of the dystrophin-glycoprotein complex (DGC) **(Figure 3.1)**, which is localized to the sarcolemma and acts as a link between the extracellular matrix (ECM) and cytoskeleton [192]. The DGC is believed to protect muscle cells from contraction-induced injury and preserve cell viability [60,139]. However, in the absence of dystrophin, there is a loss of associated

DGC proteins, which leads to muscle fragility, contraction-induced damage, necrosis, and inflammation [181].

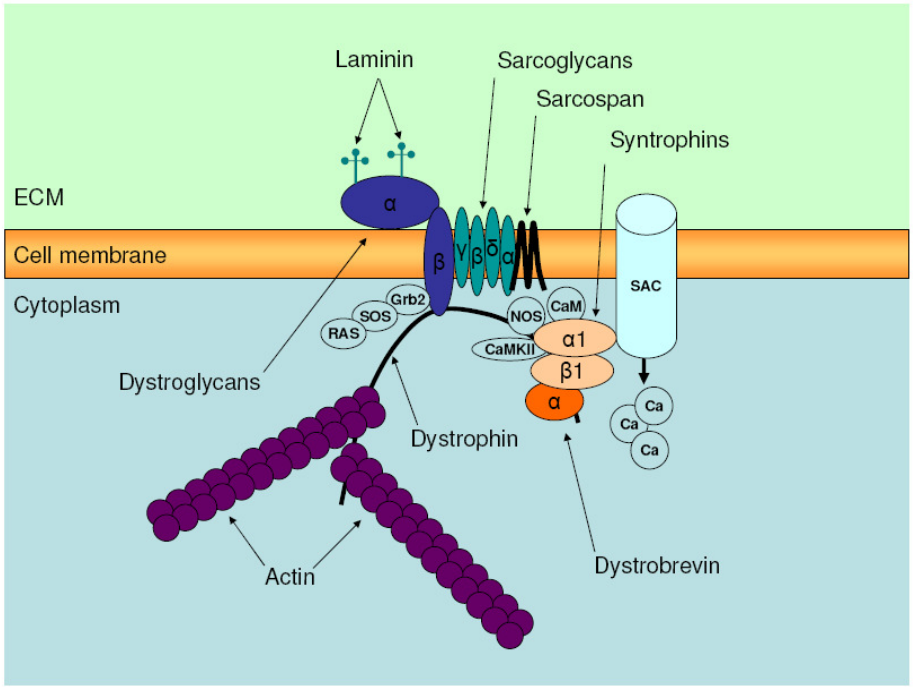

Figure 3.1 – The dystrophin glycoprotein complex (DGC) in normal myofibers. Illustration of the link formed between laminin in the extracellular matrix (ECM) and the cytoskeleton by the DGC. Also shown, interaction of DGC components (dystrophin, dystroglycans, dystrobrevin, laminin, sarcoglycans, syntrophin, and sarcospan) with potential signaling proteins (Grb2, SOS, RAS, NOS, CaM, CaMKII), and with stretch activated channels (SAC) through which calcium (Ca) can enter the cell.

Research has suggested that "cycles" of degeneration and regeneration in dystrophic muscle eventually deplete satellite replacement cells (i.e., muscle stem cells) [17,55,209]. Once satellite cells are depleted, muscle regeneration ceases, promoting progressive replacement of muscle tissue with adipose and fibrous connective tissues [41]. The morphopathological characteristics of both muscle degeneration and regeneration have been detailed [3,17]; however, the mechanisms regulating the degeneration/regeneration cycles have not been clearly defined.

Dystrophin deficiency and DGC dysfunction do not consistently produce muscle wasting at all life stages, in all muscle phenotypes, or in all animal models of DMD [156,157]. Compared to DMD, dystrophin-deficient mice (*mdx*) present with a mild phenotype that does not accurately reflect the severe nature of the human disease [41]. Among the several other animal models of DMD, the golden retriever muscular dystrophy (GRMD) dog has been the most studied and exhibits the severe phenotype of DMD patients [41]. Although time course studies of the immune response in *mdx* mice are limited, they are even more limited in the GRMD dog. Therefore this review focuses on the findings from *mdx* mice.

DMD patients show progressive physical impairment leading to death by age 20-30 years, while mature *mdx* mice are capable of substantial muscle regeneration, exhibit little physical impairment, and have a relatively normal life span (~1-2 years) [32,82]. Overt onset of clinical disease occurs between age 3-5 years in DMD patients; however, muscle degeneration and elevated serum creatine kinase levels can be observed prior to birth **(Figure 3.2A)** [20,21,62,63,67,116,191]. In contrast, initial disease onset in *mdx* mice, occurring at age ~21 days, is characterized by the initiation of muscle degeneration and elevated serum creatine kinase [45,55,122]. The process of degeneration in *mdx* skeletal muscles wanes by age 24 to 28 days at which time muscle regeneration predominates [28,45,55,90]. Muscle degeneration/regeneration is suppressed by age 3-4 months, but continues at low levels for the remainder of the animal's life **(Figure 3.2B)** [41,55,122]. Even though the *mdx* mouse model exhibits considerable phenotypic variation compared to DMD, this model continues to be very important during early maturation for understanding mechanisms of disease pathogenesis.

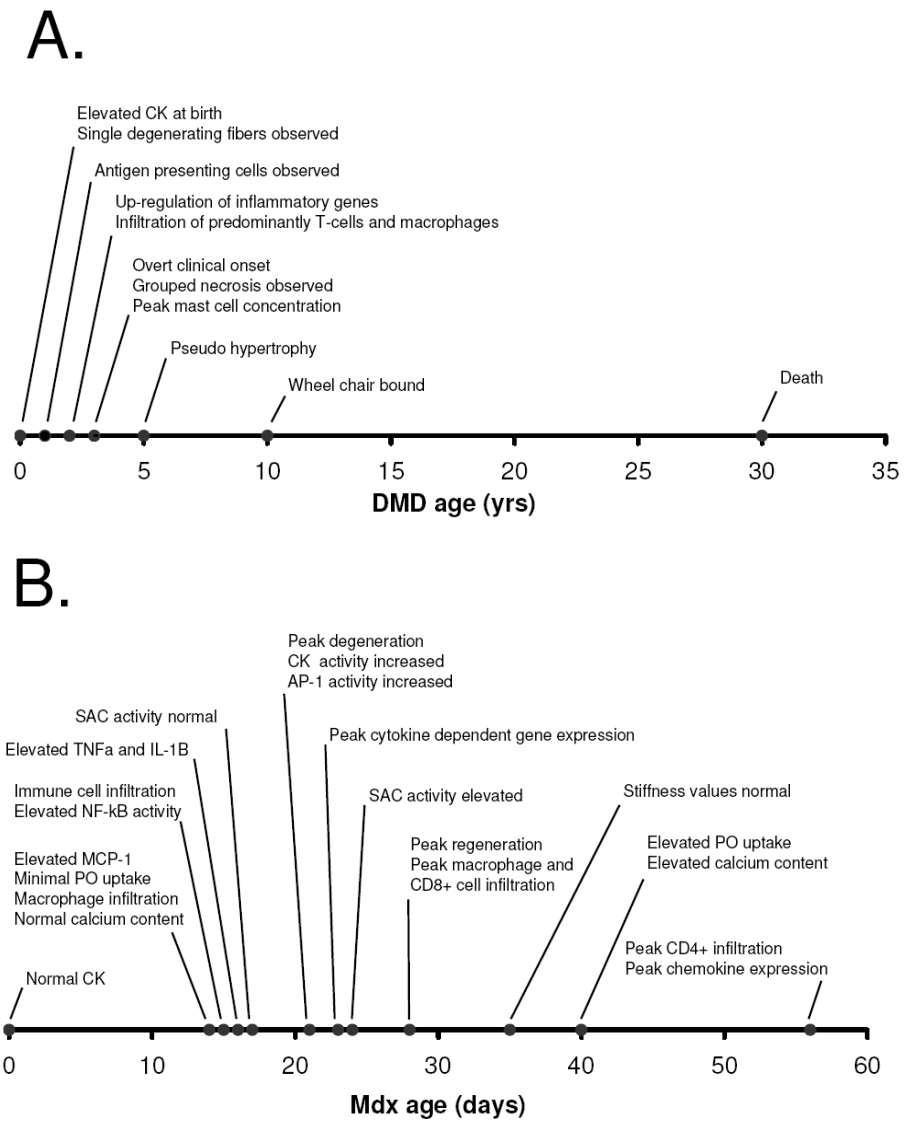

Figure 3.2 – The time course of dystrophin-deficiency in DMD patients and mdx mice. The clinical time course of (A) DMD is well known, but only limited data are available for the time course of immune cell infiltration, cytokine levels, and signaling pathways. Although these have been characterized in the (B) *mdx* mouse, the time course during early disease stages remains incomplete.

Mechanical injury and membrane defects are important factors promoting dystrophic disease pathology, but do not fully explain DMD disease onset and progression [146,152]. Aberrant intracellular signaling cascades, which regulate both inflammatory and immune processes, appear to contribute substantially to the degenerative process [105,106,155]. Observations of up-regulated inflammatory genes (e.g. complement components,

cytokines, and major histocompatibility complexes) and activated immune cell infiltrates (e.g., T lymphocytes and macrophages) during critical disease stages in dystrophic muscle suggest that these processes may play a critical role in initiating and exacerbating muscle wasting [28,37,150,154,157,186,210].

In this review, mechanical and signaling roles for the DGC, the profile of inflammatory gene expression and the intracellular signaling pathways that could be responsible for dystrophic disease onset and progression in the absence of the DGC are described. The available literature supports the immune response as an initiator of DMD, but the available data are inadequate to fully define its role. A review of available time course studies will help to clarify the role of the immune response in the onset and progression of the disease, and identify specific immune targets and time points. A clearer understanding of the role of the immune response in dystrophic muscle pathogenesis could provide invaluable guidance to clinicians to develop and ultimately implement effective therapeutic interventions to treat DMD.

3.2 Mechanical and signaling roles for the DGC

3.2.1 Mechanical role

In healthy muscle, the DGC is thought to bind to and strengthen the sarcolemma by maintaining mechanical integrity during muscle contraction. In the absence of dystrophin, the components of the DGC are not localized to the sarcolemma and the connection between the ECM and the cytoskeleton is lost [218]. The lack of dystrophin compromises the mechanical integrity of myofibers, and results in membrane lesions that allow calcium ions to freely transverse the membrane and initiate muscle cell injury [121]. This hypothesis has

been supported by evidence that dystrophic myofibers have increased membrane permeability, decreased membrane stiffness and reduced force production [6,101,121,152,169,218]. However, available time course data suggest these changes occur only after initial disease onset is first observed in dystrophic muscle [28,45,101,121,169,218]. Furthermore, the mechanical integrity of dystrophic muscles appears to be unchanged during early disease stages [83,218].

Changes in dystrophic muscle membrane permeability have been associated with elevated serum creatine kinase activity, elevated intracellular calcium concentrations, and increased fluorescent dye uptake by fibers; however, these changes are predominantly observed after the initial onset of muscle degeneration [6,121,140,152]. Creatine kinase (CK), usually found at low concentrations outside of muscle fibers, is dramatically elevated in the serum of dystrophic *mdx* mice during initial disease onset [121,122,222]. Serum CK levels are 10-fold higher than normal in *mdx* mice age 21 days, but are not elevated in *mdx* mice age 14 days [121,122]. Although serum CK is not elevated prior to the time of disease onset in *mdx* mice, it can be elevated in DMD patients prior to birth and normally peaks around age 3 years. Histological muscle abnormalities are also observed in human fetuses with elevated CK and suggest that the onset of muscle degeneration can occur before birth [62,63,116,191]. The possibility that inflammation is contributing to this early onset has not been investigated in humans. In addition, calcium (Ca^{2+}) content of *mdx* extensor digitorum longus (EDL) muscles is reported to be normal at age 14 days, but is significantly increased at 40 days, when compared to wild type (WT) control mice [121]. Procion orange (PO), a low molecular weight fluorescent dye that is impermeable to intact muscle fibers, is commonly used to asses sarcolemma permeability. *Mdx* EDL muscles incubated in PO at resting length have minimal dye uptake at age 14 days but increased permeability (~15% of the fibers) is

observed at 40 days [121]. Eccentric contractions increase PO uptake in EDL muscles of *mdx* mice age 90-110 days, but no difference is observed for PO uptake at age 9-12 days compared to un-stretched *mdx* muscles [83,152]. Taken together, these results suggest the dystrophic membrane does become 'leaky", but potentially after disease onset.

Differences in contractile properties have been noted in *mdx* skeletal muscle [44,48,83,101,147]; however maximal force output (tetanic tension), when normalized for muscle mass or cross sectional area, is unchanged before initial disease onset [169,218]. Compared to WT, tetanic tension is not different in *mdx* mice age 2 weeks [169,218], but is significantly depressed in *mdx* mice age 3 to 6 weeks [101,169]. Dystrophin deficiency appears to result in minimal changes in muscle function prior to initial disease onset. The reason for the significant loss in force output only after initial disease onset remains unclear.

Assessments of mechanical integrity suggest that tensile strength of muscle fibers and whole muscle stiffness values are not different in young *mdx* mice [73,83,92,218]. Tensile strength, measured as the amount of suction force required to rupture the sarcolemma of either dissected myofibers (from mice age 3-7 weeks) or cultured myotubes (from mice age 7 days), is not different for *mdx* and WT mice [73,92]. Sarcolemma repair in muscle fibers damaged with a laser pulse is also similar in *mdx* and WT mice [14]. Stiffness is a mechanical measure of a material's ability to resist deformation when under load and is defined as the change of force divided by the change of length [218]. Muscle stiffness is an important measure of muscle integrity and function because it affects the amount of force needed for normal limb movement. EDL muscles from *mdx* mice age 9-12, 14, 21, 28, and 35 days have whole muscle stiffness values that are similar to age matched WT control muscles [83,218]. These data suggest that mechanical integrity of individual dystrophic myofibers and

whole muscles is unchanged during early maturation, despite disease onset and progression.

The absence of dystrophin/DGC proteins results in membrane fragility and contraction-induced injury, characterized by increased membrane permeability and reduced force production; however, currently available data suggest these properties are altered only after initial disease onset [83,101,121,152,169]. In addition, mechanical properties of skeletal muscle are unchanged during early disease processes in *mdx* mice [73,83,92,218]. The mechanisms responsible for the initiation of initial disease onset in dystrophic muscle have not been clearly identified. Further studies to determine if and how membrane lesions form during early maturation are critical to determining the mechanisms that trigger initial disease onset in dystrophic muscle. Identifying these mechanisms could provide valuable insight for clinicians because therapies could then be tailored to blunt or eliminate them. Ideally, time course studies would first focus on determining membrane permeability, contractile properties and mechanical properties in *mdx* mice age 14, 21, 28, 35, and 42 days, ages that represent early maturation and disease onset. Subsequently, studies should be conducted in the GRMD, and finally in DMD patients at the time of overt onset to determine if similar changes occur. On the basis of the available literature, it is not clear if membrane fragility is an initiator or a consequence of the disease process. This outcome could suggest that altered signaling may be responsible for disease onset.

3.2.2 Signaling role

There is evidence that the DGC serves as a scaffold for protein signaling complexes that regulate muscle cell viability. At least four important signaling proteins are known to

associate with the DGC: calmodulin (CaM), calmodulin kinase II (CaMKII), growth factor receptor bound protein 2 (Grb2), and neuronal nitric oxide synthase (nNOS). CaM and CaMKII regulate the interactions of dystrophin and utrophin with actin and cell-survival cascades such as the phosphatidylinositide 3-kinase/Akt cascade and the calcineurin/nuclear factor of activated T-cells (NFAT) pathway. Grb2 promotes cell survival by initiating the Ras/mitogen activated protein kinase (MAPK) signaling cascade through the adaptor protein son-of-sevenless (SOS). nNOS produces nitric oxide, which is believed to mediate vasodilatation during contractile activity [164]. Recently, α1-syntrophin, a member of the DGC, has been shown to bind with TRPC1 to form stretch activated channels (SAC). This may indicate that the DGC scaffolding plays an important role in regulating transmembrane ion fluxes **(Figure 3.1)** [206]. Although the total muscle intracellular Ca^{2+} concentration is reported to increase after initial disease onset [121], SAC activity is reported to increase before initial disease onset [106], and may induce temporary changes in intracellular Ca^{2+} concentration that alter cell signaling. Notably, many of these signaling pathways activate transcription factors that regulate cell viability and the immune response [105,106,154,155,164].

Increased activation of NFAT, activator protein-1 (AP-1) and nuclear factor-kappaB (NF-κB) are observed in dystrophic muscle. These transcription factors regulate cell viability and inflammatory gene expression. Activation of NFAT has only been assessed in *mdx* mice after initial disease onset, therefore it's role in this process is difficult to determine; however, AP-1 and NF-κB activity are both elevated before initial disease onset in the *mdx* mouse [105,106]. Aberrant regulation of AP-1 and NF-κB has been implicated in several disease processes and the early activation of these factors in dystrophic muscle may

suggest a possible role in the immunopathogenesis of DMD. Interestingly, activation of AP-1 and NF-κB in dystrophic muscle is augmented by mechanical stretch [106]. NFAT, AP-1 and NF-κB are known to induce the transcription of inflammatory genes that are reported to be expressed in dystrophic muscle before initial disease onset **(Table 3.1-Table 3.4)**. Understanding both the changes in signaling that lead to disease pathogenesis and when these occur could provide clinicians with the best therapeutic strategies to ablate muscle wasting.

3.3 Profile of inflammatory gene expression early in dystrophic muscle

Temporal gene expression profiles of human dystrophic skeletal muscle, using microarray technology, indicate that inflammation is a primary component of the early disease time course **(Table 3.1)** [37,150]. For example, increased expression of complement components, human leukocyte antigens (HLA's), and chemokines occur during pre-symptomatic (< age 2 years) and symptomatic (age 5 to 12 years) disease stages [37,150]. ECM remodeling genes are also altered in both disease stages and may induce fibrotic scarring. Many homologous inflammatory genes are up-regulated in the *mdx* mouse before and after initial disease onset at age ~21 days **(Table 3.2)** [155,157]. The time course of inflammatory gene expression in dystrophic muscle may play an important role in the onset and progression of muscle wasting.

DNA microarray studies indicate elevated expression of pro-inflammatory genes begins before DMD patients are age 2 years [37,150]. Expression of HLA class I and II (Major Histocompatibility Complex (MHC) I and II) and complement components are elevated in pre-symptomatic and symptomatic DMD patients [37,150]. Overall, elevated inflammatory

gene expression does not continue to increase during the transition from pre-symptomatic to symptomatic disease stages. However, expression of the following genes do increase: HLA-A (1.6-4.4-fold), HLA-B(1.2-2.2-fold), HLA-C (1.2-2.2-fold), HLA-D (1.9-3.1-fold), and complement factor D (1.4-2.5-fold) [37,150]. HLA genes code for MHC proteins that bind and present antigens at the cell surface [37]. MHC class I includes HLA-A, HLA-B, and HLA-C genes, while MHC class II includes the six HLA-D genes [72]. Complement components are activated during innate and acquired immune responses and result in disruption of the plasma membrane [188,215].

Although cytokine expression has not been thoroughly assessed during early DMD disease stages, chemokine expression is up-regulated in pre-symptomatic DMD patients [112,150]. Over expressed chemokines include: CCL2/MCP-1 (1.4-fold), CCL14 /HCC-1 (1.3-fold), CXCL12/SDF-1 (2.3-fold), and CXCL14/BRAK (2.1-fold) [150]. The chemokine CXCL14, also known as breast and kidney expressed chemokine (BRAK), is chemotactic for dendritic cells, B-cells, and monocytes [150,155] and may regulate the increased infiltration of these cells in dystrophic muscle. CCL2, or monocyte chemotactic protein 1 (MCP-1), is likely involved in the recruitment and infiltration of macrophages and T-cells to sites of dystrophic muscle injury [155].

The expression of genes involved in ECM remodeling and fibrosis are augmented in pre-symptomatic and symptomatic DMD patients [37,150]. Expression of collagen type I (~4- to 5-fold) and III (~4-fold) demonstrate the largest elevation, but other collagen types (types IV, V, VI, XIV, XV, and XVIII) are also up-regulated. Elevated expression of matrix metalloproteinase 2 (MMP2; 1.41-fold) and the MMP inhibitors TIMP1 (3.31-fold) and TIMP2 (1.22-fold) are observed. An imbalance in the expression/activation of

MMP/TIMP has been implicated as a factor contributing to fibrosis in DMD [150]. Expression of transforming growth factor (TGF)-β family members, TGFB1 and TGFB3, are also elevated. TGFB1 (1.65-fold) is the predominantly expressed isoform in presymptomatic patients; however, both TGFB1 and TGFB3 are over expressed in patients after age 6 months [150]. The up-regulation of TGFB1 and TGFB3 can be interpreted either as a reparative mechanism or as a compensatory anti-inflammatory response aimed at maintaining homeostasis at the skeletal muscle level.

In *mdx* muscle, DNA microarray studies indicate that ~30% of all differentially expressed genes may be associated with inflammation [154,158]. Analysis of hindlimb muscles from *mdx* mice, age 14, 28, 56, and, 112 days, reveal that markers indicative of cytokine production, complement response, major histocompatibility response, and ECM remodeling all closely correspond with *mdx* disease progression [157]. Up-regulated cytokine-dependent gene expression (e.g., TNF-α receptor (p75 TNF) and Stat 6) is reported in *mdx* mice age 56 days, but cytokine expression is unchanged when assayed with microarray techniques [154]. RT-PCR analysis indicates that elevated expression of tumor necrosis factor alpha (TNFα) and Interleukin-1 beta (IL-1β) are detectable in diaphragm muscles of *mdx* mice age 16 days. Expression of these cytokines is also evident in age 60 day *mdx* mice [105].

Increased expression of inflammatory chemokines (e.g., CCL2/MCP-1, CCL5/Rantes, CCL6/mu C10, CCL7/MCP-2, CCL8/MCP-3, and CCL9/MIP-1γ) and receptors (CCR1, CCR2, and CCR5) have been observed in *mdx* mice with microarray analysis as early as age 23 days with transcripts peaking at age 56 days [155,157]. Similar to DMD patients, BRAK (~2-fold) and its receptor (~5-fold) are up-regulated in *mdx* hind

limbs [155,157]. RT-PCR analysis demonstrates that both MCP-1 and mu C10, are detectable at elevated levels as early as age 14 days after birth and remain elevated at age 112 days in hind limb muscles of *mdx* mice [155]. Many of the chemokine ligands or receptors that show increased expression in *mdx* hind limb muscles are not increased in spared extra ocular muscles (EOM) [157], suggesting an important role for these proteins in the pathology of affected muscles.

Genes associated with ECM remodeling are also altered in *mdx* muscles. Augmented expression of fibril-forming collagen (Col1a2, Col3a1, Col5a2, and Col8a1) transcripts are observed in *mdx* leg muscles. Osteopontin (Spp1), which is produced by macrophages to enhance ECM synthesis, is repressed in *mdx* mice age 7 days (-22.4-fold), but is then highly induced by age 28 days (74.1-fold) [157]. Matrix metalloproteinase 3 (MMP3) is up-regulated in *mdx* mice age 56 days [157], which may prove important because Spp1 activation is dependent on MMP3 cleavage [154]. Similar gene profiles are observed in highly affected *mdx* diaphragm muscles but not in EOM [157,158]. RT-PCR analysis indicates that expression of TGF-β1,2,3 and TGF-β receptors (TβR) I, II, III are elevated following initial disease onset. Increased expression of theses genes is not observed in quadriceps or diaphragm muscles of *mdx* mice age 21 days, but by 56 days there is a significant increase in expression of these genes in both quadriceps (TGF-β1: 8.4-fold, TGF-β2: 1.6-fold, TβRI: 1.4-fold, TβRII: 2.2-fold TβRIII: 2.3-fold) and diaphragm muscles (TGF-β1: 3.4-fold TGF-β2: 1.9-fold, TGF-β3: 2.8-fold, TβRI: 3.0-fold, TβRII: 2.3-fold, TβRIII: 1.2-fold) [224]. Expression of TGF-β is associated with increased fibrosis in dystrophic tissue [81,205].

Microarray technology has been instrumental in identifying gene clusters and disease time points that contribute to dystrophic muscle pathology. Induction of inflammatory and

ECM remodeling gene expression occurs soon after birth and remains active in symptomatic DMD patients [37,150]. Increased inflammatory gene expression is observed in the *mdx* mouse before and after initial disease onset [157]. Approximately 67% of the inflammatory genes induced in *mdx* mice, display comparable behavior in DMD patients [150]. Chemokines and cytokines are important regulators of immune cell infiltration and activation; however their time course has not been completely characterized during early disease stages in DMD patients or *mdx* mice [112,154]. RT-PCR analysis of *mdx* muscles indicate that elevated expression of chemokines (MCP-1 and mu C10) and cytokines (TNFα, and IL-1β) are detectable prior to the overt onset of muscle degeneration at ~21-days [105,155]. The differences observed for the gene expression time course between microarray and RT-PCR techniques highlight discrepancies in the sensitivity of these methods and reveals the need to further validate the role of cytokine and chemokines in dystrophic muscle. Determining the time course of gene expression for cytokines and chemokines is essential because these molecules represent possible therapeutic targets for decreasing inflammation and muscle pathology. Up-regulated expression of ECM remodeling genes in pre-symptomatic and symptomatic DMD patients indicates an early initiation of inflammatory repair processes [81,205]. Expression of inflammatory genes is up-regulated during unique disease stages of *mdx* muscle pathology; however, a thorough time course evaluation of these genes should be further assessed in *mdx* mice and in DMD patients. The inflammatory transcription profile in the early dystrophic disease process is likely driven by the transcription factors NFAT, AP-1 and NF-κB, all of which contribute to cell viability. Upstream regulation of these pathways with already available therapeutics may have a dramatic impact on blunting or preventing the disease process.

Table 3.1 - DMD quadriceps muscles microarray data.

Affymetrix Probe ID	Gene name	Fold Change		References
		<2y	5-12y	
Complement				
35822_at	Complement factor B	3.2	3.0	37
40282_s_at	Complement factor D	1.4	2.5	37
218232_at	Complement component 1q, alpha	3.12	_	150
202953_at	Complement component 1q, beta	2.16	_	150
212067_s_at	Complement component 1r	2.65	_	150
208747_s_at	Complement component 1s	2.29	_	150
217767_at	Complement component 3	3.69	_	150
214428_x_at	Complement component 4A	0.68	_	150
213800_at	Complement factor H	1.88	_	150
215388_s_at	Complement factor H-related 1	2.29	_	150
Human Leukocyte Antigen (HLA)				
36773_f_at	HLA-DQ-beta (DR7 DQw2)	1.9	3.1	37
41723_s_at	HLA-DR beta (DR2.3)	2.3	3.0	37
38095_i_at	HLA-DP beta	2.4	2.8	37
38096_f_at	HLA-DP beta	2.9	2.7	37
38833_at	HLA-DPA1	2.0	2.7	37
37039_at	HLA-DR alpha	2.2	2.6	37
36878_f_at	HLA-DQ-beta (DQB1,DQw9)	2.4	2.4	37
216231_s_at	Beta-2-microglobulin class I MHC invariant chain	1.69	_	150
215313_x_at	HLA-A	1.83	_	150
209140_x_at	HLA-B	1.82	_	150
208812_x_at	HLA-C	1.70	_	150
200905_x_at	HLA-E	1.46	_	150
204806_x_at	HLA-F	1.52	_	150
211528_x_at	HLA-G	1.41	_	150
209619_at	CD74 antigen, class II MHC invariant chain	2.52	_	150
217478_s_at	HLA-DMA	2.39	_	150
211990_at	HLA-DPA1	3.51	_	150
201137_s_at	HLA-DPB1	2.82	_	150
210982_s_at	HLA-DRA	3.24	_	150
209312_x_at	HLA-DRB1	2.82	_	150
215193_x_at	HLA-DRB3	2.87	_	150
Interferon (IFN)-inducible factors				
208436_s_at	IFN regulatory factor 7	1.41	_	150
205483_s_at	IFN, alpha-inducible protein (clone IFI-15K)	2.14	_	150
204415_at	IFN, alpha-iducible protein (clone IFI-6-16)	2.15	_	150
208996_x_at	IFN, gamma-inducible protein 16	2.64	_	150
214453_s_at	IFN-induced protein 44	1.65	_	150
201601_x_at	IFN-induced transmembrane protein 1	1.76	_	150
201315_x_at	IFN-induced transmembrane protein 2	1.66	_	150
212203_x_at	IFN-induced transmembrane protein 3	1.72	_	150
203153_at	IFN-induced with tetracopeptide repeats 1	1.44	_	150
Chemokines				
205392_s_at	CCL14 (HCC-1)	1.3	_	150
216598_s_at	CCL2 (MCP-1)	1.4	_	150
209687_at	CXCL12 (SDF-1)	2.3	_	150
218002_s_at	CXCL14 (BRAK)	2.1	_	150
Receptors				
220146_at	Toll-like receptor 7	1.1	6.6	37,150
ECM remodeling				
202310_s_at	Collagen, type I, alpha1	4.27	_	150
202404_s_at	Collagen, type I, alpha2	5.13	_	150
211161_s_at	Collagen, type III, alpha1	4.22	_	150
211980_at	Collagen, type IV, alpha1	1.56	_	150
211964_at	Collagen, type IV, alpha2	1.61	_	150
214641_at	Collagen, type IV, alpha3	0.70	_	150
212489_at	Collagen, type V, alpha1	2.17	_	150
221729_at	Collagen, type V, alpha2	3.75	_	150
213428_s_at	Collagen, type VI, alpha1	1.93	_	150
209156_s_at	Collagen, type VI, alpha2	2.21	_	150
201438_at	Collagen, type VI, alpha3	2.47	_	150
212865_s_at	Collagen, type, XIV, alpha 1 (undulin)	1.54	_	150
203477_at	Collagen, type XV, alpha1	1.53	_	150
209082_s_at	Collagen, type XVIII, alpha 1	1.32	_	150
201069_at	Matrix metalloproteinase (MMP2)	1.41	_	150
203085_s_at	Transforming growth factor, beta 1 (TGFB1)	1.65	_	150
209747_at	Transforming growth factor, beta 3 (TGFB3)	1.15	_	150
201666_at	Tissue inhibitor of metalloproteinase 1 (TIMP1)	3.31	_	150
203167_at	Tissue inhibitor of metalloproteinase 2 (TIMP2)	1.22	_	150

Table 3.2 - *Mdx* hindlimb muscle microarray data.

Affymetrix Probe ID	Gene name	Fold Change						References
		7d	14d	23d	28d	56d	112d	
Complement								
98562_at	Complement component 1q, alpha	NC	NC	2.79	3.61	6.21	3.06	[157]
96020_at	Complement component 1q, beta	NC	NC	3.59	6.86	10.15	4.56	[157]
92223_at	Complement component 1q, c	NC	NC	3.10	2.53	3.79	2.25	[157]
93454_at	Complement component 1q, receptor 1	NC	NC	NC	NC	1.80	NC	[157]
93497_at	Complement component 3	NC	NC	2.15	NC	4.43	NC	[157]
103707_at	Complement component 3a, receptor 1	NC	NC	3.04	NC	5.31	2.92	[157]
103033_at	Complement component 4	NC	NC	1.88	NC	3.61	NC	[157]
101853_f_at	Complement factor H	NC	NC	NC	NC	1.88	NC	[157]
MHC-associated anitgens								
928866_at	H2-Aa	NC	NC	4.55	15.13	9.97	3.06	[157]
100998_at	H2-Ab1	NC	NC	3.56	7.79	7.48	2.65	[157]
94285_at	H2-Eb1	NC	NC	2.10	1.84	3.46	1.56	[157]
98034_at	H2-DMb1	NC	NC	NC	NC	6.77	NC	[157]
97541_f_at	H2-D1	NC	NC	2.09	1.82	2.97	1.93	[157]
97540_f_at	H2-D1	NC	NC	1.63	1.71	2.50	NC	[157]
101886_f_at	H2-D1	NC	NC	1.59	1.73	2.19	NC	[157]
93120_f_at	H2-K	NC	NC	1.59	1.87	2.78	NC	[157]
93714_f_at	H2-L	NC	NC	1.49	1.57	4.82	NC	[157]
102161_f_at	H2-Q2	NC	NC	1.35	NC	2.34	NC	[157]
98472_at	H2-T23	NC	NC	1.63	NC	2.15	NC	[157]
Interferon (IFN)-inducible factors								
93321_at	Interferon activated gene 203 (Ifi203)	NC	NC	1.64	NC	NC	NC	[157]
98466_r_at	Interferon activated gene 204 (Ifi204)	NC	NC	NC	NC	4.00	NC	[157]
98465_f_at	Interferon activated gene 204 (Ifi204)	NC	NC	2.22	3.29	3.65	NC	[157]
94224_s_at	Interferon activated gene 205 (Ifi205)	NC	NC	2.31	2.49	3.82	NC	[157]
103634_at	Interferon dependent positive acting transcription factor 3 gamma (Isgf3g)	NC	NC	1.70	NC	NC	NC	[157]
160933_at	Interferon gamma induced GTPase (Igtp)	NC	NC	NC	NC	NC	1.98	[157]
97444_at	Interferon gamma iducible protein 30 (Ifi30)	NC	NC	NC	NC	5.96	NC	[157]
98410_at	Interferon-g induced GTPase (Gtpi-pending)	1.48	NC	NC	1.71	NC	2.46	[157]
100981_at	Interferon-induced protein with tetratricopeptide repeats 1 (Ifit1)	NC	NC	5.95	NC	NC	NC	[157]
93956_at	Interferon-induced protein with tetratricopeptide repeats 3 (Ifit3)	NC	NC	1.97	NC	NC	NC	[157]
96764_at	Interferon-inducible GTPase (Iigp-pending)	NC	NC	2.03	NC	NC	NC	[157]
98822_at	Interferon-stimulated protein (15 kDa) (Isg 15)	NC	NC	2.39	NC	NC	NC	[157]
Chemokines								
102736_at	CCL2 (MCP-1)	NC	NC	15.92	25.13	17.52	12.22	[157]
92849_at	CCL6 (mu C10)	NC	NC	NC	NC	3.07	NC	[157]
94761_at	CCL7 (MCP-3)	NC	NC	5.78	18.08	15.00	6.12	[157]
92459_at	CCL8 (MCP-2)	NC	NC	8.51	7.71	25.54	NC	[157]
104388_at	CCL9 (MIP-1γ)	NC	NC	3.18	3.90	5.49	2.82	[157]
93397_at	CCR2	NC	NC	14.84	14.14	5.44	2.53	[157]
161968_f_at	CCR5	NC	NC	36.90	57.95	111.1	19.05	[157]
ECM remodeling								
94305_at	Procollagen, type I, alpha 1 (Col1a1)	NC	NC	NC	NC	2.00	2.07	[157]
101130_at	Procollagen, type I, alpha 2 (Col1a2)	NC	NC	NC	NC	2.40	2.09	[157]
102990_at	Procollagen, type III, alpha 1 (Col3a1)	NC	NC	NC	1.91	4.53	3.71	[157]
98331_at	Procollagen, type III, alpha 1 (Col3a1)	NC	NC	NC	NC	3.07	2.87	[157]
161984_f_at	Procollagen, type III, alpha 1 (Col3a1)	NC	NC	NC	NC	2.47	2.74	[157]
101093_at	Procollagen, type IV, alpha 1 (Col4a1)	NC	NC	NC	NC	1.39	1.55	[157]
92567_at	Procollagen, type V, alpha 2 (Col5a2)	NC	NC	1.48	1.71	3.75	3.07	[157]
162459_f_at	Procollagen, type VI, alpha 1 (Col6a1)	NC	NC	NC	NC	1.83	NC	[157]
95493_at	Procollagen, type VI, alpha 1 (Col6a1)	NC	NC	NC	NC	1.75	NC	[157]
93517_at	Procollagen, type VI, alpha 2 (Col6a2)	NC	NC	1.36	NC	1.57	1.55	[157]
101110_at	Procollagen, type VI, alpha 3 (Col6a3)	NC	NC	1.21	1.38	2.36	2.20	[157]
100308_at	Procollagen, type VIII, alpha 1 (Col8a1)	NC	NC	1.66	NC	3.87	NC	[157]
100481_at	Procollagen	-2.10	NC	NC	NC	NC	NC	[157]
95338_s_at	Matrix metalloproteinase 12 (MMP12)	NC	NC	NC	NC	27.39	6.51	[157]
95339_r_at	Matrix metalloproteinase 12 (MMP12)	NC	NC	NC	7.46	8.70	17.25	[157]
100484_at	Matrix metalloproteinase 13 (MMP13)	-14.09	NC	NC	NC	NC	NC	[157]
160118_at	Matrix metalloproteinase 14 (MMP14)	NC	NC	1.75	NC	NC	NC	[157]
98833_at	Matrix metalloproteinase 3 (MMP3)	NC	NC	NC	NC	6.47	NC	[157]
99957_at	Matrix metalloproteinase 9 (MMP9)	-34.54	NC	NC	NC	NC	NC	[157]
97519_at	Secreted phosphoprotein 1 (Spp1)	-22.42	2.35	29.58	74.09	26.16	10.44	[157]

3.4 Dysregulated cell signaling in dystrophic muscle pathogenesis

Intracellular signaling pathways, particularly those related to inflammation, may be responsible for triggering initial disease onset and regulating disease severity in various muscles. As noted above, expression of genes that regulate inflammatory signaling (i.e., cytokines, chemokines, major histocompatibility complex and ECM remodeling genes) are elevated early in the dystrophic muscle disease time course [37,105,150,154,155,157]. Elevated expression of these genes has been suggested to trigger extracellular signaling that results in infiltration and activation of immune cells in dystrophic muscle [154,155,187]. Populations of lymphocytes, macrophages and neutrophils, which are present in high concentration during early disease progression are capable of facilitating dystrophic muscle wasting, through a process of cell injury and scarring [11,66,187]. Thus, these inflammatory signaling proteins may play a critical role in the onset and progression of DMD. Many inflammatory signaling proteins are dependent on the activation and interaction of the transcription factors, NFAT, AP-1, and NF-κB **(Figure 3.3)**. Each of these plays a critical role in determining cell viability and the expression of inflammatory molecules **(Table 3.3 and Table 3.4)** in diseased myofibers. Signaling cascades that regulate these transcription factors may be dependent on the presence of the DGC, and in its absence become disregulated, ultimately inducing DMD disease pathogenesis [104-106,114,144,194].

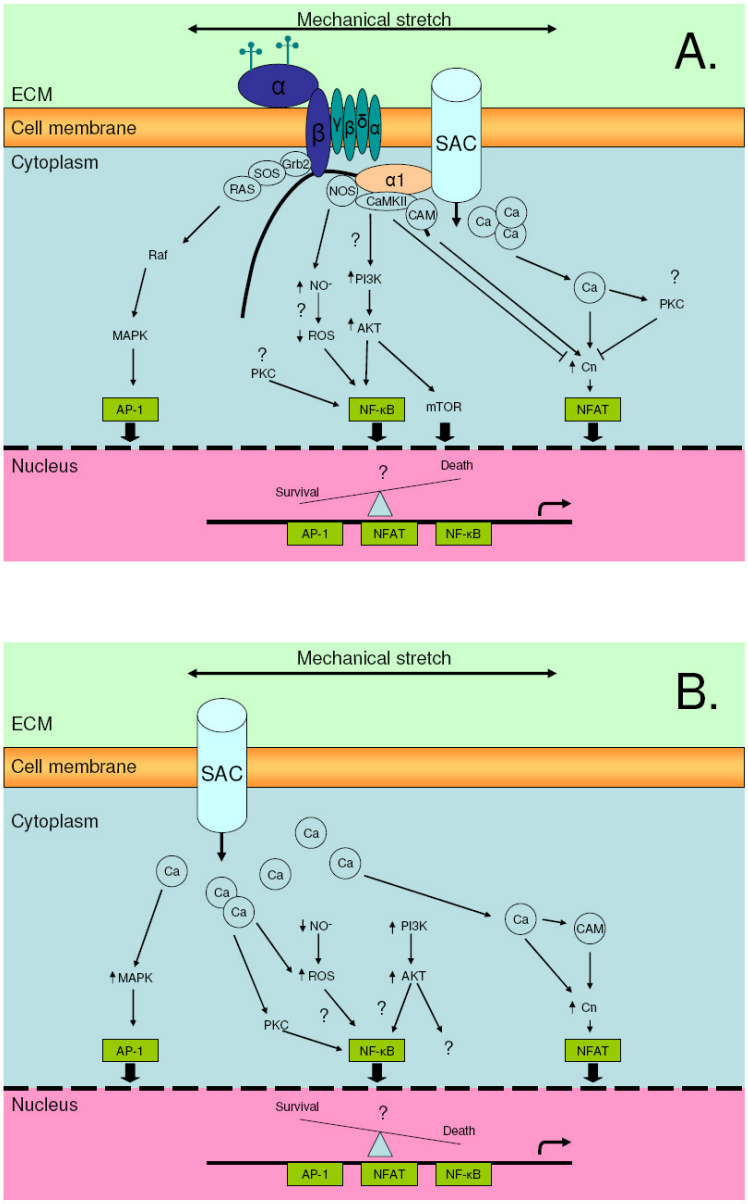

Figure 3.3 – Intracellular signaling pathways. (A) Potential pathways by which mechanical stretch of normal muscle fibers with intact DGC signaling regulate Ca^{2+} influx and transcription factors that control expression of genes for hypertrophy/maintenance, inflammation, and cell survival. (B) Stretch - contractions of dystrophin-deficient muscle fibers causes a large influx of Ca^{2+} through SAC and results in increased activation of transcription factors that regulate fiber phenotype, inflammatory gene expression, and cell viability. Increased activation of AP-1 and NF-κB in *mdx* results from increased activation of upstream signaling in response to mechanical stretch whereas increased NFAT activation does not. However, NFAT activation may be the result of increased cytosolic Ca^{2+}, but this has not yet been studied.

Table 3.3 - Transcription factor target genes.

Transcription Factor	Targets Genes	Function	References
NFAT	IFN-γ	Interferon	104,114,144
	TNF-α and TNF-β	Tumor Necrosis Factor	104,114,144
	CD40L		104,114
	IL-2	Interleukin	104,114,144
	Genes controlling slow twitch programming		104,114
	Utrophin	Dystrophin homologue	31,75,149
AP-1	IFN-γ	Interferon	104,114,144
	TNF-α and TNF-β	Tumor Necrosis Factor	104,114,144
	CD40L		104,114
	IL-2	Interleukin	104,114,144
	Genes controlling slow twitch programming		104,114
	Utrophin	Dystrophin homologue	31,75,149
NF-κB	IFN-γ	Interferon	104,114,144
	IL-1α	Interleukin	144
	IL-1β	Interleukin	144
	TNF-α and TNF-β	Tumor Necrosis Factor	104,114,144
	MIP-1 and MIP-2	Macrophage inflammatory protein 1 and 2, β chemokine	144
	Rantes	Regulated upon Activation Normal T lymphocyte Expressed and Secreted, β chemokine	144
	c-Rel	Transcription Factor	144
	IκBα	NF-κB inhibitor	144
	Collegenase I	Matrix Metalloproteinase	144
	nfkb1	NF-κB p100 precursor	144
	nfkb2	NF-κB p105 precursor	144
	iNOS	Nitric Oxide synthesis	144
	VCAM-1	Vascular Cell Adhesion Molecule	144
	MHC Class I	Mouse histocompatibility antigen	144
	CCR5	Chemokine receptor	144
	CD48	Antigen of stimulated lymphocytes	144
	MCP-1	Macrophage chemotactic protein	144
	IL-2	Interleukin	104,114,144

Table 3.4 - Transcription factor inducers

Transcription Factor	Inducers	Description	References
NFAT	Calcineurin	Calcium signaling pathway	104,114
	IGF-1		5
AP-1	Mechanical stretch		105,106,123
	MAPK/PKC	signaling pathway	5,104 114,176
NF-κB	IL-1	Inflammatory Cytokine	144
	IL-2	Inflammatory Cytokine	144
	TNF-α and TNF-β	Inflammatory Cytokine	144
	Ischemia		144
	Physiological Stress Conditions		144
	Physical Stress		144
	Sheer Stress		144
	Oxidative Stress		144
	MHC Class I	Over-expressed protein	144
	Mechanical stretch		105,106,123
	MAPK/PKC	signaling pathway	5,104 114,176

3.4.1 NFAT

NFAT is a transcription factor which is dephosphorylated and activated by calcineurin [143]. Calcineurin (Cn) is a Ca^{2+}-CaM-dependent phosphatase that is activated by sustained elevations of intracellular Ca^{2+} and induces muscle hypertrophy mainly by dephosphorylating and activating NFAT [142]. CaM and several other proteins that regulate NFAT are known to associate with the DGC and therefore may be affected by its absence [164,206]. Elevated Cn-NFAT activity has been reported in *mdx* mice, but its role in initial disease onset has not been fully defined. NFAT may be important in dystrophic disease pathogenesis because it regulates gene expression for hypertrophy, utrophin, cytokine production and inflammation **(Figure 3.3)** [29,165].

In normal muscle, the DGC may regulate Cn-NFAT signaling through its interaction with TRPC1, CaM and CaMKII [164,206]. CaM activates Cn/NFAT signaling, but CaMKII is believed to inhibit NFAT expression and block Cn activity [165]. SAC activity and Ca^{2+} influx are increased in dystrophic muscle and are attributed to aberrant stretch activation due to the absence of the DGC [6,206]. Sustained intracellular Ca^{2+} content drives Cn-NFAT signaling and the expression of utrophin and oxidative proteins [38,142]. In dystrophic muscle there is an increase in the slow muscle fiber phenotype and an increase in utrophin which is thought to be driven by Cn-NFAT signaling [29,38]. Utrophin expression in *mdx* skeletal muscle is ~4 fold greater than in WT and is associated with increased cell viability [211,212]. Cn-NFAT signaling facilitates a fiber type shift towards the slow phenotype and increased muscle hypertrophy, which improves muscle viability [38,128,209].

The content of Cn is significantly decreased in EDL but unchanged in soleus muscles of *mdx* compared to WT mice age 33-34 days [194]. In mature *mdx* diaphragm muscles (age 5.5 months), Cn and active NFAT protein content are significantly greater (~2-fold) than in WT [194]. Cn phosphatase activity is also increased by ~1.5-fold [194]. Cn and NFAT protein content are significantly higher in TA muscles compared to diaphragm muscles; however, the differences between *mdx* and WT TA muscles are not as great as in diaphragm muscles [194]. Modulation of Cn-NFAT pathway is a key regulator of dystrophic muscle pathology. Constitutively active Cn expression in *mdx* mice attenuates dystrophic pathology while inhibition of Ca^{2+}/CaM signaling exacerbates the dystrophic phenotype [30,31,194]. Immunosuppressive drugs can both enhance (i.e., deflazacort) or inhibit (i.e., cyclosporine A) NFAT-dependent gene expression in dystrophic muscle [51,189]. These divergent drug effects may explain how NFAT is deleterious during early disease stages, but beneficial at later disease stages. Young *mdx* mice treated with cyclosporine A to block NFAT activation have decreased muscle mass and fiber regeneration with increased fiber degeneration and immune cell infiltration [193]. Whereas, *mdx* mice treated with deflazacort to enhance NFAT activation have increased muscle mass and fiber regeneration, with decreased fiber degeneration and immune cell infiltration [7,189]. Therefore, muscle degeneration during initial disease onset in *mdx* mice may overwhelm Cn-NFAT signaling similar to treatment with cyclosporine A, so fiber degeneration is favored. During later disease stages, elevated Cn-NFAT signaling favors fiber regeneration. This possibility could suggest that muscle regeneration with endogenous NFAT activity is not adequate to fully compensate for degeneration in dystrophic muscle during the early onset of the disease, but instead exacerbates disease progression by increasing inflammation.

3.4.2 AP-1

Another transcription factor that can influence cell viability is AP-1. AP-1 activity is regulated by a multitude of stimuli including cytokines, growth factors, and mechanical stress [89,106]. Mechanical stress signals in skeletal muscle are modulated by mitogen activated protein kinase (MAPK) pathways, some of which associate with the DGC [89,106,164,177]. Because dystrophic muscle lacks dystrophin and is susceptible to mechanical stress, these signaling pathways may be responsible for onset and progression of the disease [106]. The role of AP-1 in cell survival is not simply related to increased or decreased activity because this signaling cascade can have both positive and negative affects on muscle viability **(Figure 3.3)** [89,177].

Mdx diaphragm muscles from mice age 17-18 days have an increased basal activation of the MAPK signaling through extracellular signal related kinase 1/2 (ERK1/2), which are upstream of AP-1 activation [106]. ERK1/2 activation is significantly greater in the *mdx* diaphragms in response to mechanical stretch than in WT. Activation of ERK1/2 requires phosphorylation by MAPK kinase 1/2 (MEK1/2). Pretreatment of both *mdx* and WT diaphragms with a MEK1/2 inhibitor results in inhibition of ERK1/2 activation after stretch. This outcome confirms the role of this pathway in the signal transduction mechanism of mechanical stretch. Calcium influx through SAC also induces ERK1/2 activation in dystrophic muscle. WT diaphragm muscles (age 17-18 days) have decreased ERK1/2 activation when treated with the intracellular Ca^{2+} antagonist, TMB-8; however, there is no change in ERK1/2 activation of *mdx* muscles [106]. Conversely, in a Ca^{2+}-free solution, only *mdx* diaphragm muscles (age 17-18 days) have reduced ERK1/2 activation. Treatment of *mdx* diaphragm muscles with L-type Ca^{2+} channel blockers (i.e., nifedipine

and verapamil) does not significantly reduce ERK1/2 activation following mechanical stretch, but treatment with a SAC blocker (i.e., gadolinium chloride) significantly decreases ERK1/2 activation. ERK1/2 activation is believed to be responsible for most of the AP-1 activation observed in mechanically stretched dystrophic muscles [106]. Basal activation of AP-1 is increased in *mdx* diaphragm muscles (age 17-18 days) and is augmented by mechanical stretch when compared to WT. AP-1 activation is blocked when *mdx* muscles are stretched in solution without Ca^{2+} or when MEK1/2 activation is inhibited, indicating AP-1 activation is facilitated by ERK1/2 activation and Ca^{2+} flux through SAC [106]. Many inflammatory genes have AP-1 consensus binding sites in their promoter regions including cytokines and chemokines **(Table 3.3)** [49,106,163]. This may explain why these genes are elevated early in the disease process.

3.4.3 NF-κB

NF-κB is a widely studied transcription factor thought to contribute to dystrophic muscle wasting. NF-κB proteins are DNA-binding, dimeric transcription factors from the Rel family, which are involved in the inflammatory response [94]. NF-κB is sequestered to the cytoplasm by I-kappaB (IκB) inhibitor proteins. IκB undergoes ubiquitin dependent degradation upon its phosphorylation by IκB kinase (IKK). IKK is composed of two catalytic subunits: IKKα, and IKKβ [96,105]. When IκB is degraded the nuclear localization signal is exposed allowing NF-κB to enter the nucleus and drive transcription of cytokines, chemokines, adhesion molecules and enzymes that produce secondary inflammatory mediators [96]. The DGC may interact with NF-κB through the phosphatidylinositol 3-kinase/AKT cascade or the regulation of free radical formation **(Figure 3.3)** [102,151,164]. In DMD patients, NF-κB immunoreactivity is observed in 20-30% of necrotic muscle fibers

and all regenerating fibers [130], suggesting an important role for this transcription factor in dystrophic muscle pathology.

Mdx diaphragm muscles have significantly higher NF-κB/DNA binding activity at ages 15, 18, 30, and 60 days when compared to WT [105]. Elevated TNFα and IL-1β expression is also detectable in these tissues [105]. The increased NF-κB activation and pro-inflammatory cytokine expression prior to *mdx* initial disease onset may signify the importance of immune related signaling mechanisms in this process. Mechanical stretch results in greater NF-κB activity in WT and *mdx* diaphragm muscles; however NF-κB/DNA-binding activity is increased to a greater extent in *mdx* diaphragm muscles [105]. In stretch-activated WT and *mdx* diaphragms, the NF-κB complex is mainly comprised of p50 and p65 subunits [105]. NF-κB stretch activation appears to be the result of increased IKKβ activity which peaks 15 minutes post stretch. Increased IKKβ activity leads to phosphorylation and degradation of IκBα, which exposes the nuclear localization signal, allowing NF-κB to translocate to the nucleus where it binds to DNA [105]. Treatment of WT diaphragms with a Ca^{2+} channel blocker (nifedipine) or with a SAC blocker (gadolinium chloride) does not decrease stretch activation of NF-κB; however treatment with a free radical inhibitor (N-acetyl cysteine) does decrease NF-κB activity [105]. Therefore, during mechanical stretch, free radical formation appears to be the primary contributor to increases in NF-κB activity and may be enhanced by increased oxidative stress seen in dystrophic muscle [59,105,200]. Ca^{2+} influx into cells is coupled with the formation of free radicals such as $^{\cdot}O_2^-$, H_2O_2, and $^{\cdot}OH$ [102]. *Mdx* mice are known to have aberrant SAC activity [221]. Although Ca^{2+} channel blockers do not affect NF-κB activity in WT muscle, marginal NF-κB activity

can be amplified by Ca^{2+} signaling and could be involved in dystrophic disease onset [47,105,213].

The phosphatidylinositol 3-kinase/Akt (PI3K/Akt) signaling pathway regulates muscle hypertrophy and NF-κB activation [57,151]. PI3K/Akt's association with the DGC is unclear, but this pathway may indirectly interact with the DGC through CaMKII [151,164]. The loss of the DGC may potentially result in the disregulation of the PI3K/Akt signaling cascade. Phosporylated Akt (P-Akt) and Akt are elevated in *mdx* mice as early as age 2 weeks [151]. However, significant increases do not occur until *mdx* mice reach age 4 weeks (P-Akt: ~1.9 fold and Akt: ~2.3 fold) and remain elevated in adult *mdx* mice ages 41-59 weeks (P-Akt: ~1.3 fold and Akt: ~1.9 fold) when compared to WT [151]. Mechanical stretch further enhances Akt levels which are specifically dependent on increases in PI3K activation [57]. Downstream targets of the PI3K/Akt pathway (GSK3β, mTOR, FKHR) show an increase in phosphorylation due to mechanical stretch [57]. A PI3K specific inhibitor prevents stretch-induced activation of NF-κB and IKK in *mdx* mice [57]. NF-κB can mediate cell survival through the expression of Bcl-2 and cIAP1. The protein levels of Bcl-2 and cIAP1 are significantly increased in *mdx* diaphragms compared to WT, indicating a potential role of NF-κB in dystrophic muscle cell survival [57]. Although the PI3K/Akt activation of NF-κB is implicated in cell survival in dystrophic muscle, the predominant effect of NF-κB activation is to promote muscle wasting. *Mdx* mice treated with pyrrolidine dithiocarbamate (PDTC), an NF-κB inhibitor that blocks IκBα degradation, from age 5 to 10 weeks have a 20% increase in forelimb strength, 24% increase in strength normalized to weight, and 61% lower fatigue than control *mdx* mice [127]. A significant decrease in percent necrotic area and increase in regenerating area are also reported in PDTC-treated *mdx* mice.

In WT mice, PDTC does not significantly change any of these parameters. PDTC-treated *mdx* mice have significantly reduced NF-κB binding activity and TNFα expression when compared to WT and *mdx* control mice [127].

3.4.4 Signaling Interactions

NFAT, AP-1, and NF-κB signaling cascades not only work alone to enhance gene expression, but also interact with each other to balance cell viability and inflammation. For example, MAPK signaling through C-Jun-N-terminal kinases (JNK) may be a mechanism of cross talk that regulates the upstream signaling activity of these transcription factors [97,100,219]. NF-κB inhibits JNK activity, but JNK itself can induce AP-1 activation and inhibit NFAT activation [97,100,219]. In dystrophic muscle tissue there is believed to be an increase in JNK activation [100,137], but how changes in upstream signaling effect transcription factor activation have not been fully studied in dystrophic muscle. These transcription factors also directly interact in the nucleus to regulate gene expression. NFAT and AP-1 can interact by binding to adjacent sites on DNA. This interaction results in ~20-fold increase in the stability of NFAT DNA binding [165]. NFAT:AP-1 transactivation binding sites have been indentified in the promoter/enhancer regions of many cytokine genes (e.g., IL-2, IL-4, IL-5, and IFN-γ) that are subsequently increased in dystrophic muscle [165]. AP-1 and NF-κB also interact to augment transactivation of both κB and AP-1 enhancer-dependent gene expression [74,190]. AP-1 and κB promoter/enhancer binding sites are found in many inflammatory and cytokine genes that are subsequently increased in dystrophic muscle [49,105,106,144,163,167]. In the absence of the DGC, changes in the regulation of NFAT, AP-1, and NF-κB may be a key mechanism that induces a shift in the balance between cell viability and inflammation in dystrophic muscle.

Regulation and activation of NFAT, AP-1, and NF-κB may play a crucial role in modulating the balance of cell viability and inflammatory gene expression in dystrophic disease pathogenesis [29,89,96,106,165]. The DGC acts a scaffolding that binds regulatory proteins that control signaling and activation of these transcription factors. In the absence of the DGC these signaling cascades appear to be disregulated resulting in aberrant activation of these transcription factors [30,31,105,106]. Influx of extracellular Ca^{2+} through SAC may facilitate the formation of free radicals and may contribute to altered signaling leading to initial disease onset in dystrophic muscle [102,105,106]. Aberrant activation of NFAT, AP-1, and NF-κB may result in a shift in cell viability and inflammatory gene expression. Although NFAT activation before disease onset has not been studied, both AP-1 and NF-κB activity are elevated in *mdx* mice before initial disease onset [30,31,105,106]. Currently available therapeutics may provide clinicians with the tools they need to treat dystrophic disease progression. However, further characterization of these pathways is needed to provide insight into specific disease mechanisms that regulate initial disease onset and the severity of muscle wasting in different muscle groups and at different disease stages. Future research should be focused on identifying mechanisms by which the DGC regulates cell viability and determining the time course and content of these signals in dystrophic muscle.

3.4.5 Currently available anti-inflammatory therapeutic options

Glucocorticoids (GC) are a primary treatment for DMD patients. The most widely used of these are Prednisone/Prednisolone and Deflazacort [9]. Several time course studies in both DMD patients and *mdx* mice with these drugs show improvements in muscle strength and mobility [13,42,99,159,189]. Treatments initiated during early disease stages may result in the

greatest improvements in these parameters [125,159]. GC bind to their receptors (GCR) in the cytoplasm, which then dimerize and translocate to the nucleus where they regulate expression of developmental, metabolic and immune response genes through both transactivation and transrepression [15,50]. Transactivation occurs when the GCR-dimer binds to glucocorticoid response elements (GRE) within gene promoter regions and drives gene expression (e.g. glucose-6-phosphatase, glutamine synthetase, glucocorticoids-induced leucine zipper, lipocortin-1, interleukin-10, interleukin-1 receptor antagonist) [15,50]. The most prominent effect of GC is to inhibit expression of numerous inflammatory genes, but transactivation is unlikely to account for all of the anti-inflammatory properties of GC since GRE regions are absent in the majority of inflammatory genes [15]. Activated GCR can also interact with transcription factors to block their inflammatory activity through the process of transrepression. GC are known to alter NFAT, AP-1, and NF-κB activities, but the exact mechanisms by which this occurs are still unknown [12,95,189]. The activated GCR is thought to directly interact with AP-1 resulting in transcriptional interference and may also regulate AP-1 through inhibition of JNK [2]. In contrast, the GCR is believed to stimulate production of IκBα which directly inhibits NF-κB activity [12,120]. Although GC are shown to reduce NFAT DNA-binding activity and NFAT-AP-1 complex formation, decreases in muscle pathology and NFAT-dependent gene expression in GC treated *mdx* mice is thought to result from an increase in NFAT translocation into myonuclei [189,203,216,217]. One interpretation of this data is that GC treatment results in increased translocation of NFAT and expression of a subset of genes that decrease *mdx* muscle pathology. However, total NFAT DNA-binding activity, NFAT-AP-1 complex formation, and expression of inflammatory genes are decreased. The pleiotrophic actions of these drugs make exclusive

blockade of key pathways difficult. In addition, their many negative side effects such as weight gain, reduced bone density, and impaired glucose tolerance makes long term use of these drugs problematic for DMD patients [9].

Cytokines and chemokines are potential targets for specific therapeutic immuno-modulation. Drugs such as infliximab (Remicade) and etanercept (Enbrel) have been used successfully to specifically block TNFα activity in inflammatory diseases such as rheumatoid arthritis and Crohn's disease [162]. Using these drugs in the treatment of *mdx* mice prior to the onset of muscle necrosis results in decreased muscle pathology and immune cell infiltration during initial disease onset [84,90]. Blockade of TNFα can reduce activation of AP-1 and NF-κB along with other inflammatory factors resulting in an overall decrease in inflammation [84,90]. Other anti-cytokine drugs are also available that have yet to be tested in *mdx* mice or DMD patients, but may also decrease muscle pathology.

Several dietary supplements with no obvious toxicity have been identified as good anti-inflammatory agents and could potentially be added to DMD patients diets or given as nutraceuticals to decrease muscle pathology. Epigallocatechin gallate (EGCG), a component of green tea extract (GTE), is believed to decrease the production of free radicals and modulate the activity of both the Akt and NF-κB pathways. *Mdx* mice treated with either GTE or EGCG have increased antioxidant capacity, improved contractile properties, and decreased muscle pathology [58]. These studies indicate the GTE and EGCG may provide beneficial treatment options for reducing oxidative stress and decreasing dystrophic muscle pathology. EGCG has been shown to inhibit Akt activation [160,170]. EGCG also inhibits NF-κB activation by blocking IKK activity [36,220]. Since NF-κB activity is elevated in dystrophic muscle and Akt may contribute to NF-κB activation, this may be

one way in which EGCG decreases muscle pathology. However, the role EGCG plays in modulating cell signaling has not been studied in dystrophic muscle.

Curcumin a dietary component of the spice tumeric is a recognized inhibitor of NF-κB activation [61]. Curcumin has been shown to have an array of biological activities which include inhibition of sarcoplasmic reticulum Ca^{2+} ATPase, cyclooxygenase-2 expression, and JNK activity [115,145]. In *mdx* mice, dietary administration of curcumin did not decrease muscle pathology or decrease NF-κB activity; however, intraperitoneal injection of curcumin decreased muscle pathology and was able to reduce NF-κB activity and iNOS expression which catalyzes the production of NO [61,145]. Additionally, serum levels of TNFα and IL-1β were also reduced [145]. Nutraceuticals provide a low toxicity treatment option that may be very effective at reducing muscle pathology and inflammation by targeting specific signaling pathways. Although the exact dose and ideal administration route for EGCG and curcumin have not been determined. Under appropriate guidance by clinicians, these supplements could be used to treat DMD patients.

Currently there are many anti-inflammatory drugs/nutraceuticals available to clinicians with strong anti-inflammatory properties. These drugs provide a distinct advantage over other treatment options such as gene therapy where unknown complications and side effects may arise. GC have been the primary drugs used to decrease DMD muscle pathology, but have substantial side effects. A clearer understanding of the disease mechanisms has lead to the identification of other potential treatments for DMD. Anti-cytokine drugs which are already used for rheumatoid arthritis and Crohn's disease have highly specific targets and result in decreased inflammation and muscle pathology in *mdx* mice; however, more studies should be conducted to determine if the prolonged

immunosuppression would be problematic for DMD patients. Nutraceuticals are promising therapeutic options that can be used to suppress inflammation. EGCG and curcumin are widely consumed dietary compounds that have no apparent toxicity. Both EGCG and curcumin decrease muscle pathology and decrease *mdx* muscle pathology. Although ideal administration of these compounds as nutraceuticals has not yet been determined, they could be used as a dietary therapy for DMD patients now.

3.5 Conclusion

In this review, inflammatory signaling pathways involved in the initiation and progression of dystrophic muscle lesions have been assessed, and potential therapeutic drug candidates have been identified from already available clinically tested drugs and dietary componds. Signaling pathways are known to be altered in dystrophic muscle, but our understanding of how the absence of the DGC changes the balance between cell survival and death is limited [105,106,164]. The available evidence strongly suggests that altered activation of NFAT, AP-1, and NF-κB pathways alone or together could contribute to inflammatory gene expression initiating dystrophic pathogenesis. Understanding the dynamic interactions of signaling pathways in the dystrophic disease time course will undoubtedly provide new insight into DMD disease processes and reveal the best treatment options available for those afflicted with this disease.

Although mechanical injury and membrane defects are important pathological factors that impact dystrophic muscle wasting, these features have only been reported after the initiation of muscle degeneration or initial disease onset. In contrast, altered cell signaling, elevated immune cell infiltration and expression of immuno-regulatory proteins has been

reported in dystrophic muscle before and during the onset of morphopathological changes. The absence of dystrophin and DGC proteins likely contributes to altered mechanical integrity of muscle fibers, but these have more recently been linked to aberrant cellular signaling. Greater basal activation and stretch activation of transcription factors, in connection with Ca^{2+} influx and free radical production, involved in the expression of inflammatory genes are reported in dystrophic muscle before initial disease onset. Specifically, increased expression of cytokines and chemokines, which regulate infiltration and activation of immune cell populations are observed during this time. Cytokines and chemokines represent clear therapeutic targets for regulating inflammation and could be targeted with already available drugs. In dystrophic muscle, immune cells contribute substantially to muscle wasting and are known to modulate apoptosis, necrosis, and fibrosis. Early therapeutic interventions, which disrupt immune processes through NFAT, AP-1, and NF-κB in *mdx* mice result in greatly decreased muscle pathology and may provide the most beneficial treatments for DMD. Although many immune-mediated disease processes have been identified in dystrophin-deficient muscle, characterization of a detailed time course of these mechanisms has been neglected in both human patients and in dystrophic models. Thus, time course studies should first focus on determining immune cell infiltration, cytokine production, and inflammatory signaling in *mdx* mice at ages 14, 21, 28, 35, and 42 days to represent the periods before, during, and after the onset of lesion development in muscle. Similar studies should then follow in other animal models and when possible in DMD patients. This information should provide valuable guidance for clinicians to develop and to ultimately design studies to demonstrate the clinical efficacy of these interventions to treat DMD.

Chapter 4 Immune mediated mechanisms potentially regulate the disease time course of Duchenne muscular dystrophy and provide targets for therapeutic intervention

Nicholas P. Evans[a*], Sarah A. Misyak[b], John L. Robertson[c], Josep Bassaganya-Riera[b], and Robert W. Grange[a]

[a] Department of Human Nutrition, Foods and Exercise, Virginia Polytechnic Institute and State University, Blacksburg, Virginia 24061, USA

[b] Virginia Bioinformatics Institute, Virginia Polytechnic Institute and State University, Blacksburg, Virginia 24061, USA

[c] Department of Biomedical Sciences and Pathobiology, Virginia Polytechnic Institute and State University, Blacksburg, Virginia 24061, USA

[*]Correspondence to Nicholas P. Evans, Department of Human Nutrition, Foods and Exercise, Virginia Polytechnic Institute and State University, 338 Wallace Hall, Blacksburg, Virginia 24061, USA

Reprinted from PM R, 1(8), Evans NP, Misyak SA, Robertson JL, Bassaganya-Riera J, Grange RW, Immune mediated mechanisms potentially regulate the disease time course of Duchenne muscular dystrophy and provide targets for therapeutic intervention, 755-68, 2009, with permission from Elsevier.

Abstract

Duchenne muscular dystrophy is a lethal muscle wasting disease that affects boys. Mutations in the dystrophin gene result in the absence of the dystrophin glycoprotein complex (DGC) from muscle plasma membranes. In healthy muscle fibers, the DGC forms a link between the extracellular matrix and the cytoskeleton to protect against contraction-induced membrane lesions and to regulate cell signaling. The absence of the DGC results in aberrant regulation of inflammatory signaling cascades. Inflammation is a key pathological characteristic of dystrophic muscle lesion formation, but the role and regulation of this process in the disease time course has not been sufficiently examined. The transcription factor, NF-κB has been shown to contribute to the disease process and is likely involved with increased inflammatory gene expression, including cytokines and chemokines, seen in dystrophic muscle. These aberrant signaling processes may regulate the early time course of inflammatory events that contribute to disease onset. This review critically evaluates the possibility that dystrophic muscle lesions in both DMD patients and *mdx* mice are the result of immune-mediated mechanisms that are regulated by inflammatory signaling and also highlights new therapeutic directions.

4.1 Introduction

Duchenne muscular dystrophy (DMD) is a lethal, human muscle wasting disease caused by mutations in the dystrophin gene that result in the loss of the dystrophin protein [19,197]. In normal muscle cells, the dystrophin-glycoprotein complex (DGC) **(Figure 4.1)** is localized to the sarcolemma forming a link between the extracellular matrix (ECM) and cytoskeleton [192]. This complex is thought to protect muscle cells from contraction-induced injury and preserve cell viability through both mechanical and signaling roles [60,139]. In DMD, dystrophin and the associated DGC proteins are absent from the sarcolemmal membrane resulting in altered mechanical and signaling functions which contribute to membrane fragility, necrosis, inflammation, and progressive muscle wasting [181].

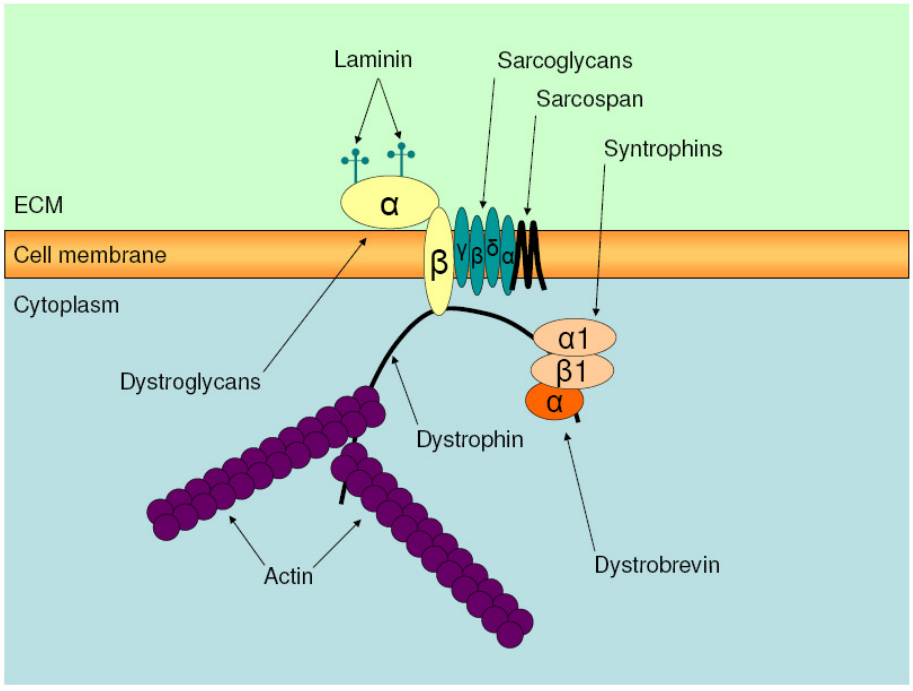

Figure 4.1 – The dystrophin glycoprotein complex (DGC) in normal myofibers. Illustration of the link formed between laminin in the extracellular matrix (ECM) and the cytoskeleton by the DGC. Also shown, interaction of DGC components (dystrophin, dystroglycans, dystrobrevin, laminin, sarcoglycans, syntrophin, and sarcospan) with potential signaling proteins (Grb2, SOS, RAS, NOS, CaM, CaMKII), and with stretch activated channels (SAC) through which calcium (Ca) can enter the cell.

Although mechanical injury and membrane defects are important factors promoting dystrophic disease pathology, neither fully explains DMD disease onset and progression [146,152]. Aberrant intracellular signaling cascades that regulate both inflammatory and immune processes contribute substantially to the degenerative process [105,106,155]. Up-regulated inflammatory gene expression (e.g. cytokines, chemokines, and major histocompatibility complexes) and activated immune cell infiltrates (e.g., T lymphocytes and macrophages) are evident during early disease stages in dystrophic muscle and play a critical role in muscle wasting [28,37,150,154,157,186,210]. The purposes of this review are (1) to propose and evaluate the possibility that the onset of dystrophic muscle lesions in both DMD patients and *mdx* mice are the result of immune-mediated mechanisms, (2) to explore the roles of NF-κB, cytokines, and chemokines as regulators of these immune mechanisms and, (3) to highlight therapeutic options to blunt these processes.

4.2 Immune mediated dystrophic muscle lesion formation

An understudied area to delineate the time course of DMD pathology during early disease onset is the contribution of immune mechanisms. Time course refers to the characteristics of dystrophic pathology that arise over time from pre onset through early progression of the disease. One advantage of this knowledge is that it can reveal significant information to guide treatment at a specific disease stage. For example, immune cell infiltration in dystrophic muscle was once thought to be a non-specific reaction to damaged muscle fibers [11,66,67], but is now considered to be a specific response that directly contributes to muscle lesion formation [87,119,186,207,210]. Because immune cell infiltration (i.e., neutrophils and macrophages) precedes initial disease onset in dystrophic muscle [28,186,210],

it is not surprising that immunosuppressive therapies can significantly blunt muscle wasting when administered prior to disease onset [51,84,90,161,186,189,210]. Although comprehensive time course data sets are limited, those that are available suggest early immune cell infiltration in DMD patients and *mdx* mice represent an important, but underappreciated aspect of dystrophic muscle pathology.

Immune cells can contribute substantially to the initiation and progression of muscle pathology **(Figure 4.2)** [198,199]. In dystrophic muscle, macrophages and T-cells are the primary infiltrating immune cell types [11,66,124,186,210]. Macrophages, when triggered by inflammatory stimuli, lyse muscle fibers through the production of nitric oxide [207,210]. Macrophages may also engulf and present antigens to T-cells to induce their activation; however, this process has not been characterized in dystrophic muscle [187]. CD8+ T-cells trigger muscle fiber death and CD4+ T-cells can contribute to this process by providing inflammatory stimuli (i.e. cytokines) to CD8+ cells and other immune cells [186,187]. The high concentrations of macrophages and T-cells observed in dystrophic muscle from early disease stages and persisting through later stages indicates the importance of these cells in the initiation and progression of dystrophic muscle lesions [11,66,124,186,210]. Additionally, mast cells, eosinophils, and neutrophils are believed to contribute to dystrophic muscle fiber wasting [25,78-80,90]. The role of these cells in dystrophic muscle lesion formation is less clear, but data indicates that they are significant factors in disease progression.

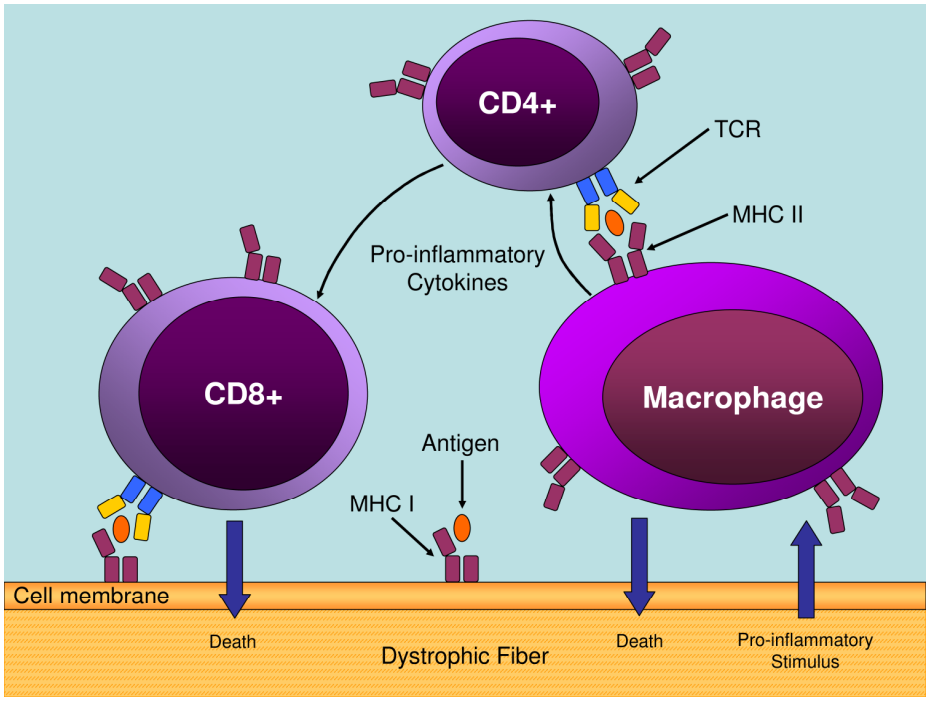

Figure 4.2 – Possible immune cell interactions in dystrophic muscle. Macrophages, CD4+, and CD8+ cells appear to primarily interact within the muscle tissue of *mdx* mice, whereas in a typical immune response, APC's would engulf antigens and carry them back to draining lymph nodes to interact with CD4+ and CD8+ T cells. Dystrophic muscle fibers likely produce antigens which are engulfed by macrophages and are activated by additional inflammatory stimuli. In DMD patients, T cells have specific TCR rearrangements that may allow them to interact with APC which express MHC I and II. Therefore, one possibility is that macrophages (which have both MHC I and II proteins on their surface) could induce muscle fiber death through nitric oxide mediated cell lysis or present antigen, bound to MHC II, to CD4+ T cells through their T cell receptors. Activated CD4+ T cells would then produce cytokines to activate CD8+ T cells. When receptors on CD8+ T cells come in contact with antigen, they bind to MHC I on the surface of muscle fibers and can induce muscle fiber death.

4.2.1 DMD Patients.

In DMD patients, immune cells are present throughout perivascular, perimysial, and endomysial regions of skeletal muscle [66]. At age 2-8 years, the infiltrating mononuclear cells are predominantly macrophages (~38%) and T-cells (~62%), with minimal B-cell (~1%) infiltration [11,66]. The infiltrating T-cell population is composed predominantly of CD4+ cells with some CD8+ cells [124]. Mast cells have also been implicated in the initiation

and progression of muscle lesions in DMD. Peak mast cell infiltration occurs by age 3 years and there is a 10-fold increase in these cells in skeletal muscle from DMD patients when compared to healthy individuals [79].

Major Histocompatibility Complex (MHC) class I proteins are expressed on most nucleated cells, whereas MHC class II proteins are only expressed on professional antigen presenting cells (APCs) like macrophages, and B-cells. Infiltrating mononuclear cells are strongly reactive for both MHC class I and II proteins in DMD skeletal muscle [124]. In patients >1-year-old, MHC II proteins are consistently observed on infiltrating mononuclear cells indicating the presence of APC's in the muscle tissue from an early age [123]. Skeletal muscle fibers are one of a few cell types that have very little or no detectable MHC I proteins on their surface [10,65,98,123,124], so it is striking that muscle fibers from DMD patients have a ~3-fold increase of these proteins [123]. MHC I proteins are detectable on skeletal muscle fibers from these patients as early as age 6 months [123,124]. MHC I staining can be observed on morphologically normal muscle fibers , necrotic fibers, regenerating fibers and fibers invaded by inflammatory cells [10,65,98,123,124]. This striking pattern of MHC production in dystrophic muscle could indicate that immune effector mechanisms are targeting specific dystrophic muscle antigens and contributing to disease pathology. Specifically, T-cells may recognize antigens bound to the surface of MHC proteins located on muscle fiber cell membranes [11].

Evidence of polyclonal expansion of T-cells has been noted in DMD patients and suggests increased immunoreactivity, albeit to unknown antigens [87,187]. T-cells isolated from DMD patients contain Vβ2 T-cell receptor (TCR) rearrangements [87,187]. The majority of these patients exhibit a conserved amino acid sequence in the highly variable region of

the TCR believed to interact with antigen, which is not observed in muscle tissue from healthy individuals. In other inflammatory muscle diseases, such as polymyositis, there is a predominance of Vβ15 rearrangements not the Vβ2 rearrangements that occur in DMD. These data indicate that the TCR rearrangements observed in DMD patients are specific for this disease [119]. Collectively, these data indicate that APC's and T-cells are present early (e.g., age 6-12 months) and may contribute to disease pathogenesis by targeting unknown antigens present on dystrophic muscle fibers. However, there is still insufficient data that fully characterizes the immune response in DMD patients, and therefore, much of the understanding about the role of the immune system and its effects on dystrophic muscle have come from mdx mice, a reasonable but not complete animal model for DMD.

4.2.2 *Mdx* mice.

Mdx mice have been used to study the muscle lesion formation that results from immune cell infiltration because the immune cell populations in their muscles resemble those seen in DMD patients [11,66,124,184,186,210]. In DMD patients and *mdx* mice, muscle lesion formation is associated with immune cell infiltration that is clearly different from non-specific inflammatory responses to muscle injury [25,78,79,186,198,210]. The primary immune cells evident in skeletal muscle of *mdx* mice are macrophages, T-cells and neutrophils; however, other inflammatory cells are also believed to contribute to the observed muscle pathology **(Table 4.1)**. In *mdx* mice, immune cell infiltration is an early pathological event that occurs between age 2-4 weeks and then decreases in severity by age 3 months [184].

Table 4.1 - Peak immune cell infiltration in *mdx* mice.

Infiltrating Immune cells	Peak Age	Peak Infiltration	References
Macrophages	4 - 8 weeks	>80,000 cells/mm^3	186,210
T-cells	4 - 8 weeks	>1200 cells/mm^3	184,186
Neutrophils	ND	ND	90
Eosinophils	4 weeks	>4000 cells/mm^3	25
Mast Cells	4 weeks	30 fold increase	79

ND, No data

Macrophage infiltration is the most prominent immune feature observed in *mdx* muscles. The concentration of these cells are elevated in *mdx* muscles as early as age 2 weeks and peak between ages 4 to 8 weeks [28,184,186,210]. Macrophages have a variety of important immunoregulatory and inflammatory functions that are not fully understood. Recently, two subpopulations of macrophages have been identified in *mdx* muscle tissue that may influence muscle degeneration and regeneration depending on the proportion of these cells present [207]. The M1 population are pro-inflammatory and promote muscle cell lysis through inducible nitric oxide synthase (iNOS) dependent mechanisms while the M2 population enhance muscle regeneration by inducing satellite cell proliferation [207]. Cytokines play an important role in the regulation of the two populations of macrophages present in dystrophic muscle [207]. TNFα and IFNγ stimulate the expression of iNOS in M1 macrophages while IL-4 and IL-10 decrease iNOS expression and promote M2 activation [207]. IL-10 activated M2 macrophages are thought to promote satellite cell proliferation and muscle regeneration [207]. Although there is a population of macrophages in dystrophic muscle that supports regeneration, antibody-mediated depletion of macrophages in *mdx* mice, beginning at age 6 days and continuing to age 4 weeks, results in a >75% reduction of injured muscle fibers, suggesting an important role of these cells in the development of muscle lesions [210]. Future research might focus on ways to block the production of

cytokines promoting the M1 phenotype and shift the balance of these cells to the M2 phenotype to dramatically improve the regenerative process.

Elevated concentrations of activated CD8+ and helper CD4+ T-cells are present in affected muscles of *mdx* mice between age 4-8 weeks, but rapidly decrease in concentration by age 14 weeks [184,186]. Activated CD4+ (18-fold) and CD8+ (17-fold) cells are significantly elevated in skeletal muscle from *mdx* mice compared to WT mice. No increases of these cells have been observed in axillary or inguinal lymph nodes of *mdx* mice, suggesting that their activation is occurring in the muscle tissue, and not systemically [186]. T-cells may be involved in the pathogenesis of DMD through three mechanisms that promote cytotoxicity: perforin-induced killing, fatty acid synthetase [fas]-induced killing and cytokine-induced killing. Fas-induced killing has been ruled out as a main contributor to dystrophic muscle fiber death; however, both perforin- and cytokine-induced killing are likely to be significant contributors [184,186,187]. Antibody-mediated depletion of CD8+ or CD4+ cells in *mdx* mice, beginning at age 6 days and continuing to age 4 weeks, results in a 75% and 61% reduction in muscle histopathology, respectively [186]. This positive outcome suggests an important role for these cells in the development of muscle lesions.

Clusters of neutrophils are observed in the muscles of *mdx* mice as early as age 2 weeks [28]. Muscle injury and membrane lysis can be caused by superoxide production mediated by infiltrating neutrophils [198]. Antibody-mediated depletion of neutrophils starting at age 19 days significantly reduces muscle necrosis (age ~21 days) and subsequent regeneration (age ~28 days) [90]. For example, ~17% of the tibialis anterior (TA) muscle is necrotic in *mdx* mice during acute disease onset, while neutrophil depleted age-matched *mdx* mice have less than 3% muscle necrosis [90]. This reduction in the early necrotic process

indicates the importance of neutrophils as key regulators of the dystrophic disease time course and may provide insight into mechanisms of immunopathogensis since they are one of the earliest infiltrating cell types.

Eosinophil concentrations in quadriceps muscles of *mdx* mice age 4 weeks are elevated (~20-fold) compared to WT controls [25]. By 30 to 32 weeks, the concentration in *mdx* quadriceps significantly decreases, but is still significantly elevated compared to age matched WT controls (~7-fold) [25]. In diaphragm muscles of *mdx* mice age 4 weeks, the concentration of eosinophils is only marginally elevated, but then the concentration significantly increases by 30 to 32 weeks when compared to WT control [25]. The time course of eosinophil infiltration in each muscle appears to parallel the overall muscle pathology time course and may indicate that these cells have an unknown function in muscle wasting [25]. Electron micrographs of *mdx* hindlimb muscles show that eosinophils infiltrate the basement membrane of muscle fibers and are found in close proximity to the surface of necrotic fibers. Eosinophils contain vesicles with rod-like inclusions, consisting of major basic protein (MBP), which are oriented parallel to the surface of non-pathological muscle fibers. However, eosinophils lying next to pathological muscle fibers have MBP rods oriented perpendicular to muscle fibers and appear to protrude through fiber membranes [25]. MBP and other cationic proteins released by eosinophils form pores in target cell membranes that result in cell swelling, Ca^{2+} influx, and the leakage of cytosolic proteins [1,103].

Mast cells have been implicated in dystrophic disease processes in *mdx* mice and in DMD patients [78,79]. Mast cells contain granules filled with biogenic amines (e.g., histamine), proteoglycans, cytokines, and other enzymes, which are released upon

stimulation [78,79]. Mast cell proliferation and degranulation is commonly observed in areas of grouped fiber necrosis [78,79]. Mast cell degranulation results in the release of proteases (chymase, tryptase, carboxypeptidase), which can induce membrane lysis of nearby cells and promote local areas of ischemia [79]. Additionally, the release of molecules like TNFα and histamine from mast cell granules can contribute to a pro-inflammatory environment that promotes muscle necrosis [161]. Treatment of *mdx* mice beginning prior to acute disease onset (age 19 days) with sodium cromoglycate (cromolyn), a blocker of mast cell degranulation, results in ~30% decrease in cumulative TA muscle damage by age 28 days [161]. Additional research of mast cells in dystrophic muscle may provide insight into mechanisms that regulate the microenviroment and ischemic conditions that result in fiber necrosis.

Muscle tissue from DMD patients and *mdx* mice is infiltrated with large populations of immune cells during the early stages of the disease [28,66,77,186,187,210]. In DMD patients and *mdx* mice, the high concentration of macrophages and T-cells and the low concentration of B-cells present in the muscle during inital disease onset indicate a cell-mediated immune response [11,66,123,124,186,210]. In *mdx* mice, elevated concentrations of macrophages and neutrophils are observed as early as age 2 weeks [28,87,210], while peak mast cell and eosinophil infiltration are observed during acute disease onset [25,78]. Remarkably, the dramatic increase in immune cell infiltration in the *mdx* mouse rapidly decreases after initial disease onset and may be one mechanism by which *mdx* mice are spared the debilitating pathology suffered by DMD patients [184]. Although many studies have reported elevated populations of immune cells, mechanisms of immune cell infiltration and the initiation of myonecrosis have not been fully quantified in either DMD patients or in *mdx*

mice; this greatly limits our current understanding of these mechanisms and their regulation. However, because several studies demonstrated that depletion of inflammatory cells results in a dramatic improvement in dystrophic muscle pathology, it is likely that inflammation is a key contributor to muscle wasting. If true, then potential regulators of dystrophic muscle pathology could be cytokines and chemokines, which are known to increase immune cell activity and may directly trigger muscle cell death signals [112,154,155,157]. Additionally, upregulation of cyokines and chemokines in dystrophic muscle prior to disease onset could be due to changes in NF-κB activity resulting from disrupted DGC signaling [2,105]. As noted below, there is reasonable evidence to support this regulatory scheme. A clear benefit of understanding the processes that regulate inflammation is that new therapeutic strategies to ameliorate DMD may emerge.

4.3 NF-κB, cytokines, chemokines, and immune mediated responses in dystrophic muscle

Intracellular signaling pathways are chronically activated in dystrophic muscle due to the loss of intact DGC signaling, Ca^{2+} influx through stretch activated channels and the production of ROS [105,106,164,206,213]. In addition, it is well recognized that dystrophic muscle membranes are susceptible to contraction-induced injury; however mechanical stretch can also induce the activation of transcription factors like NF-κB that regulate the balance of cell survival and cell death. NF-κB has been shown to regulate the expression of many inflammatory genes, including cytokines and chemokines in both immune cells and muscle fibers [2,57,105,144]. Cytokine inflammatory mediators are secreted from infiltrating lymphocytes (e.g. T-cells), myeloid cells (e.g. macrophages), and from damaged muscle fibers to induce further immune cell infiltration and activation [112,154]. Chemokines regulate

T-cell differentiation, leukocyte extravasation, and chemotaxis of various immune cells, including macrophages and T-cells, to sites of tissue damage and inflammation [155,157]. The mechanisms that orchestrate immune cell infiltration and activation have not been identified [37,150,154,155], but evidence suggests these immune-mediated mechanisms could be regulated by cytokine and chemokine signaling in response to upregulated NF-κB.

4.3.1 NF-κB

NF-κB encompasses the Rel family of transcription factors and regulates the expression of many inflammatory genes. Humans express five different Rel/NF-κB proteins which can be separated into two different classes. The first class is synthesized as mature proteins and includes: RelA (p65), c-Rel and Rel-B. The second class must be proteolytically processed from large precursors to the mature proteins p50 and p52. RelA, c-Rel and RelB have nuclear localization signals while p50 and p52 do not. p52 and p50 must dimerize with either RelA, c-Rel or RelB to act as transcription factors. NF-κB dimers containing RelA or c-Rel are sequestered to the cytoplasm by I-kappaB (IκB) inhibitor proteins. Activation of NF-κB is a ubiquitin-dependent process which requires the phosphorylation of IκB inhibitor proteins by IκB kinase (IKK) triggering the nuclear localization signal. NF-κB is then free to enter the nucleus and activate gene expression for inflammatory mediators [94,96]. The DGC appears to be involved in the regulation of NF-κB and in dystrophic muscle there is aberrant activation of this pathway during early disease stages **(Figure 4.3)**. For example, NF-κB /DNA binding activity is significantly higher in *mdx* diaphragm muscles at ages 15, 18, 30, and 60 days when compared to WT [105]. Increased NF-κB activity during the early *mdx* disease time course coincides with and appears to be involved in cytokine and chemokine expression.

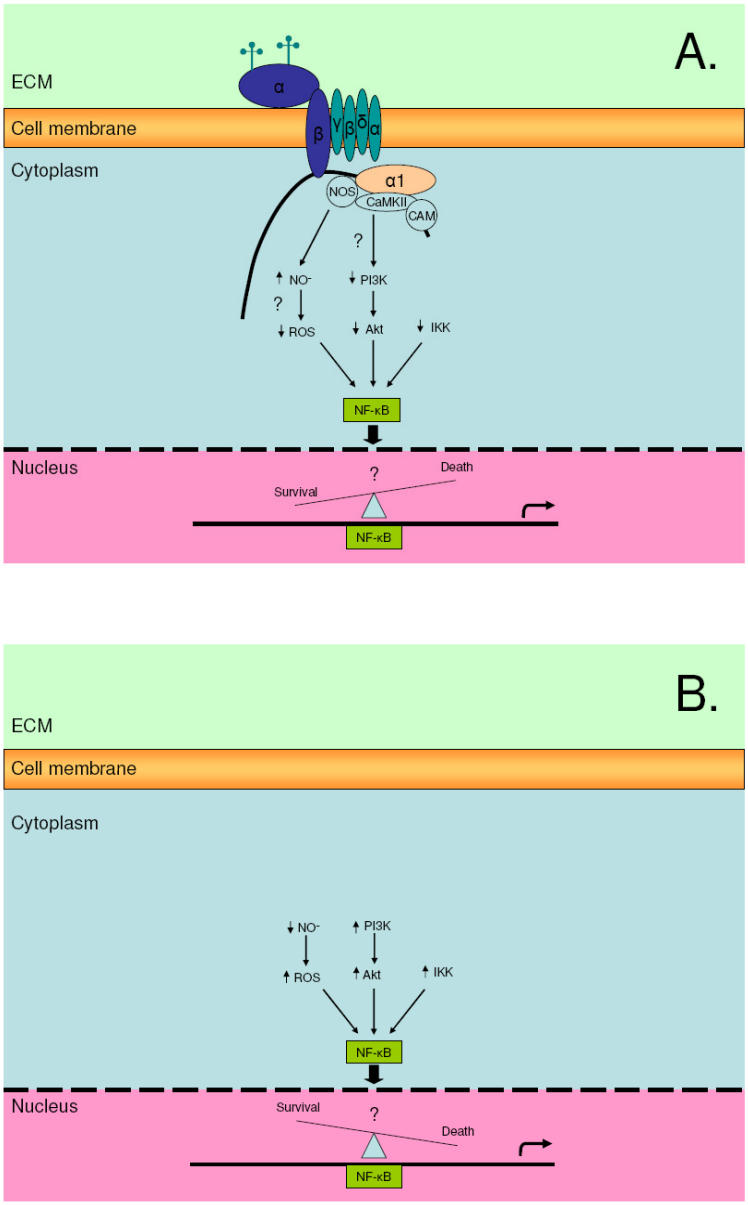

Figure 4.3 – Possible pathways resulting in NF-κB activation. (A) In WT muscle fibers the DGC may play key role in regulating or suppressing NF-κB activation but the mechanism for how this happens has not been defined. (B) In *mdx* muscle fibers, the loss of the DGC has been reported to contribute to changes in signaling pathways that increase NF-κB activation.

NF-κB activity is increased in the diaphragm, TA, and gastrocnemius muscles of *mdx* mice [2]. In these muscles, NF-κB is composed of the p50 and p65 subunits with p50 appearing to predominate in the TA and gastrocnemius [2,105]. Other NF-κB subunits (c-Rel, Rel-B, and Bcl-3) do not contribute significantly to DNA binding activity [2]. Although total p65 levels are not increased in *mdx* muscles, the activated or phosphorylated (p-p65) levels are increased in immune cells and regenerating muscle fibers of *mdx* mice and also DMD patients [2]. Heterozygous deletion of the p65, but not the p50, subunit results in decreased muscle pathology and decreased macrophage infiltration.

Results of recent studies indicate that activation of p65 by IKKβ is independent of classical IκB degradation [2,173]. A conditional deletion of IKKβ in myeloid cells decreases p-p65 in macrophages but not in regenerating muscle fibers. Deletion of IKKβ in macrophages results in a 51% decrease in necrotic foci, a 58% decrease in TNFα, a 66% decrease in IL-1β, and a 45% decrease in MCP-1α. However, the reduction of pro-inflammatory cytokines does not reduce p-p65 in dystrophic myofibers indicating that additional factors contribute to NF-κB activation in muscle fibers. When IKKβ deletion is targeted for muscle, noticeable increases in regeneration occur; yet, no decreases in immune cells are observed. A reduction in TNFα is reported, but no significant change in expression of IL-1β, MCP-1, RANTES, and MIP-1α are apparent [2]. TNFα is believed to inhibit myogenesis by activating NF-κB, which regulates MyoD expression [2,88]. IKKβ-deficient *mdx* muscles have a 41% increase in MyoD immunostaining, indicating NF-κB activity may hinder dystrophic muscle differentiation. *Mdx* mice treated with an IKK specific inhibitor have an 80% decrease in macrophage infiltration and 77% reduction of

membrane lysis of muscle tissue, emphasizing the role of NF-κB in the dystrophic disease process [2].

4.3.2 Cytokines and chemokines

Cytokine and chemokine expression appears to be entwined with the disease time course of dystrophic muscle in DMD patients and *mdx* mice **(Figure 4.4)** [8,81,105,150,154,155,224]. In DMD patients, expression of chemokines, including MCP-1, are up-regulated before age 2 years [150]. Elevated TNFα concentrations are observed in the serum of DMD patients; however, elevated expression of TNFα and IL-1β is not consistently observed in muscle tissuec[112,153,196]. Overexpression of TGF-β is observed in DMD patients older than 6 months and likely contributes to loss of muscle function due to fibrotic scarring [150,224]. In *mdx* mice, pro-inflammatory cytokine and chemokine expression have been reported prior to onset of muscle degeneration and are believed to contribute to this process [28,105,154,157,184,186]. Elevated expression of MCP-1 is detectable at age 14 days and 112 days [155]. Increased TNFα and IL-1β expression are detectable in *mdx* mice age 16 and 60 days. Muscle degeneration is followed by regeneration, fibrosis, and a decrease in immune cell infiltration [8,28,81,184,224]. TGF-β expression is elevated in *mdx* mice during the time following peak muscle denegation (>age 42 days) [8,81]. Increased expression of TGF-β is believed to contribute to a decrease in pro-inflammatory immune response and the increased muscle fibrosis following disease onset [8,81,150,224]. Although there is evidence to support the role of cytokines and chemokines in the time course of dystrophic muscle wasting, the mechanisms have not been fully characterized.

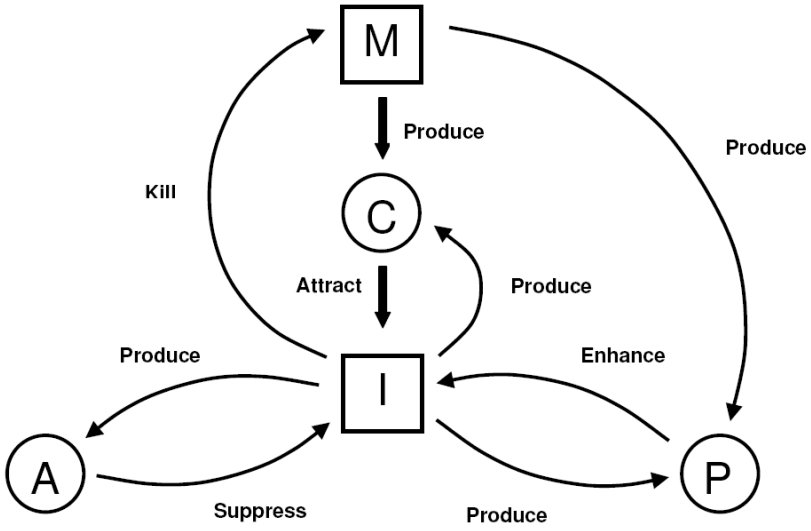

Figure 4.4 – Possible interactions of extracellular immune signaling pathways in dystrophic muscle. In DMD and *mdx* (M) muscle tissue, elevated levels of (C) chemokines and (P) pro-inflammatory cytokines are produced, which when released into the ECM can act as chemoattractants for a variety of (I) immune cells. Although the process has not been described in dystrophic muscle, activated immune cells may travel to sites of muscle damage where they can release pro-inflammatory and anti-inflammatory (A) anti-inflammatory cytokines. The balance between pro-inflammatory and anti-inflammatory cytokines may regulate the level of immune cell activation in dystrophic muscle and resulting muscle fiber death.

MCP-1 is thought to be an important factor in skeletal muscle regeneration and macrophage chemotaxis. MCP-1 expression increases after muscle injury and promotes muscle repair. In the absence of MCP-1 muscle regeneration and strength recovery are impaired [178,179,208]. Macrophages respond to the release of MCP-1 after muscle injury and contribute to muscle regeneration and the removal of necrotic debris [179,195]. Satellite cells can induce macrophage chemotaxis through the release of MCP-1. Once macrophages arrive on site, they amplify chemotaxis and muscle repair [35]. In dystrophic muscle, macrophages have been shown to significantly contribute to dystrophic muscle wasting [210]. Therefore, MCP-1 and macrophage infiltration in dystrophic muscle is likely an attempt at muscle repair; however, excessive macrophage infiltration results in additional muscle

damage. The mechanisms that regulate macrophage infiltration and muscle damage have not been fully assessed, but may be linked with MCP-1 release.

IL-1 has been associated with inflammatory responses in muscle [54]. Both IL-1α and IL-1β have been identified as key contributors of inflammation in inflammatory myopathies [86,113]. In muscle of patients with inflammatory myopathies, IL-1α is localized to endothelial and inflammatory cells and IL-1β is localized to inflammatory cells. The IL-1 receptors, IL-1RI and IL-1RII are localized to muscle fibers [86]. IL-1 is thought to have negative effects on muscle function, protein synthesis and metabolism [43]. Very low concentrations of IL-1β, have been shown to inhibit insulin-like growth factor (IGF)-I stimulated protein synthesis and myoblast differentiation [22]. IGF-1 is an important component that regulates satellite cell recruitment to injured muscle and the resolution of inflammation [134], so IGF-1 regulation by IL-1β may be very important in dystrophic muscle. Increases in IL-1β expression have been noted in dystrophic muscle; however, its contribution to dystrophic muscle wasting has not been addressed.

TNFα is responsible for mediating many immune processes and has been prominently studied in connection with muscle pathology [109,167]. This cytokine is mostly synthesized by macrophages in response to antigens, but can also be produced by muscle cells. Skeletal muscle expresses TNFα receptors I (TNFR1) and II (TNFR2), which bind with TNFα to initiate intracellular signaling pathways. TNFα is known to inhibit contractile function of skeletal muscle, induce muscle wasting, and may be involved in nitric oxide (NO) production [167]. TNFα/TNFR1/NF-κB signaling is believed to increase the production of reactive oxygen species (ROS) via mitochondrial electron transport and increase activity of the ubiquitin/proteasome pathway [167]. ROS can also regulate TNFα/NF-κB signaling,

and thereby influence further catabolic processes, including protein loss, in mature muscle fibers [109].

TNFα-deficient *mdx* mice (*mdx*/TNFα$^{-/-}$) have been used to determine the role of this cytokine in dystrophic muscle pathology [185]. *Mdx*/TNFα$^{-/-}$ mice age 4-8 weeks display no change in CK levels or muscle strength compared to *mdx* controls, although their body mass and muscle mass are significantly decreased by age 8 weeks. *Mdx*/TNFα$^{-/-}$ mice have significantly lower (~2-fold) pathological markers (macrophage and neutrophil invasion, hyaline fibers, and necrosis) in quadriceps muscles at age 8 weeks. In diaphragm muscles of these mice, pathological markers are significantly increased (~2-fold) at age 4 weeks, but not at age 8 weeks [185]. Pharmacological blockade of TNFα with a neutralizing antibody (Remicade), beginning at age 7 days, significantly reduces myofiber necrosis (~17%) in TA muscles of *mdx* mice age 21 days when compared to both untreated *mdx* and *mdx*/TNFα$^{-/-}$ mice [84,90]. The reason for the differences in muscle pathology resulting from the two TNFα depletion techniques is unknown; however, TNFα appears to have a biphasic effect by which it can stimulate myogenesis in undifferentiated myocytes and increase catabolism in mature muscle fibers [109]. Therefore, one possibility is that treatments that deplete the concentration of TNFα, instead of eliminating gene expression, allow for low levels of TNFα to stimulate myogenesis without inducing muscle catabolism.

TGF-β1 suppresses the immune system by preventing proliferation and function of specific T- and B-cell subsets by down regulating MHC I and II expression and inflammatory cytokine activity [224]. Elevated expression of TGF-β is associated with increased fibrosis in dystrophic tissue [81,205]. T-cells play an important role in mediating fibrosis in dystrophic muscle [107,132,133]. The TGF-β family of ligands and receptors are

significantly elevated in the muscles of both DMD patients (age >6 months) and *mdx* mice (age 56 days); however they are not elevated in younger patients [150,224]. *Mdx* mice depleted of T-cells and/or B-cells have significantly less fibrosis and TGF-β1 expression [70,132,133]. Antibody-mediated depletions of TGF-β1 result in a significant reduction of connective tissue to near normal levels in diaphragm muscles of *mdx* mice age 12 weeks [8]. TGF-β1 depletion also results in a significant increase in CD4+, but not CD8+ T-cells in *mdx* diaphragm muscles [8]. Although CD4+ cells concentration is increased, no difference in muscle degeneration is observed at age 12 weeks [8]. The increase in the concentration of CD4+ cells after the removal of TGF-β1 indicates that this molecule may be an important suppressor of the immune response that contributes to dystrophic muscle wasting. The decrease in fibrosis and TGF-β1 after the removal of lymphocytes indicates an important role for this molecule in the regulation of these cells. The induced expression of TGF-β following the initial disease onset phase may be one inhibitory mechanism attempting to suppress the immune response in dystrophic muscle, but may ultimately result in muscle fibrosis.

Increased activation of transcription factors, like NF-κB, that regulate inflammatory genes are observed in dystrophic muscle which can ultimately result in the expression of cytokines and chemokines that regulate immune cell infiltration and activation [29,105,106]. Immune cells play a critical role in dystrophic muscle wasting [187]. In dystrophic muscle, chemokine expression is believed to be elevated before initial disease onset and likely initiates T lymphocyte and macrophage infiltration [150,155]. Increased expression of TNFα and IL-1β before initial disease onset can trigger a pro-inflammatory immune response in dystrophic muscle. TNFα expression is associated with muscle wasting and is believed to

be involved in dystrophic muscle pathology [84,90,185]. Expression of TGF-β is likely a mechanism that suppresses the pro-inflammatory immune response that occurs during disease onset, but results in fibrosis [8,81,150,224]. The role of chemokines and cytokines in the dystrophic disease time course has not been thoroughly investigated in DMD patients or *mdx* mice. Expression of these genes can be difficult to measure because they are transiently expressed and not representative of the concentrations of released proteins. Although the role of these important regulatory molecules has not been thoroughly studied in DMD, they likely contribute substantially to the initiation and progression of this disease. Time course studies detailing cytokine and chemokine protein levels in *mdx* mice spanning before and after disease onset may enable the identification of potential time points at which anti-inflammatory therapies would provide the most beneficial results to blunt or prevent muscle wasting.

4.4 Emerging therapeutic options

In DMD patients and *mdx* mice, inflammation is a large component of muscle pathology [11,25,66,78,79,91,186]. Primarily macrophages and T cells are thought to contribute to muscle wasting in dystrophic muscle; however, as described above other inflammatory cells are also significant contributors to this process [11,25,66,78,79,91,186]. Depletion or inhibition of these cells has been shown to significantly decrease dystrophic muscle pathology [25,90,161]. Although inflammation is a necessary part of the healing process, it can also contribute to the injury process [198,199]. Glucocorticoids have anti-inflammatory properties and have been used to treat DMD with some success; however, the side effects of these drugs often outweigh their benefit [9,13,42,99,125,159,189]. Numerous other anti-inflammatory therapies have been reported to improve healing, many of which may be useful in the treatment of DMD.

Some of these emerging therapeutic options include stem cell treatment, anti-cytokine drugs, and inhibition of NF-κB activity.

Stem cell therapies offer promising treatment options because of their ability to differentiate into different tissue types [16,108]. However, recent research has revealed that several types of stem cells have the ability to strongly suppress the immune response. Mesenchymal stem cells, hematopoietic stem cells, and placenta-derived multipotent stem cells exhibit immunosuppressive properties that are being studied for use in autoimmune diseases [18,33,118,168]. When these stem cells are in the presence of pro-inflammatory cytokines (i.e. TNFα, IL-1, IFNγ) they can produce chemokines that result in T-cell migration into these areas [168]. Once T-cells are in close proximity, their activity is suppressed by the production of nitric oxide, IL-10, and TGF-β by these stem cells [33,168]. There is also data to suggest that mesenchymal stem cells can regulate APC activation of T-cells through cell to cell interactions [18]. Although these findings are very exciting, the use of these therapies in DMD patients will require extensive research to demonstrate their clinical efficacy.

Several anti-cytokine drugs, which are already available for use in human patients, are capable of decreasing dystrophic muscle pathology [84,90]. Infliximab (Remicade) and etanercept (Enbrel) have been used to block TNFα in rheumatoid arthritis and Crohn's disease [162]. These drugs have also been shown to greatly improve muscle pathology in *mdx* mice [84,90]. Because TNFα is known to inhibit contractile function of skeletal muscle and induce muscle wasting, blockade of this cytokine is a logical therapeutic option for DMD patients [167]. Interleukin 1 receptor antagonist (Anakinra) could potentially be used in DMD patients and has already been used in the treatment of rheumatoid arthritis and other

inflammatory diseases [93]. There are also newly developed drugs that block MCP-1 (Bindarit) and TGF-β (TGF-β antagonist), but they are only in the initial stages of assessment [4,129]. A thorough investigation of the cytokines responsible for regulating the dystrophic disease process and their regulation of the disease time course has not been conducted, but will undoubtedly result in the identification of other targets for the amelioration of DMD. Several anti-cytokine therapies have been shown to improve *mdx* muscle pathology and may be useful treatments for DMD patients.

As described above, the transcription factor NF-κB may be responsible for muscle wasting [2,57,105,127]. NF-κB regulates the expression of numerous cytokines which are shown to be elevated in dystrophic muscle [2,57,105,144], and therefore represents a suitable target for therapy. Epigallocatechin gallate (EGCG), a component of green tea extract, is a potent antioxidant that can regulate NF-κB activation [36,71,220]. EGCG inhibits NF-κB activation by blocking IKK activity; however, the mechanism through which EGCG regulates this pathway is not fully understood [36,220]. Since NF-κB activation is sensitive to free radicals, EGCG's ability to reduce their formation may be a key mechanism. Although there are no reports of DMD patients being treated with green tea extract, treated *mdx* mice have increased antioxidant capacity, improved contractile properties, and decreased muscle pathology [23,26,58,136]. Another inhibitor of NF-κB activation is curcumin, a dietary component of the spice tumeric [145]. *Mdx* mice treated with injections of curcumin have reduced NF-κB activation and iNOS expression. TNFα and IL-1β levels in the serum of these mice are also reduced [61,145].

The antioxidants, pyrrolidine dithiocarbamate (PDTC) and *N*-acetylcysteine (NAC), have been used to treat human diseases and are reported to block NF-κB activation [174]. In

mdx mice. PDTC treatment greatly improves force deficit, forelimb strength, and overall body strength [127,180]. These mice have decreased NF-κB activation and TNFα production in their muscle tissue [127]. Histologically, these muscles demonstrate significant decreases in necrosis and increases in regenerating fibers [127]. Similar results are seen in mice treated with NAC [214]. Encouraging results from *mdx* mice indicate that these inhibitors of NF-κB may provide beneficial treatments for DMD patients and could be put to use relatively quickly.

The development of new therapeutic options would greatly benefit from thorough time course studies in DMD patients and animal models that detail the signaling processes that regulate inflammation in dystrophic muscle. Once key signaling processes are identified, treatments can then be tailored to alter these processes in DMD patients. Nevertheless several anti-inflammatory therapies could have clinical relevance in the very near future. These include the use of nutritional therapies (i.e. EGCG and curcumin) and anti-cytokine therapies (i.e. infliximab or etanercept). Stem cell therapies hold great promise to both regenerate muscle tissue and suppress inflammation. Once fully developed, this therapeutic approach could ultimately lead to a cure for DMD patients.

4.5 Conclusion

Mechanical injury and membrane defects are important pathological factors that impact dystrophic muscle wasting; however, these features do not fully explain dystrophic muscle lesion formation and these changes are reported only after overt disease onset. In contrast, altered cell signaling, elevated immune cell infiltration and expression of immuno-regulatory proteins has been reported in dystrophic muscle before and during the

overt onset. The absence of dystrophin and DGC proteins is thought to contribute to altered mechanical integrity of muscle fibers, but has more recently been linked to aberrant cellular signaling. Increased activation of transcription factors (e.g. NF-κB), in connection with Ca^{2+} influx and ROS production, involved in the expression of inflammatory genes are reported in dystrophic muscle before disease onset. NF-κB regulates the expression of numerous inflammatory genes and has been indicated as a key factor in the initiation and progression of dystrophic muscle wasting. Increased expression of cytokines and chemokines, which regulate infiltration and activation of immune cell populations are observed in connection to NF-κB activation. The role of cytokines and chemokines in the pathogenesis of DMD has not been comprehensively examined, but may provide valuable insight into disease mechanisms that regulate muscle pathology. In dystrophic muscle, immune cells contribute substantially to muscle wasting and are known to modulate apoptosis, necrosis, and fibrosis. Early therapeutic interventions, which disrupt immune processes in *mdx* mice greatly decrease muscle pathology and may provide the most beneficial treatments for DMD. Many of these treatments are presently in use to treat other human diseases (e.g. rheumatoid arthritis and Crohn's disease), and therefore could be applied to DMD relatively quickly when compared to treatments that still require extensive testing (e.g., gene therapy). Although many immune-mediated disease processes have been identified in dystrophin-deficient muscle, characterization of a detailed time course of these mechanisms has been largely neglected in both human patients and in dystrophic models. Specifically, time course studies that profile the inflammatory/immune response in detail during the period before and after initial disease onset will be invaluable to identify new therapeutic targets.

Chapter 5 Green tea extract decreases muscle pathology and NF-κB immunostaining in regenerating muscle fibers of *mdx* mice

Nicholas P. Evans[a], Jarrod A. Call[b], Josep Bassaganya-Riera[c], John L. Robertson[d], and Robert W. Grange[a]

[a] Department of Human Nutrition, Foods and Exercise, Virginia Polytechnic Institute and State University, Blacksburg, Virginia 24061, USA

[b] Department of Physical Medicine and Rehabilitation, University of Minnesota, Minneapolis, Minnesota 55455, USA

[c] Virginia Bioinformatics Institute, Virginia Polytechnic Institute and State University, Blacksburg, Virginia 24061, USA

[d] Department of Biomedical Sciences and Pathobiology, Virginia Polytechnic Institute and State University, Blacksburg, Virginia 24061, USA

[*]Correspondence to Nicholas P. Evans, Department of Human Nutrition, Foods and Exercise, Virginia Polytechnic Institute and State University, 338 Wallace Hall, Blacksburg, Virginia 24061, USA

Abstract

BACKGROUND & AIMS: Duchenne muscular dystrophy is a debilitating genetic disorder characterized by severe muscle wasting and early death in afflicted boys. The primary cause of this disease is mutations in the dystrophin gene resulting in massive muscle degeneration and inflammation. The purpose of this study was to determine if dystrophic muscle pathology and inflammation were decreased by pre-natal and early dietary intervention with green tea extract. METHODS: *Mdx* breeder mice and pups were fed diets containing 0.25% or 0.5% green tea extract and compared to untreated *mdx* and C57BL/6J mice. Serum creatine kinase was assessed as a systemic indicator of muscle damage. Quantitative histopathological and immunohistochemical techniques were used to determine muscle pathology, macrophage infiltration, and NF-κB localization. RESULTS: Early treatment of *mdx* mice with green tea extract significantly decreased serum creatine kinase by ~85% at age 42 days ($P \leq 0.05$). In these mice, the area of normal fiber morphology was increased by as much as ~32% ($P \leq 0.05$). The primary histopathological change was a ~21% decrease in the area of regenerating fibers ($P \leq 0.05$). NF-κB staining in regenerating muscle fibers was also significantly decreased in green tea extract-treated *mdx* mice when compared to untreated *mdx* mice ($P \leq 0.05$). CONCLUSION: Early treatment with green tea extract decreases dystrophic muscle pathology potentially by regulating NF-κB activity in regenerating muscle fibers.

5.1 Introduction

Duchenne muscular dystrophy (DMD) is a lethal muscle wasting disease affecting approximately one in 3,500 boys [19,197]. Mutations in the dystrophin gene result in the loss of this protein from the sarcolemma of muscle fibers [19,197]. Dystrophin deficiency does not consistently produce muscle degeneration at all life stages, in all muscle phenotypes, or in all animal models [155]. In dystrophin-deficient skeletal muscle mechanical injury and proteolysis may be important factors but do not fully explain DMD pathogenesis. Mechanisms such as the immune/inflammatory response to injury appear to contribute substantially to muscle pathophysiology. Observations of activated immune cell infiltrates in dystrophic muscle suggest that the immune/inflammatory response may play a role in exacerbating the disease [154,155,184,186,210]. Recently, individual macrophage subpopulations have been reported to influence muscle degeneration and regeneration depending on the proportion of these cells present. M1 macrophages are cytotoxic and pro-inflammatory while M2 macrophages promote muscle regeneration [207]. Therefore, a shift in macrophage phenotype may be one mechanism that can regulate the dystrophic disease time course [207].

Complementary and alternative medicine (CAM) approaches, including the use of botanicals, are being pursued in the amelioration of DMD. Green tea is a widely consumed beverage believed to elicit anti-oxidant and anti-inflammatory properties [36,204]. Green tea extract (GTE) is the hot water-soluble portion of unfermented *Camellia sinensis* leaves, which contains high levels of polyphenols. The polyphenols in GTE are mainly composed of the catechins: gallocatechin (GC), epigallocatechin (EGC), epicatechin (EC), and epigallocatechin gallate (EGCG) [71,204]. These catechins are strong antioxidants that can quench reactive oxygen species (ROS) such as super oxide radical, singlet oxygen,

hydroxyl radical, peroxyl radical, nitric oxide, nitrogen dioxide, and peroxynitrile [71]. In GTE, EGCG is the most abundant polyphenol, accounting for 30-50% of total polyphenols, and is believed to provide the majority of the beneficial effects observed with green tea consumption [58]. EGCG may lead to decreased inflammation through its antioxidant properties or through other mechanisms. EGCG has been shown to have effects on several signaling pathways including blockade of NF-κB activation by inhibiting IκB kinase (IKK) activity [36,110,160,170,175,220,223].

The antioxidant potential of GTE may be beneficial in treating dystrophic muscle, because oxidative stress is believed to contribute substantially to muscle pathology [164,213]. Evidence suggest that oxidative stress is involved in early disease stages and occurs before disease onset in *mdx* mice [56]. In one study, diets supplemented with GTE (0.01% or 0.05%) were provided to *mdx* breeder pairs and their pups prior to and following weaning. At age 28 days, extensor digitorum longus (EDL) muscles of GTE treated *mdx* pups had significant reductions in areas of necrosis and regeneration [23]. In a separate study, *mdx* mice treated with either GTE (0.05% or 0.25%) or EGCG (0.1%) for one to five weeks after weaning had increased antioxidant capacity, improved contractile properties, and decreased muscle pathology [58]. These studies indicate the GTE and EGCG may provide beneficial CAM modalities for reducing oxidative stress and decreasing dystrophic muscle pathology during early disease stages, however; the role of these polyphenols in altering muscle pathology and inflammation has not been fully characterized. This study represents a detailed time-course characterization of pathological and inflammatory markers at which pre-natal and early GTE treatment of *mdx* mice decreases muscle wasting.

5.2 Methods

5.2.1 Mice

C57BL/6J and *mdx* mice, originally from Jackson Laboratories (Bar Harbor, Maine), were obtained from our colony. Breeding mice and offspring were maintained in a supervised laboratory animal facility in polypropylene shoebox cages. Mice were given free access to public tap water via an automatic watering system, and fed a standard pelleted diet ad libitum. Decaffeinated GTE (90DCF-T; Sunphenon) [polyphenols >80%, catechins >80%, (-)-epigallocatechin-3-gallate (EGCG) >45%, caffeine <1%], was a kind gift from Taiyo International (Minneapolis, MN). *Mdx* breeder pairs were provided standard breeding pelleted diets (7004; Harlan Teklad) with no GTE, 0.25% GTE, or 0.5% GTE. *Mdx* pups (n = 4-6 for each diet and age group) were weaned at age 21 days and then supplied with a standard maintenance diet (2018; Harlan Teklad) containing the same percentage of GTE provided to the breeder pair from which they came. C57BL/6J breeders were fed the standard breeding diet and weaned pups (n = 3-4 for each age group) were fed the maintenance control diet without GTE. The GTE diets correspond to a human consuming ~ 2.5 (0.25% GTE) – 5 (0.5% GTE) grams of GTE a day. Experimental procedures were approved by the Institutional Animal Care and Use Committee of Virginia Polytechnic Institute and State University and met or exceeded requirements of the Public Health Service/National Institutes of Health and the Animal Welfare Act.

5.2.2 Tissue Collection

Mice of each genotype and treatment were selected at random from available cages. For tissue collection and for humane euthanasia, mice were sacrificed by carbon dioxide

narcosis followed by secondary thoracotomy. Blood was collected via cardiac puncture. Tibialis anterior (TA) muscles were removed and were either flash frozen in liquid nitrogen and stored at -80°C or fixed in 10% neutral buffered formalin until prepared for sectioning.

5.2.3 Serum Analysis

Blood collected from mice was placed directly into Microtainer serum separator tubes (Becton Dickinson). Whole blood samples were allowed to clot for 30 minutes at room temperature. The tubes were then centrifuged for 2 minutes at 10,000 x g to separate serum. Serum creatine kinase (CK) assays were performed in the Clinical Pathology Laboratory at Virginia Tech, using an Olympus AU400 chemistry analyzer (Olympus America, Center Valley, PA).

5.2.4 Histological Analysis

Formalin fixed TA muscles were prepared for light microscopy by dehydrating using increasing concentrations of ethanol and xylene as transitional solvents. Tissues were infiltrated with paraffin polymer, sectioned at 3 micrometers, and stained with hematoxylin-eosin (HE) on automated staining equipment. A quantitative analysis of muscle histopathology was performed as follows. Degenerating fibers were identified as swollen eosinophilic, hyalinized, and pyknotic muscle fibers. Regenerating muscle fibers were identified by small diameter, centralized nuclei and basophilic cytoplasm. Necrotic fibers were identified as swollen muscle fibers with disrupted cell membranes, invaded by inflammatory cells. Image analysis software (Image-Pro Plus, Media Cubernetics, Inc. Silver Spring, MD) was used to analyze tissue sections for pathological markers in fields selected with battlement technique from the entire cross section of the TA muscle. A grid

was superimposed over each selected field and the number of intersections that overlay pathological markers was reported as a percent of the total intersections that overlay muscle tissue.

Frozen serial sections 10 micrometers thick were transferred to positively charged slides for immunohistochemical staining. Sections were fixed in 2% formalin for five minutes and rinsed in PBS. Macrophages were identified by staining for anti-F4/80 (1:500; Serotec). After fixation, sections to be stained for NF-κB were permeabilized in 1% Triton X-100, rinsed in PBS, and covered with anti-NF-κB p65 specific for phosphorylated Serine 536 (1:100; Abcam). Sections were incubated with primary antibody overnight at 4°C, rinsed in PBS, and immunodetection was performed using an anti-rat or anti-rabbit IgG labeled with horseradish peroxidase-diaminobenzidine system (R&D Systems). Additional sections were also incubated without primary antibody to ensure the presence of minimal background staining. The sections were then mounted and cover slipped for evaluation. The presence of macrophages and NF-κB staining was quantified using image analysis software (Image-Pro Plus, Media Cubernetics, Inc. Silver Spring, MD).

5.2.5 Statistics

Data were analyzed in a completely randomized design. Differences in muscle histopathology and serum CK were analyzed to determine the significance of the main effects and interactions. For the histopathology time course, the model was analyzed as a 2 X 5 factorial arrangement for genotype (C57BL/6J and *mdx*) versus age (14, 21, 28, 35 and 42 d). For histopathology and serum CK in GTE treatment studies, the model was analyzed as a 2 X 3 factorial arrangement for age (28 and 42 days) versus treatment (0%, 0.25%,

0.5% GTE). To determine the significance of the model, two-way analysis of variance (ANOVA) was performed using the general linear model. When the model was significant, the analysis was followed by Fisher's Least Significant Difference multiple comparisons method (JMP 6.0.2 software. SAS Institute Inc. Cary, NC). Predetermined comparisons between GTE treated *mdx* mice and control *mdx* mice were made using Dunnett's multiple comparisons method. Differences in macrophage infiltration and NF-kB staining between GTE treatment groups were analyzed with one-way ANOVA. When significant differences were detected, Tukey's Honestly Significant Difference post hoc test was used to determine differences between means. Differences for all analyses were considered significant at $P \leq 0.05$ and data were presented as the mean ± standard error.

5.3 Results

5.3.1 Microscopic muscle lesions in *mdx* mice

Muscle histopathology was quantified for *mdx* mice during the initial disease onset stages to further characterize and determine time points that represent early disease progression **(Figure 5.1)**. Systematically selected fields from TA muscles for both C57BL/6J and *mdx* mice were quantified **(Figure 5.2)**. *Mdx* TA muscles had normal fiber morphology at age 14 days, but by age 21 days the percent area of normal fiber morphology was decreased compared to C57BL/6J and was further decreased at age 42 days ($P \leq 0.05$). Degenerating muscle fibers peaked at age 21 days and represented 3.5% of the *mdx* TA area, but declined to lower levels thereafter. Immune cell infiltration of the muscle tissue and necrotic fibers were seen at age 21 days and peaked at age 28 days. At age 28 days immune cell infiltration and necrotic fibers accounted for 3.6% and 1% of

abnormal morphology, respectively. Regenerating muscle fibers were the most abundant histopathological feature accounting for 28% to 61% of the TA area between ages 28 and 42 days. Ages 28 and 42 days were selected as the primary time points for determining the effects of GTE on muscle pathology and inflammation because they represent critical time points in the *mdx* disease process.

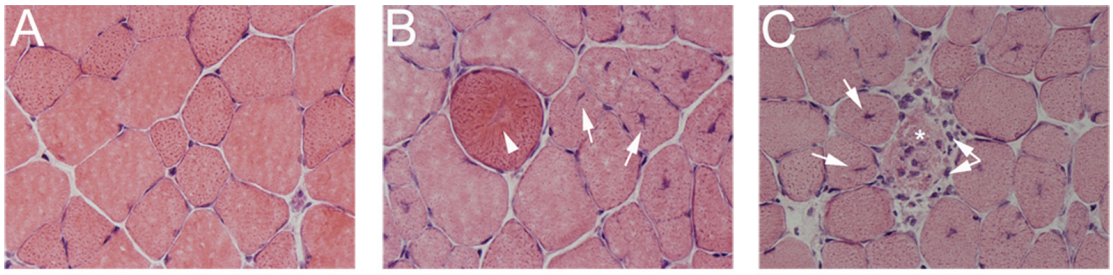

Figure 5.1 – Histopathological features of TA muscles from C57BL/6J and *mdx* mice age 28 days. (A) Normal muscle morphology was seen in C57BL/6J muscle sections. (B and C) Regenerating fibers (arrow), degenerating fibers (arrowhead), necrotic fibers (asterisk) and immune cell infiltration (double arrow) were apparent in *mdx* muscle sections. 400X H&E.

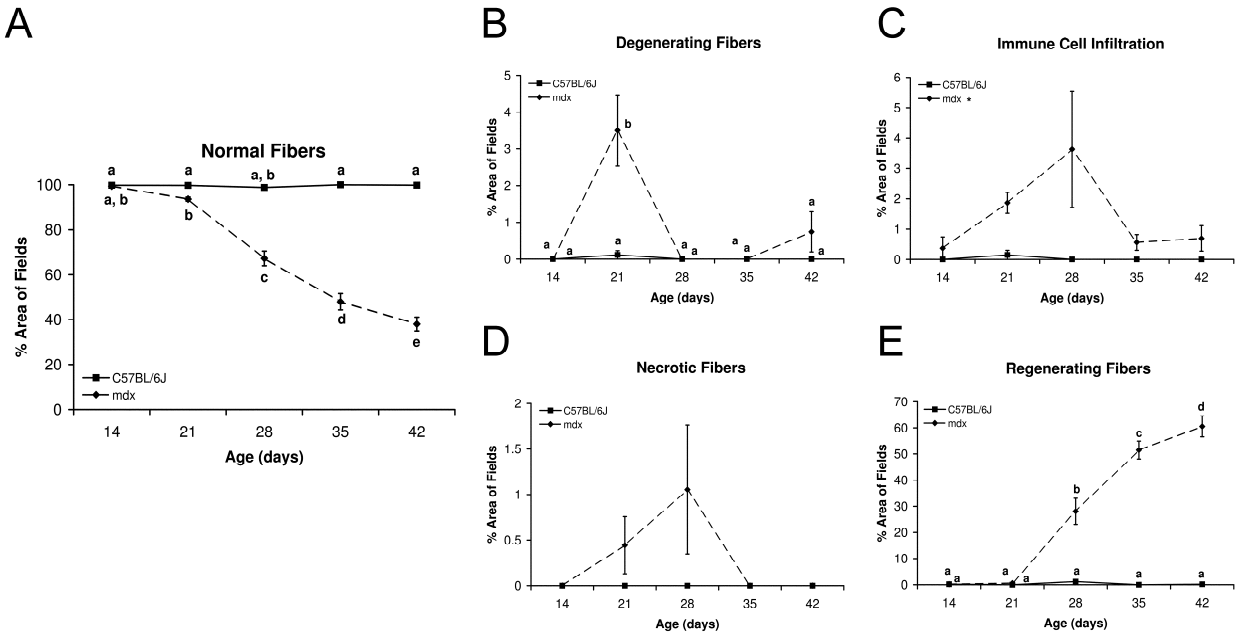

Figure 5.2 – Histopathology time course for C57BL/6J and mdx TA muscles. (A) Fiber morphology appeared normal in *mdx* mice at age 14 days, but by 21 days (B) degenerating fibers and (C) immune cell infiltration were evident, followed by the formation of (D) necrotic fibers and (E) regenerating fibers by age 28 days. Mean values not connected by the same letter were significantly different (P≤0.05). *Mean *mdx* values greater than C57BL/6J (P≤0.05).

5.3.2 GTE treatments in *mdx* mice

Body mass was recorded for treated *mdx* mice and compared to control *mdx* mice to determine how GTE supplementation affected overall health. GTE supplementation did not result in a change in body mass for either treatment when compared to untreated *mdx* mice at either age (Average body mass in grams: 28 day: *mdx* = 13.4, *mdx* 0.25% GTE = 15.9, *mdx* 0.5% GTE = 13.8; 42 day: *mdx* = 21.6, *mdx* 0.25% GTE = 21.8, *mdx* 0.5% GTE = 22.6).

5.3.3 Systemic indicator of muscle damage

Serum CK activity was not decreased in GTE treated mice at age 28 days **(Figure 5.3)**. However, at age 42 days there was a decrease (~83-85%) in 0.25% (1345.5 U/L) and 0.5% (1194.3 U/L) GTE treated *mdx* mice when compared to untreated *mdx* (7896.5 U/L) ($P \leq 0.05$). There was no difference in CK activity for age 28 days when compared to age 42 days. CK activity for GTE treated *mdx* mice was still considerably elevated when compared to C57BL/6J mice (86.8 U/L).

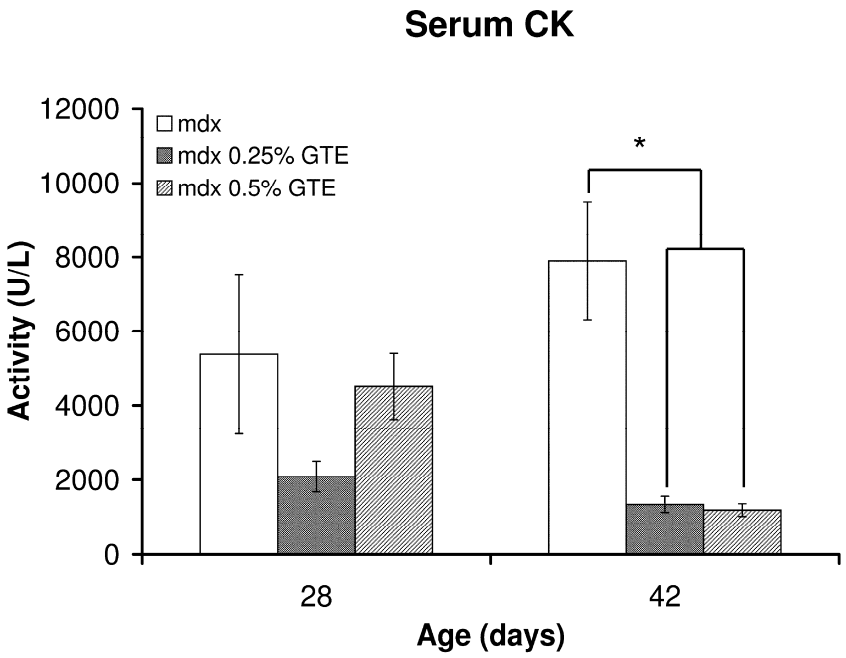

Figure 5.3 – Serum CK for *mdx* and GTE treated *mdx* mice age 28 and 42 days. *Mdx* mice treated with 0.25% or 0.5% GTE had reduced serum CK values when compared to untreated *mdx* mice at age 42 days (P≤0.05). *Mean GTE treated *mdx* values were significantly less than in untreated *mdx* mice.

5.3.4 Muscle lesions in GTE treated *mdx* mice

Histopathological features of GTE treated and untreated *mdx* mice were not different at age 28 days. By age 42 days, 38% of the TA area in untreated *mdx* mice had normal fiber morphology, while 50% and 48% normal morphology was observed for 0.25% and 0.5% GTE treated *mdx* mice, respectively **(Figure 5.4 and Figure 5.5)**. This corresponds to an improvement of 32% (0.25% GTE) and 26% (0.5% GTE) in normal fiber morphology for GTE treated *mdx* mice ($P \leq 0.05$). At age 42 days regenerating fibers were the primary histopathological feature that accounted for 61% of the TA area in untreated *mdx* mice, but only 48% in 0.25%, and 50% in 0.5% GTE treated *mdx* mice. This is a decrease of 21% (0.25% GTE) and 18% (0.5% GTE) in regenerating fibers when compared to untreated *mdx* mice ($P \leq 0.05$). There were no changes in the percent area of immune cell infiltration, necrosis, and degeneration. These markers do not appear to contribute substantially to the increase in normal fiber morphology observed in GTE treated *mdx* mice.

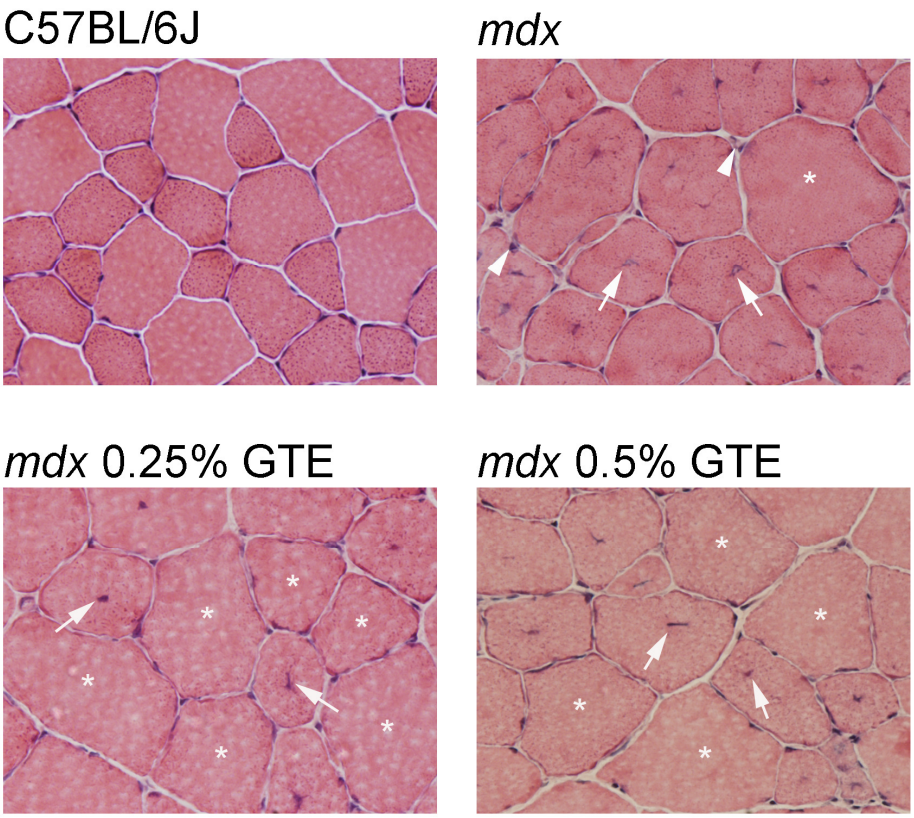

Figure 5.4 – Histopathology of TA muscles for C57BL/6J, *mdx* and GTE treated *mdx* mice age 42 days. C57BL/6J muscle sections depicting normal fiber morphology for this age. Untreated *mdx* sections showing a morphologically normal fiber (asterisks), regenerating fibers (arrow), and immune cell infiltration (arrowhead). Treated *mdx* sections from 0.25% GTE and 0.5% GTE had altered muscle pathology with an increase in morphologically normal fibers (asterisks) and fewer regenerating fibers (arrow). 400X H&E.

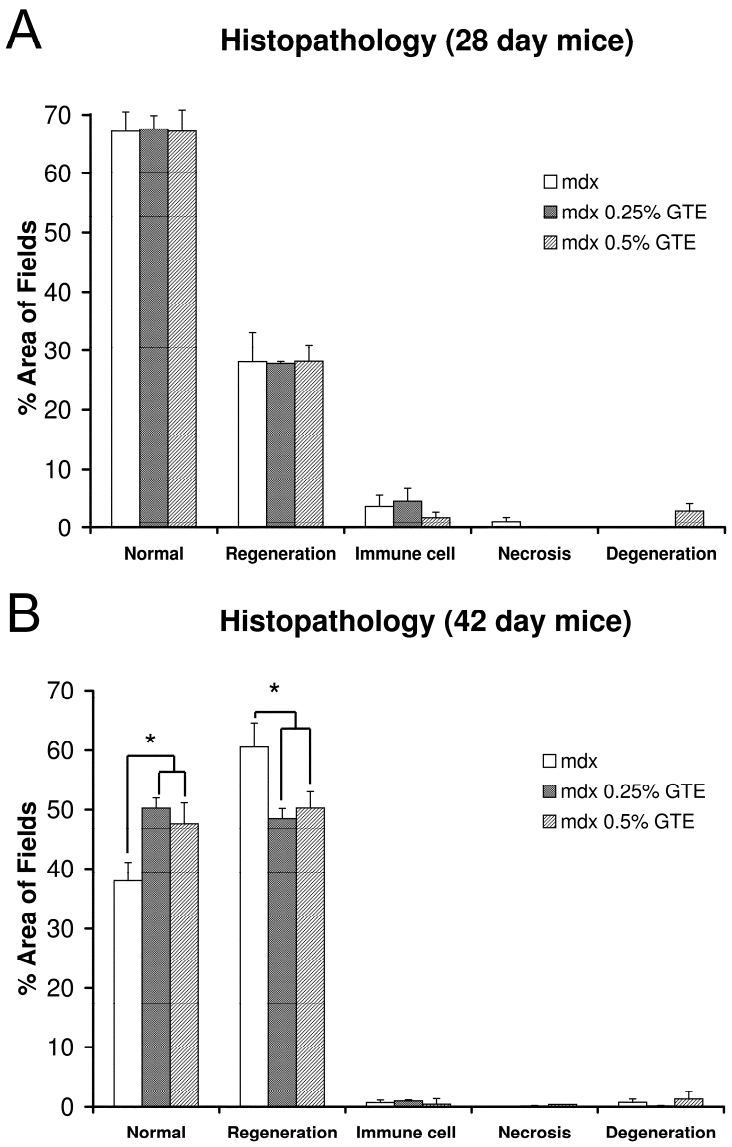

Figure 5.5 – Quantification of histopathology for *mdx* and GTE treated *mdx* TA muscles at ages 28 and 42 days. (A) Although necrotic fibers and fiber degeneration/regeneration were apparent in *mdx* TA muscles by age 28 days, there was no difference in histopathology in GTE treated *mdx* mice compared to untreated *mdx* mice at age 28 days, (B) By age 42 days there was an increase in normal fiber morphology and a decrease in regenerating fibers in GTE treated *mdx* mice ($P \leq 0.05$). *Mean untreated *mdx* values were significantly different compared to treated *mdx* mice.

5.3.5 Macrophage infiltration

Macrophage infiltration is a major histopathological feature of the dystrophic disease processes **(Figure 5.6)**. Infiltrating macrophages are found throughout *mdx* TA muscles with dense foci near necrotic, degenerating and regenerating muscle fibers. GTE is thought to reduce inflammation; however, GTE treatment at 0.25 or 0.5% did not reduce macrophage infiltration in *mdx* mice age 42 days.

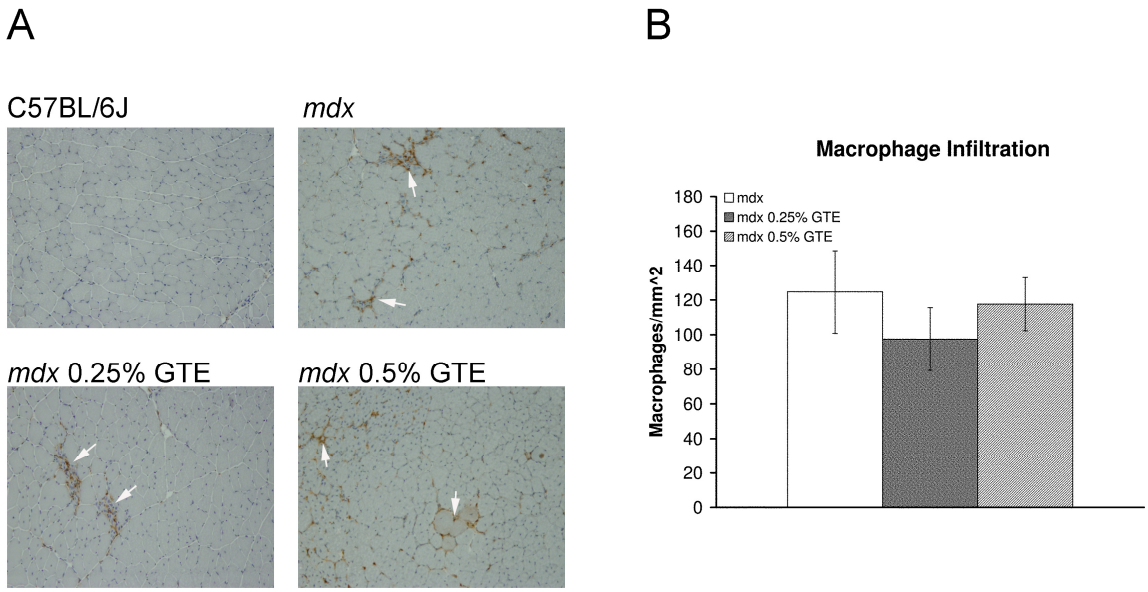

Figure 5.6 – Macrophage infiltration (F4/80) of TA muscles from mice age 42 days. (A) C57BL/6J muscle sections had very few infiltrating macrophages. Untreated *mdx* sections had macrophage infiltration (arrow) throughout with dense foci of macrophages. Treated *mdx* sections from 0.25% GTE and 0.5% GTE had similar macrophage infiltration (arrow) compared to untreated *mdx*. 100X. (B) Quantification of macrophages revealed there was no difference in the number of infiltrating macrophages for GTE treated and untreated *mdx* mice.

5.3.6 NF-κB in necrotic and regenerating fibers

NF-κB is a transcription factor that regulates the expression of many inflammatory genes [144]. An antibody specific for the phosphorylated p65 (p-p65) subunit of NF-κB was used to determine if GTE had an effect on activated NF-κB immunostaining (p-NF-κB) **(Figure 5.7)**. Activated NF-κB is normally sequestered to nuclei; however, in DMD patients necrotic muscle fibers have been reported with cytoplasmic p-NF-kB immunostaining.[130]. In TA muscles from *mdx* mice age 42 days, fibers with cytoplasmic staining were also observed. To confirm that cytoplasmic staining was specific to these fibers, negative control sections were stained without primary antibody. All negative control sections showed minimal background staining, no staining of nuclei, and no fibers with cytoplasmic staining were observed (data not shown). In tissues probed with anti-p-NF-κB, fibers with cytoplasmic staining were typically invaded or surrounded by inflammatory cells that also stained positive for p-NF-κB. The presence of inflammatory cells in and around fibers with cytoplasmic NF-κB staining indicates these muscle fibers were undergoing the process of necrosis. There was no difference in the number of fibers with cytoplasmic NF-κB staining for GTE treated and untreated *mdx* TA muscles at age 42 days (~5 fibers/mm^2 of muscle tissue). As expected, the number of *mdx* fibers with cytoplasmic NF-κB staining was elevated when compared to C57BL/6J control (0.1/mm^2 of muscle tissue). After being phosphorylated, NF-κB enters the nucleus to regulate gene expression. NF-κB has been implicated in muscle fiber regeneration and may contribute to the dystrophic disease process [2]. Nuclei in C57BL/6J mice had little or no immunostaining. Both GTE treated and untreated mice had strong immunostaining in peripheral and centralized nuclei. Strong staining in regenerating fibers was observed for 44% of

centralized nuclei in untreated *mdx*, while only 29% and 30% were observed in 0.25% and 0.5% GTE treated *mdx*, respectively. This was a decrease of 34% (0.25% GTE) and 31% (0.5% GTE) for GTE treated *mdx* mice when compared to untreated *mdx* mice (P≤0.05).

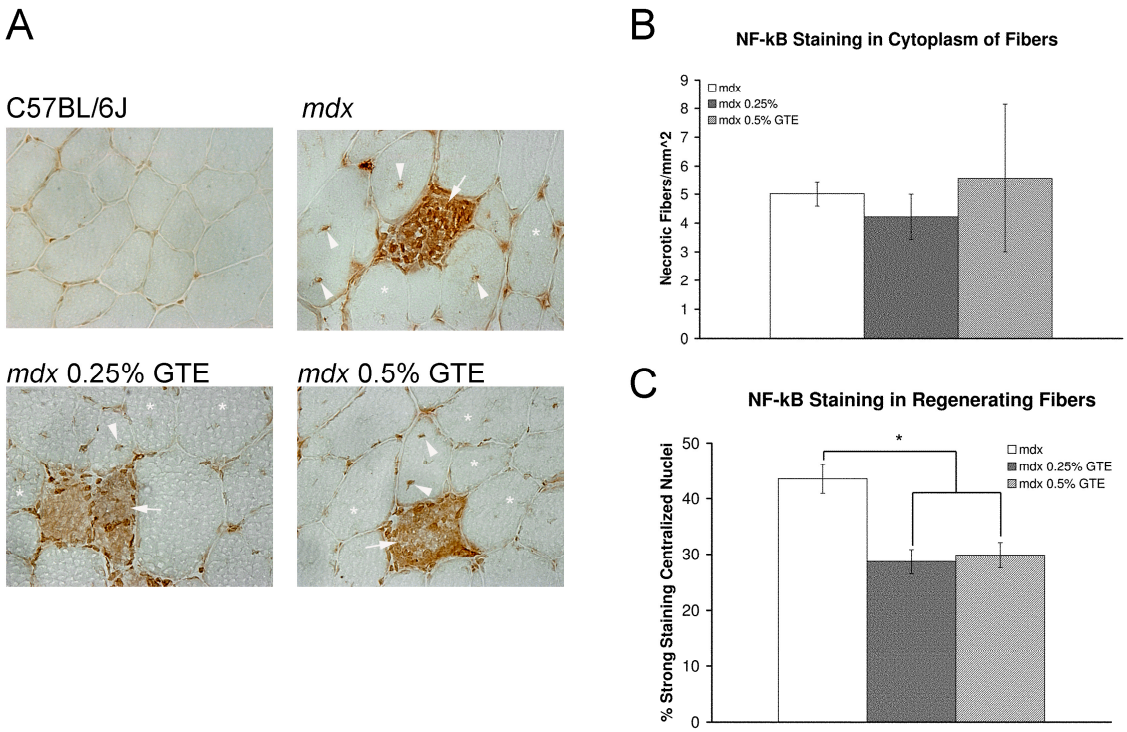

Figure 5.7 – Anit-p-NF-κB (p-p65) staining of TA muscles from mice age 42 days. (A) C57BL/6J muscle sections had no cytoplasmic staining and weak nuclear staining. Untreated *mdx* sections had staining in peripheral nuclei and the cytoplasm of necrotic fibers infiltrated by inflammatory cells (arrow). Regenerating fibers had centralized nuclei with both strong (arrowhead) and weak (asterisk) immunoreactivity. Treated *mdx* sections from 0.25% GTE and 0.5% GTE had the same number of infiltrated necrotic fibers with cytoplasmic staining (arrow), but had a decrease in the percent of regenerating fibers with strong immunoreactivity of centralized nuclei compared to untreated *mdx*. 400X. (B) Quantification of p-NF-κB (p-p65) staining revealed there was no difference in the number of fibers with cytoplasmic staining for GTE treated and untreated *mdx* mice. Cytoplasmic NF-κB staining in muscle fibers was indicative of necrotic fibers. (C) In regenerating fibers, GTE treated *mdx* mice had a decrease in strong centralized nuclear staining (P≤0.05). *Mean GTE treated *mdx* values were significantly less than untreated *mdx* mice.

5.4 Discussion

The objective of this study was to characterize and identify distinct features of dystrophic muscle pathology during the early disease time course and determine what features of dystrophic muscle pathology were reduced by pre-natal and early dietary intervention with GTE. Recent studies have relied on the percent area of centrally nucleated fibers and the area of necrotic muscle tissue to assess changes in muscle pathology and often combine these features to determine overall affected muscle tissue [23,58,84,90,126,127,136,161,193,210]. However, these studies have not discriminated the percent area of the individual fibers undergoing the histopathologically identifiable processes of degeneration, necrosis or regeneration. Therefore, it is important to note that whole muscle tissue necrosis/degeneration values that are often reported are not the same as the percent area of fiber necrosis or fiber degeneration reported here. One limitation to this approach is that the total area of tissue necrosis may not be fully realized. To compensate for this limitation, areas of immune cell infiltration where there was ongoing tissue necrosis outside of intact fibers were also measured as a separate histopathological marker and quantification of the number of infiltrating macrophages was also reported.

The time course of histopathology shows that the percent area of normal fiber morphology is the same for C57BL/6J and *mdx* TA muscles at age 14 days, but by age 21 days there is a decrease in the percent area of normal fibers for *mdx*. This time point represents the onset of disease for the *mdx* mouse. Normal fiber morphology at all other ages analyzed was decreased for the *mdx* mouse. The percent area of muscle fiber necrosis, degeneration, and immune cell infiltration represent important features of the disease process between ages 21 and 28 days, but overall account for only small percentages of the

abnormal fiber morphology (~4.5-6%). The percent area of regenerating fibers represents the largest portion of abnormal fiber morphology at ages 28 (28%) to 42 (61%) days. The large percent area of regenerating fibers compared to other histopathological features indicates that the regenerative process is a substantial contributor to dystrophic muscle pathology. Studies detailing the process of muscle regeneration have shown that in damaged muscle tissue, fibers are capable of returning to normal fiber morphology; however, many regenerated fibers retain centrally located nuclei indefinitely [46,131,171,201]. The persistence of centrally located nuclei is believed to signify that abnormal processes are occurring in these cells that prevent the nuclei from returning to the periphery of the cell [46,131,171,201]. From this initial analysis, it was determined that for the GTE treatments muscle pathology should be examined at ages 28 and 42 days because these time points represent the early degenerative and regenerative disease stages.

Serum CK is a systemic indicator of muscle pathology. CK is normally restricted to the cytoplasm of muscle fibers, but when the fibers are damaged it is released into the serum. Serum CK was not different for GTE treated *mdx* mice compared to untreated *mdx* at age 28 days, but at age 42 days there was an improvement in GTE treated *mdx* mice. Similarly, there was no difference in normal fiber morphology for GTE treated and untreated *mdx* mice at age 28 days; however, at age 42 days there was an improvement for GTE treated *mdx* mice. There was up to a 32% increase in normal fiber morphology for these mice. The increase in normal fiber morphology was largely accounted for by up to a ~21% decrease in regenerating fibers. Other histopathological features were unchanged by GTE treatments. Collectively this data indicates that overall muscle pathology was decreased in GTE treated *mdx* mice.

To further assess how GTE treatments modulate inflammation; macrophages and NF-κB immunostaining were quantified. There was no difference in the number of macrophages infiltrating the TA muscles in GTE treated or untreated *mdx* mice. Although GTE is believed to have anti-inflammatory properties, it does not appear to decrease the number of infiltrating macrophages in *mdx* mice at age 42 days. However, a recent study reported that muscle from *mdx* mice contains two subpopulations of macrophages, M1 and M2 [207]. M1 macrophages are thought to be cytotoxic and pro-inflammatory while M2 macrophages inhibit the cytotoxicity of M1 macrophages and promote muscle regeneration. In *mdx* mice there was a shift in the macrophage phenotype to the regenerative subset between age 4 weeks and 12 weeks [207]. Although there was no change in the overall number of infiltrating macrophages in GTE treated *mdx* mice age 42 days, one possibility is that GTE induces a shift in the phenotype of infiltrating macrophages. If GTE treatments did contribute to a shift in macrophage phenotype from M1 to M2 without affecting the total numbers of macrophages, it could result in an improved regenerative process. However, further studies are needed to address this possibility.

A component of GTE, EGCG, has been reported to inhibit IKK activity which results in inhibition of NF-κB [36,160,175,220]. Acharyya et al. recently reported *mdx* muscles lacking IKKβ, a subunit of the IKK complex, have an increase in regenerative capacity when compared to control *mdx* [2]. They also found that *mdx* muscles with macrophages lacking IKKβ had decreased muscle pathology and a decrease in the expression of pro-inflammatory makers [2]. Their data suggest a mechanism through which NF-kB signaling in macrophages and regenerating muscle fibers promotes degeneration and represses regeneration [2]. Several studies have reported an increase in the number of regenerating

fibers after treatments that reduce or block NF-κB activity while others have reported a decrease in regenerating fibers [2,126,127,145,214]. These differing results may stem from the way in which the NF-κB pathway is altered by treatment compounds and the methods used to administer these compounds (i.e. age of treatment initiation and termination, route of administration). Our findings indicate that prenatal and early dietary GTE treatment reduces the amount of regenerating fibers potentially through alterations in NF-κB signaling. Past studies have also shown a decrease in muscle necrosis when NF-κB activity is inhibited [2,126,127]. Our results indicate that the amount of fiber necrosis is unchanged by GTE treatment. Additionally, the number of fibers with cytoplasmic NF-κB immunostaining was unchanged by the GTE treatment. The presence of inflammatory cells infiltrating fibers with cytoplasmic NF-κB staining signifies these muscle fibers were undergoing necrosis. These findings suggest that while muscle degeneration and necrosis initiates the process of muscle wasting, impaired muscle regeneration plays a key role in the progression of muscular dystrophy [2,126,127].

GTE has been shown in several studies to decrease serum CK levels and muscle pathology while increasing force output, and endurance capacity in *mdx* mice [23,26,58,136]. The antioxidant properties of GTE are believed to be the primary element responsible for these improvements, other signaling pathways may also be responsible. Previous reports have shown that GTE treatment can result in a significant decrease in muscle pathology [23,58], which is supported by this study. However, past studies did not discriminate the different pathological markers that were reported here, including the finding that the primary change was in the percent area of regenerating fibers. In this and a previous study we reported that serum CK was decreased with pre-natal and early GTE treatment [26].

Serum CK is an indicator of the extent of muscle damage and a significant decrease of this marker indicates that GTE is having an important impact on dystrophic muscle pathology. Additionally, no other studies have attempted to determine the effect of dietary GTE on inflammation. Although no change in infiltrating macrophages was observed, a decrease in NF-κB immunostaining in regenerating fibers was observed. NF-κB is a known regulator of inflammatory genes and may play an important role in the dystrophic disease process and the recruitment of inflammatory cells. A role for GTE in the suppression of inflammation may prove to be important to decrease *mdx* muscle pathology.

CAM approaches, including the use of anti-inflammatory botanicals in general and GTE in particular, may lead to the amelioration of DMD and provide important insight into disease processes. CAM interventions can be used in conjunction with conventional therapies in a cost-effective manner to improve disease prognosis. GTE treatments of *mdx* mice resulted in increased normal fiber morphology, decreased regenerating fibers, and decreased NF-κB staining in regenerating fibers. The detailed histopathological analysis revealed that changes in the percent area of degenerating fibers, necrotic fibers, and immune cell infiltration were small in comparison to the change in regenerating fibers. These data indicates that GTE decreases NF-κB activity in regenerating fibers which may result in changes in the regenerative process leading to an increase in normal fiber morphology. Detailed muscle histopathology for pre-natal and early GTE treated *mdx* mice has not been previously reported and reveals that GTE may be an additional treatment option to decrease early muscle pathology for this incurable disease. In conclusion, GTE decreases muscle pathology potentially by suppressing NF-κB activity in regenerating fibers of *mdx* mice. While GTE did not decrease overall immune cell or macrophage

infiltration, additional studies are needed to examine the role of GTE in modulating the shift of macrophage towards and M2 phenotype and thereby ameliorate the dystrophic disease process by favoring anti-inflammatory responses.

Chapter 6 Epigallocatechin gallate decreases muscle pathology and NF-κB immunostaining in regenerating muscle fibers of *mdx* mice

Nicholas P. Evans[a], Jarrod A. Call[b], Josep Bassaganya-Riera[c], John L. Robertson[d], and Robert W. Grange[a]

[a] Department of Human Nutrition, Foods and Exercise, Virginia Polytechnic Institute and State University, Blacksburg, Virginia 24061, USA

[b] Rehabilitation Sciences, Medical School, University of Minnesota, Minneapolis, Minnesota 55455, USA

[c] Nutritional Immunology & Molecular Nutrition Laboratory, Virginia Bioinformatics Institute, Virginia Polytechnic Institute and State University, Blacksburg, Virginia 24061, USA

[d] Department of Biomedical Sciences and Pathobiology, Virginia Polytechnic Institute and State University, Blacksburg, Virginia 24061, USA

[*]Correspondence to Nicholas P. Evans, Department of Human Nutrition, Foods and Exercise, Virginia Polytechnic Institute and State University, 338 Wallace Hall, Blacksburg, Virginia 24061, USA

Abstract

BACKGROUND & AIMS: Duchenne muscular dystrophy is an inherited muscle wasting disease that results in early death of afflicted boys. Mutations in the dystrophin gene result in massive muscle degeneration and inflammation that lead to a loss of muscle function. The purpose of this study was to determine if epigallocatechin gallate was the primary component of green tea extract responsible for decreased dystrophic muscle pathology and inflammation in *mdx* mice. METHODS: C57BL/6J and *mdx* mice were fed a purified AIN-93G diet containing either 0% or 0.1% epigallocatechin gallate. Serum creatine kinase was assessed as a systemic indicator of muscle damage. Quantitative histopathological and immunohistochemical techniques were used to determine muscle pathology, macrophage infiltration, and NF-κB localization. RESULTS: Early treatment of *mdx* mice with epigallocatechin gallate did not decrease serum creatine kinase; however, the area of normal fiber morphology was increased by ~20% ($P \leq 0.05$) over ages 28 and 42 days. The primary histopathological change was a ~21% decrease in the area of regenerating fibers at age 42 days ($P \leq 0.05$). NF-κB staining in regenerating muscle fibers was also decreased in epigallocatechin gallate treated *mdx* mice when compared to untreated *mdx* mice. CONCLUSION: Epigallocatechin gallate decreases dystrophic muscle pathology potentially by regulating NF-κB activity in regenerating muscle fibers and appears to be the foremost component of green tea extract responsible for these changes.

6.1 Introduction

Duchenne muscular dystrophy (DMD) results from mutations in the dystrophin gene located on the X-chromosome. Consequently, this disease primarily affects boys and is reported to afflict approximately one in 3500 [19,197]. Mutations in the dystrophin gene lead to the absence of the dystrophin protein and the loss of the dystrophin glycoprotein complex (DGC) at the sarcolemma of muscle fibers [19,197]. The DGC is believed to provide a link between the extracellular matrix and the cytoskeleton of muscle fibers which regulates signaling pathways and sarcolemmal integrity [192]. Without the DGC muscle fibers become susceptible to degeneration and necrosis. Although the muscle fibers are capable of regeneration, DMD patients ultimately succumb to severe muscle wasting leading to death by age 30 years [19,64].

Complimentary and alternative medicine (CAM) approaches, including extracts from the green tea plant, are being investigated as potential treatment options for DMD [23,26,58,136]. Green tea extract (GTE) is derived from the unfermented leaves of the green tea plant [71,204]. GTE is composed of the catechins: gallocatechin (GC), epigallocatechin (EGC), epicatechin (EC), and epigallocatechin gallate (EGCG) [71,204]. EGCG is the predominant polyphenol comprising 30-50% of the total polyphenols in GTE [58]. Both GTE and purified EGCG have been used to successfully reduce muscle pathology in the *mdx* mouse model of DMD [23,26,58,136]. The effectiveness of GTE and EGCG to improve muscle wasting in the *mdx* mouse has mostly been attributed to their antioxidant potential; however, other potential mechanisms have not been fully explored.

Both GTE and EGCG appear to have an effect on NF-κB activity. As previously reported, early treatment with GTE decreases *mdx* muscle pathology by decreasing NF-κB staining in regenerating fibers and as a result, appears to improve the regeneration process. EGCG has been reported to inhibit IκB kinase (IKK) activation and thereby block NF-κB activity [36,175,220]. The role of GTE in improving *mdx* muscle pathology and reducing NF-κB signaling in regenerating fibers has not been fully elucidated; however, it is possible that EGCG is responsible for these positive changes. The objective of this study was to determine if EGCG could similarly decrease muscle pathology in *mdx* mice and to further characterize the role of this molecule on inflammation, regeneration, and NF-kB regulation.

6.2 Methods

6.2.1 Mice

C57BL/6J and *mdx* mice were originally obtained from Jackson laboratories (Bar Harbor, Maine). Breeding mice and offspring from our colony were maintained in a supervised laboratory animal facility in polypropylene shoebox cages. Mice were given free access to public tap water via an automatic watering system, and fed a purified pelleted diet (AIN-93G; Harlan Teklad) **(Table 6.1)**. EGCG (EGCg; Sunphenon) [(-)-epigallocatechin-3-gallate (EGCG) 96.9%, caffeine 0.1%], was a kind gift from Taiyo International (Minneapolis, MN). C57BL/6J *and mdx* breeder pairs were provided the AIN-93G pelleted diet without EGCG. *Mdx* pups were weaned at age 18 days and then provided an AIN-93G pelleted diet containing either 0% EGCG or 0.1% EGCG. In the previous study, the GTE used contained ~40-50% EGCG (see Chapter 5). Therefore, the diet containing 0.1% EGCG represents the approximate amount of EGCG contained in the

0.25% GTE diet. The purified AIN-93G diets were chosen for this study because they meet the nutritional requirements required for growth and they limit variability related to unpurified diet formulas [166]. The 0.1% EGCG diet corresponds to a human consuming ~ 1 gram of EGCG a day. Ages 28 and 42 days were investigated to parallel the previous GTE-*mdx* study (see Chapter 5). EGCG was only provided to mice after being weaned at age 18 days, which is still considered pre-disease onset for *mdx* mice. This protocol allows for detection of changes directly related to dietary intervention provided to the mice with out the compounding effects that may occur in dams. Additionally, both *mdx* and C57BL/6J mice were provided with the diet containing EGCG and the control diet, allowing for the detection of interactions related to genotype. Experimental procedures were approved by the Institutional Animal Care and Use Committee of Virginia Polytechnic Institute and State University and met all requirements of the Public Health Service/National Institutes of Health and the Animal Welfare Act.

Table 6.1 - Composition of purified diets[a].

Ingredient	Control Diet (g/kg)	EGCG Diet (g/kg)
Casein	200.0	200.0
L-Cystine	3.0	3.0
Corn Starch	397.486	396.456
Maltodextrin	132.0	132.0
Sucrose	100.0	100.0
Soybean Oil	70.0	70.0
Cellulose	50.0	50.0
Mineral Mix (AIN-93G)[b]	35.0	35.0
Vitamin Mix (AIN-93G)[c]	10.0	10.0
Choline Bitartrate	2.5	2.5
Tert-Butylhydropuinone (TBHQ)	0.014	0.014
Epigallocatechin gallate	-	1.03

[a] Provides 18.8% protein, 63.9% carbohydrates, and 17.2% fat for each kilocalorie (Kcal) and 3.8 Kcal per gram of diet.
[b] Supplied per kg of vitamin mix: 3g niacin, 1.6g calcium pantothenate, 0.7g pyridoxine HCL, 0.6g thiamine HCL, 0.6g riboflavin, 0.2g folic acid, 0.02g biotin, 2.5g vitamin B_{12} (0.1% in mannitol), 15g vitamin E (DL-α-tocopheryl acetate, 500 IU/g), 0.8g vitamin A palmitate (500,000 IU/g), 0.2g vitamin D_3 (cholecalciferol, 500,000 IU/g), 0.075g vitamin K (phylloquinone), and 974.705 g sucrose.
[c] Supplied per kg of mineral mix: 357g calcium carbonate, 196g potassium phosphate monobasic, 70.87g potassium citrate, 74g sodium chloride, 46.6g potassium sulfate, 24.3g magnesium oxide, 6.06g ferric citrate, 1.65g zinc carbonate, 0.63g manganous carbonate, 0.31g cupric carbonate, 0.01g potassium iodate, 0.01025g sodium selenate, 0.00795g ammonium paramolybdate, 1.45g sodium meta-siliate, 0.275g chromium potassium sulfate, 0.0174g lithium chloride, 0.0815g boric acid, 0.0635g sodium fluoride, 0.0318g nickel carbonate hydroxide tetrahydrate, 0.0066g ammonium vanadate, and 220.716 g sucrose.

6.2.2 Tissue Collection

Mice of each genotype were selected at random from available cages. For tissue collection, mice were sacrificed by carbon dioxide asphyxiation followed by thoracotomy. The thoracic cavity was opened to reveal the heart. Blood was collected via cardiac puncture. Tibialis anterior (TA) muscles were flash frozen in liquid nitrogen and then stored at -80°C until analyzed.

6.2.3 Serum Analysis

Blood collected from mice was placed directly into Microtainer serum separator tubes (Becton Dickinson). Whole blood samples were allowed to clot for 30 minutes at room temperature. The tubes were then centrifuged for 6 minutes at 6,000 x g to separate serum. Serum creatine kinase assays were performed in the Clinical Pathology Laboratory at Virginia Tech, using an Olympus AU400 chemistry analyzer (Olympus America, Center Valley, PA).

6.2.4 Histological Analysis

Frozen TA muscles were sectioned with hematoxylin-eosin (H&E) as previously described (see Chapter 5). A quantitative analysis of muscle pathology was performed as follows. Degenerating fibers were identified as swollen eosinophilic, hyalinized, and pyknotic muscle fibers. Regenerating muscle fibers were identified by their small size compared to normal fibers and presence of centralized nuclei. Necrotic fibers were identified as swollen muscle fibers with disrupted cell membranes, invaded by inflammatory cells. Myotubes were recognized by their small diameter when compared to

regenerating fibers, plump centralized nuclei, and basophilic staining. Image analysis software (Image-Pro Plus, Media Cubernetics, Inc. Silver Spring, MD) was used to analyze tissue sections as previously described (see Chapter 5).

Immunohistochemical staining was performed on sections to determine macrophage infiltration and NF-κB localization in muscle tissue as previously described (see Chapter 5). Macrophages were identified by staining for anti-F4/80 (1:500; Serotec). NF-κB immunolocalization was determined by anti-NF-κB p65 specific for phosphorylated Serine 536 (1:100; Abcam). Immunodetection was performed using an anti-rat or anti-rabbit IgG labeled with horseradish peroxidase-diaminobenzidine system (R&D Systems). Control sections were incubated without primary antibody to ensure the presence of minimal background staining. The presence of macrophages and NF-κB staining was quantified using image analysis software (Image-Pro Plus, Media Cubernetics, Inc. Silver Spring, MD).

6.2.5 Statistics

Data were analyzed in a completely randomized design. Analysis of variance (ANOVA) was used to determine the main effects of age, genotype, or treatment and any interactions. Differences in food consumption and body mass were analyzed as a three-way repeated measures factorial arrangement for genotype, treatment, and time. Serum CK, normal fiber morphology, and macrophage infiltration were analyzed as a three-way factorial arrangement for genotype, treatment, and age. Histopathology was analyzed as a two-way factorial arrangement for genotype and treatment. NF-kB staining in regenerating fibers of *mdx* mice was analyzed as a two-way factorial arrangement for age and treatment.

When the model was significant, the analysis was followed by Tukey's honestly significant difference multiple comparisons method (JMP 6.0.2 software. SAS Institute Inc. Cary, NC). Differences for all analyses were considered significant at $P \leq 0.05$ and data were presented as the mean ± standard error.

6.3 Results

6.3.1 Food consumption and body mass

Food consumption and body mass were recorded for C57BL/6J and *mdx* EGCG-treated and *mdx* control mice throughout the study **(Figure 6.1)**. There was an interaction in food consumption for genotype x time ($P \leq 0.05$) and treatment x time ($P \leq 0.05$), but no difference in the genotype x treatment x time interaction. Between ages 18 and 28 days there was a significant difference in food consumed by EGCG treated *mdx* mice and control *mdx* mice ($P \leq 0.05$). However, between ages 28 and 42 days there was no difference in the amount of food consumed. Between ages 28 and 42 days *mdx* mice ate less than C57BL/6J mice ($P \leq 0.05$). There was an interaction in body mass for genotype x time ($P \leq 0.05$) with no difference in treatment x time or genotype x treatment x time. Although *mdx* mice consumed less food than C57BL/6J mice, between ages 28 and 42 days, their body masses were increased compared to C57BL/6J ($P \leq 0.05$).

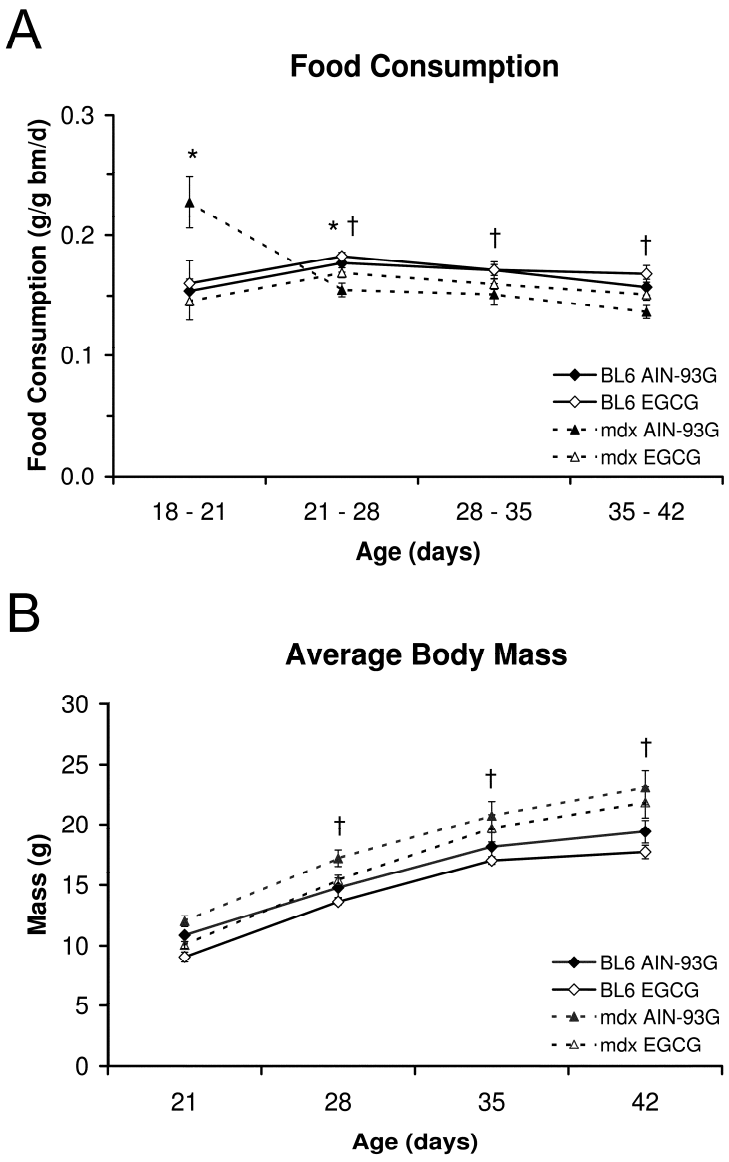

Figure 6.1 - Food consumption and body mass. (A) There was an interaction in food consumption for genotype x time (P≤0.05) and treatment x time (P≤0.05), with no difference in genotype x treatment x time. (B) For body mass, there was an interaction for genotype x time (P≤0.05) with no difference in treatment x time or genotype x treatment x time. *Mean *mdx* EGCG treated values significantly different than control *mdx* at a given age. †Mean *mdx* values significantly different compared to C57BL/6J at a given age.

6.3.2 Systemic indicator of muscle damage

For serum CK, there was a genotype effect (P≤0.05), but no other effects or interactions **(Figure 6.2)**. Serum CK activity was elevated in *mdx* mice (age 28 days: ~3500-4900 U/L; age 42 days: ~5500 U/L) when compared to C57BL/6J mice (age 28 days: ~200-400 U/L; age 42 days: ~380-580 U/L) (P≤0.05).

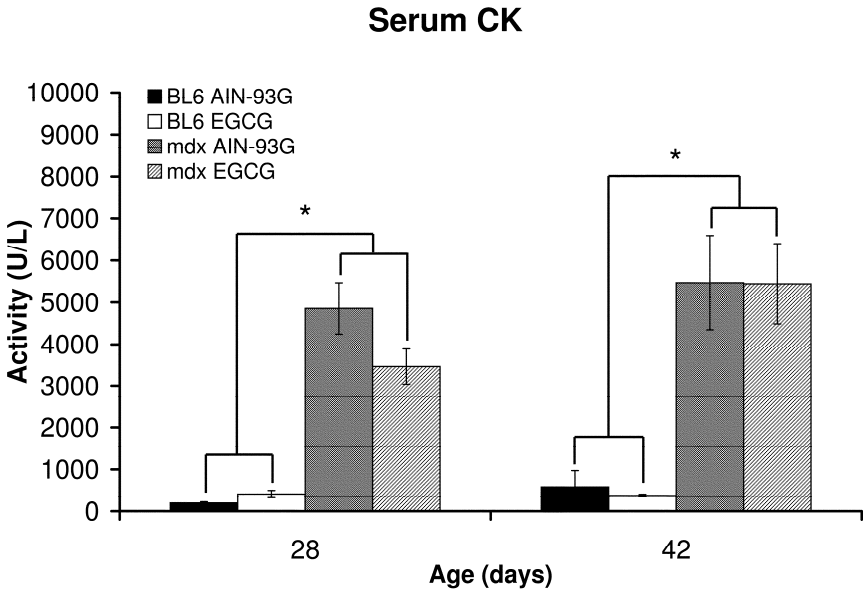

Figure 6.2 - Serum CK for EGCG treated and untreated C57BL/6J and *mdx* mice. *Mdx* mice had elevated serum CK levels compared to C57BL/6J mice at age 28 and 42 days (P≤0.05). However, EGCG treatment did not reduce serum CK for *mdx* mice at either age. *Mean *mdx* values were significantly increased compared to C57BL/6J values.

6.3.3 Muscle lesions in EGCG treated mdx mice

At both ages 28 and 42 days, TA muscles of *mdx* mice had considerable histopathological features which included necrotic fibers, degenerating fibers, regenerating fibers, immune cell infiltration and myotubes **(Figure 6.3)**. For normal fiber morphology,

there was a genotype x treatment interaction (P≤0.05), but no age effect or other interactions. In *mdx* mice, the percent area of normal fiber morphology (age 28 days: ~58%; age 42 days: ~52%) was decreased compared to C57BL/6J mice (age 28 and 42 day: ~99%) (P≤0.05). EGCG-treated *mdx* mice (age 28 days: ~63%; age 42 days: ~55%) had an increase of 20% in normal fiber morphology compared to control *mdx* mice (age 28 days: ~53%; age 42 days: ~46%) (P≤0.05). At age 28 days, there was a genotype effect for regenerating fibers and immune cell infiltration (P≤0.05) but, there were no other effects or interactions for any of the histopathological features. For *mdx* mice, the percent area of regenerating fibers and immune cell infiltration (regenerating fibers: ~30%; immune cell infiltration: ~4-9%) were increased compared to C57BL/6J (regenerating fibers and immune cell infiltration: <1%) (P≤0.05). At age 42 days there was a genotype effect for immune cell infiltration (P≤0.05) and a genotype x treatment interaction for regenerating fibers (P≤0.05). There were no other effects or interactions for any of the histopathological features. In *mdx* mice (regenerating fibers: 41-50%; immune cell infiltration: ~2.5%) the percent area of regenerating fibers and immune cell infiltration were increased compared to C57BL/6J mice (regenerating fibers: 0%; immune cell infiltration: 0%) (P≤0.05). Additionally, EGCG-treated *mdx* mice (~41%) had a decrease of ~21% in the percent area of regenerating fibers compared to control *mdx* (~51%) (P≤0.05).

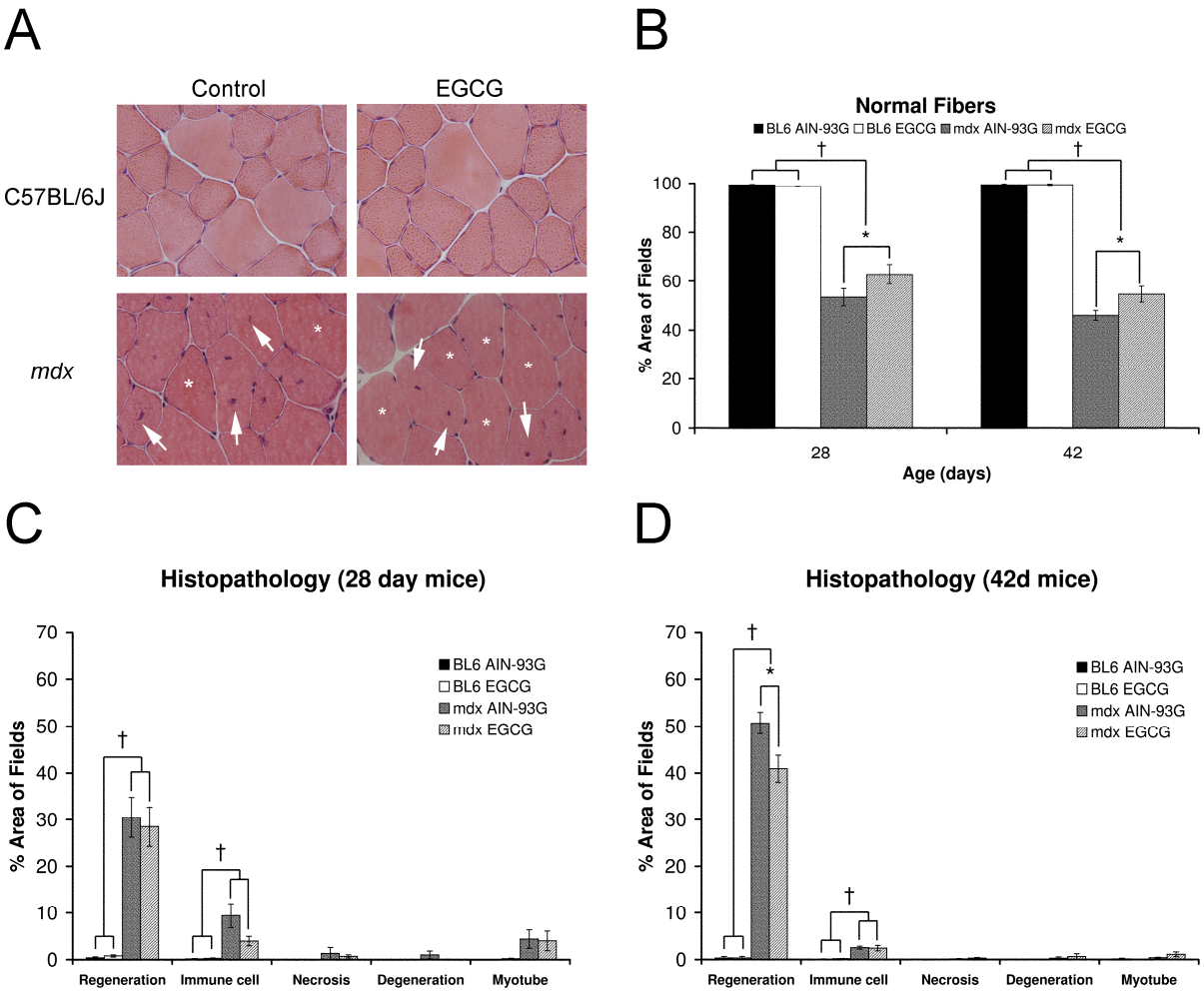

Figure 6.3 - TA muscle histopathology for EGCG treated and untreated C57BL/6J and *mdx* mice. (A) At age 42 days both control and EGCG treated C57BL/6J mice showed typical muscle fiber morphology. Control *mdx* and EGCG treated *mdx* sections both had morphologically normal fibers (asterisks) and regenerating fibers (arrow); however, treated mice had decreased regenerating fibers and increased normal fibers. 400X H&E. (B) Although normal fiber morphology was decreased for *mdx* mice compared to C57BL/6J at both ages (P≤0.05), EGCG treated *mdx* mice had an increase in normal fiber morphology compared to untreated *mdx* mice (P≤0.05). (C) At age 28 days regenerating fibers and immune cell infiltration in *mdx* mice were increased compared to C57BL/6J (P≤0.05). (D) At age 42 days both regenerating fibers and immune cell infiltration were increased in *mdx* mice compared to C57BL/6J (P≤0.05); however, EGCG treated *mdx* mice had a decrease in regenerating fibers compared to control *mdx* mice (P≤0.05). *Mean EGCG treated *mdx* values were significantly different compared to control *mdx* values. †Mean C57BL/6J values were significantly different compared to *mdx* values.

6.3.4 Macrophage infiltration

Foci of macrophages were evident in *mdx* TA muscles at ages 28 and 42 days near necrotic, degenerating and regenerating fibers **(Figure 6.4)**. Although there was a genotype and age effect (P≤0.05), there was not a treatment effect or any interactions. C57BL/6J mice (age 28 days: ~7-9 macrophages/mm^2; age 42 days: ~1-2 macrophages/mm^2) had less macrophage infiltration compared to *mdx* mice (age 28 days: ~170-220 macrophages/mm^2; age 42 days: ~68-78 macrophages/mm^2) (P≤0.05). At age 28 days, macrophage infiltration was greater than at age 42 days (P≤0.05). However, EGCG treatment did not decrease macrophage infiltration.

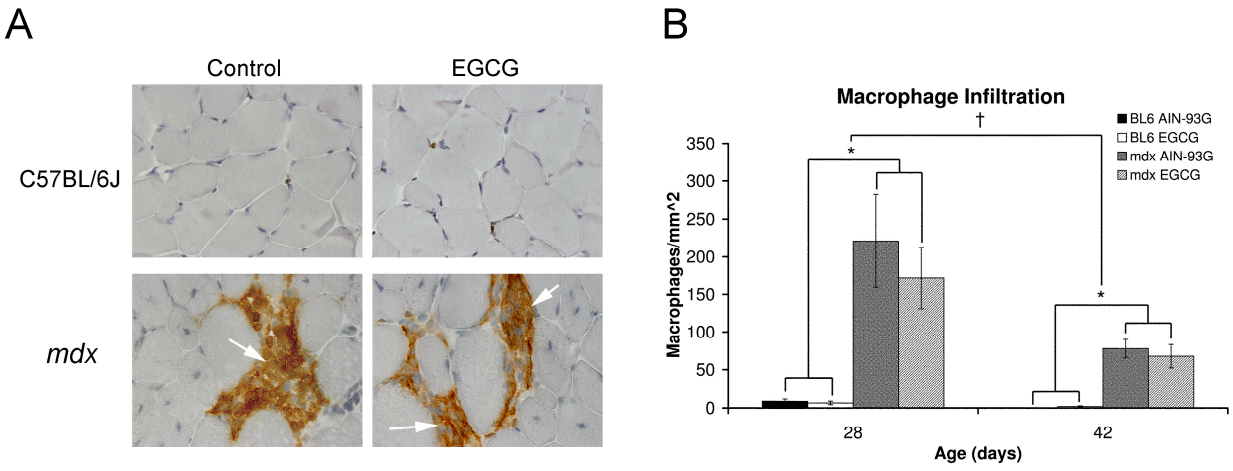

Figure 6.4 - Macrophage infiltration (F4/80) of TA muscles. (A) At age 42 days, C57BL/6J mice had very infiltrating macrophages. Both control and EGCG treated *mdx* mice had macrophages throughout the TA with dense foci (arrow) near necrotic, degenerating, and regenerating fibers. 400X (B) Macrophage infiltration was greater in *mdx* mice compared to C57BL/6J at both ages (P≤0.05); however, the EGCG treatment did not result in a decrease in macrophage infiltration for *mdx* mice. *Mean C57BL/6J values were significantly less than *mdx* values. †Macrophage infiltration was significantly greater at age 28 days compared to age 42 days.

6.3.5 NF-κB in necrotic and regenerating fibers

NF-κB staining was apparent in necrotic muscle fibers, in the nuclei of regenerating muscle fibers, and in inflammatory cells of *mdx* mice at ages 28 and 42 days **(Figure 6.5)**. There was a genotype effect for NF-κB staining in necrotic fibers ($P \leq 0.05$), but there were no other effects or interactions. In *mdx* mice (ages 28 and 42 days: ~3.0-5.5 necrotic fibers/mm^2), the number of necrotic fibers with cytoplasmic staining was increased compared to C57BL/6J (ages 28 and 42 days: <1 necrotic fiber/mm^2) ($P \leq 0.05$). For NF-κB staining in regenerating fibers, there was an interaction for treatment x age ($P \leq 0.05$). NF-κB staining in regenerating fibers of *mdx* mice at age 28 days was increased compared to at age 42 days ($P \leq 0.05$). At age 42 days, EGCG treated *mdx* mice (~34% strong staining in centralized nuclei) had a decrease of 21% in staining of regenerating fibers compared to control *mdx* mice (~43% strong staining in centralized nuclei) at age 42 days ($P \leq 0.05$).

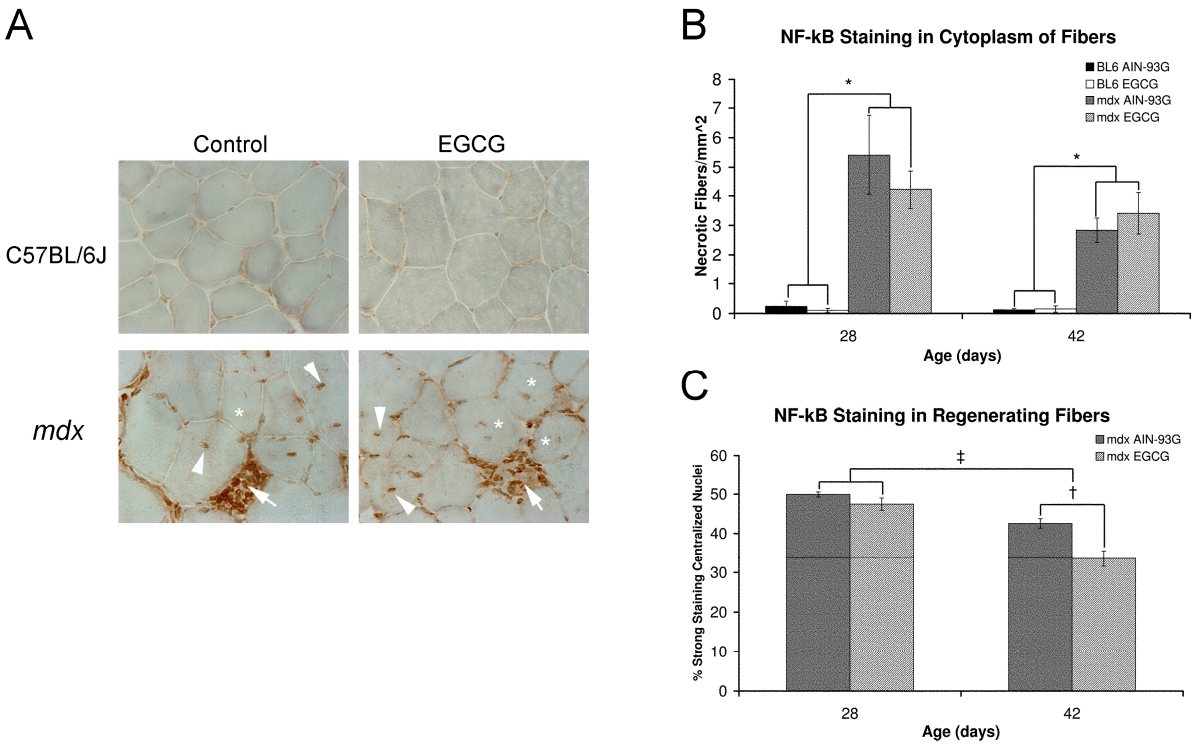

Figure 6.5 - Anti-p-NF-κB (p-p65) staining of TA muscles C57BL/6J and *mdx* mice. (A) C57BL/6J muscle sections had no cytoplasmic staining and weak nuclear staining. Control *mdx* sections had staining in peripheral nuclei and the cytoplasm of necrotic fibers infiltrated by inflammatory cells (arrow). Regenerating fibers had centralized nuclei with both strong (arrowhead) and weak (asterisk) immunoreactivity. EGCG treated *mdx* sections had a decrease in the percent of regenerating fibers with strong immunoreactivity of centralized nuclei compared to control *mdx*. 400X. (B) Quantification of p-NF-κB (p-p65) staining revealed there were less fibers with cytoplasmic staining in C57BL/6J mice compared *mdx* mice (P≤0.05), but the EGCG treatment did not reduce cytoplasmic NF-κB staining in *mdx* mice (P≤0.05). Cytoplasmic NF-κB staining in muscle fibers was indicative of necrotic fibers. (C) There was a decrease in the number of regenerating fibers with strong centralized nuclear staining from age 28 days to 42 days in *mdx* mice (P≤0.05). There was also a decrease in regenerating fibers with strong centralized nuclear staining at age 42 days for EGCG treated *mdx* mice compared to control *mdx* mice (P≤0.05). *Mean C57BL/6J values were significantly less than *mdx* values. †Mean EGCG treated *mdx* values significantly less than control *mdx*. ‡ Independent of treatment, strong centralized nuclei staining in regenerating fibers was significantly greater at age 28 days than at age 42 days.

6.4 Discussion

In this study, quantitative methods were used to determine if EGCG, like GTE, could decrease muscle pathology in *mdx* mice, and to further characterize the role of this CAM approach for altering inflammation, regeneration, and NF-kB distribution. In a previous study (see Chapter 5), 0.25% and 0.5% GTE diets were fed to *mdx* mice. Both diets reduced muscle pathology compared to the control diet. To determine if EGCG was the primary polyphenol in GTE responsible for the reduction in overall muscle pathology, in the present study we used a purified AIN-93G diet containing 0.1% EGCG.

There were no differences in food consumption for EGCG treated and control C57BL/6J mice; however, between ages 18-28 days there were significant differences for EGCG treated *mdx* mice compared to control *mdx*. *Mdx* mice also consumed less between ages 21 - 42 days compared to C57BL/6J mice. Body mass for *mdx* mice was increased between ages 28 - 42 days; however, body mass was not affected by treatment. These data indicate that differences at ages 28 - 42 days were primarily related to genotype.

Serum CK was reduced in GTE treated *mdx* mice at age 42 days (see Chapter 5), but not for EGCG treated *mdx* mice. There are at least two possible explanations for why EGCG did not decrease serum CK as seen with GTE. First, GTE contains a mixture of polyphenols and other extracts; potentially, synergistic effects of the combined polyphenols in GTE are required to decrease serum CK. However, subcutaneous injection of EGCG prior to disease onset has been reported to reduce serum CK in *mdx* mice age 56 days [136]. Although there may be factors that alter EGCG's ability to reduce serum CK when provided as a dietary treatment, this data shows that EGCG alone is capable of reducing

serum CK. Another possibility is that the extended treatment time when provided before age 18 days is more beneficial for reducing serum CK than treatments beginning at age 18 days. GTE treatments provided to *mdx* mice before birth and as pups appears to be more beneficial for reducing serum CK than treatments that only begin several days prior to disease onset. Studies have indicated that dietary GTE is taken up by rat fetuses *in utero* indicating that these polyphenols can be used to treat disease prior to birth [39,40]. Additionally, as the pups mature they begin to eat pelleted food before being weaned. Therefore, GTE and EGCG treatments that begin at or before birth may provide even more benefits than treatments that begin just prior to disease onset.

Generalized histopathological features are often reported for *mdx* skeletal muscles [23,58,84,90,126,127,136,161,193,210]. We recently demonstrated the value of detailed quantitative histopathological techniques to detect alterations in specific disease features in skeletal muscle of GTE treated *mdx* mice (see Chapter 5). As occurred in GTE treated *mdx* mice, muscle histopathology was decreased for EGCG treated *mdx* compared to control *mdx* mice. There was a ~20% increase in normal fiber morphology for EGCG treated *mdx* mice compared to control *mdx* mice over ages 28 and 42 days. The primary histopathological change was a ~21% decrease in regenerating muscle fibers at age 42 days. The necrotic fibers, degenerating fibers, immune cell infiltration, and myotubes were relatively small features of overall muscle histopathology and were not changed by EGCG treatments.

Both GTE and EGCG are believed to have anti-inflammatory properties. Macrophage infiltration is a substantial feature of *mdx* muscle pathology, yet neither GTE nor EGCG treatments reduced macrophage infiltration in *mdx* mice. Although neither treatment decreased macrophage infiltration the treatments may have induced a change in

macrophage phenotype. Two populations of macrophages, with opposite effects have been identified to play a role in dystrophic muscle pathology. M1 macrophages are pro-inflammatory and M2 macrophages are anti-inflammatory [207]. EGCG is reported to inhibit IKK activity which ultimately results in decreased NF-κB activity [36,160,175,220]. Specifically, IKKB, has been shown to be an important component in macrophage regulation of dystrophic muscle pathology [2]. Further studies using flow cytometry techniques could be useful in assessing EGCG role in regulating macrophage phenotype.

NF-κB is believed to be a key regulator of muscle regeneration, although its mode of action has not been fully characterized [2,126,127,145,214]. As previously reported GTE did not reduce the number of necrotic fibers with NF-κB, but reduced the number of centralized nuclei of regenerating fibers with strong NF-κB staining. EGCG treatment resulted in similar findings. EGCG treatment did not reduce the number of necrotic fibers with NF-κB staining at ages 28 or 42 days. However, the number of centralized nuclei of regenerating fibers with strong NF-κB staining was reduced at age 42 days. As with GTE, EGCG appears to alter NF-κB activity in regenerating fibers and may ultimately result in a greater area of morphologically normal fibers.

CAM approaches, including the use of GTE and EGCG, are promising treatments for incurable disease because they are inexpensive and can be used in conjunction with conventional treatment options. Additionally, CAM may improve disease prognosis through specific mechanisms that are not yet fully understood or can not be duplicated by other therapeutics. Both GTE and EGCG have been shown to reduce muscle pathology and reduce NF-κB immunostaining in regenerating fibers. Although EGCG did not decrease serum CK, EGCG appears to elicit other beneficial effects noted for GTE, including:

increasing normal fiber morphology, decreasing regenerating fibers, and decreasing centralized nuclei in regenerating fibers with NF-κB staining. Therefore, EGCG is likely to be the primary polyphenol in GTE responsible for these changes. In conclusion, EGCG decreases muscle histopathology potentially by reducing NF-κB activity in regenerating fibers.

Chapter 7 Conclusion

7.1 Summary and discussion

Current treatments for Duchenne muscular dystrophy (DMD) minimally improve muscle function and longevity. For DMD patients and their families, these treatments produce unacceptable outcomes because they are associated with many detrimental side effects and are not curative [9,162]. Inflammatory signaling pathways are thought to be up-regulated prior to disease onset in dystrophic muscle. These signaling cascades likely initiate and regulate the disease time course of immune mediated mechanisms in dystrophic muscle wasting [37,105,150,155,154]. Therefore, treatments that blunt these pathways promise to be very beneficial to DMD patients. Specifically, complimentary and alternative medicine (CAM) approaches provide unique treatment options and insight into disease mechanisms [23,26,58,145,162]. Green tea extract (GTE) and epigallocatechin gallate (EGCG), the primary polyphenol in GTE, have been reported to substantially decrease muscle pathology, improve muscle function, and improve serum antioxidant properties in the *mdx* mouse model [23,26,58]. Potentially, both GTE and EGCG alter NF-κB regulation [36,220], which is believed to be a primary contributor to inflammation and dystrophic muscle wasting.

In the first literature review (see Chapter 3), the DGC was shown to be an important scaffold for signaling molecules that regulate cell viability [69]. Available time course studies indicate that although mechanical integrity and membrane defects are important features of the dystrophic process, they are not evident until after disease onset. In contrast, cell signaling pathways that are altered in the absence of the DCG are up-regulated prior to disease onset. Many of these signaling pathways regulate inflammatory gene expression.

Furthermore, both inflammatory gene expression and immune cell infiltration are also observed prior to disease onset. These findings strongly suggest that aberrant signaling, leading to inflammatory disease processes, contributes to the initiation of muscle degeneration. Specifically, the transcription factors NFAT, AP-1, and NF-κB are believed to play a key role in dystrophic cell viability. These transcription factors regulate gene expression for a plethora of inflammatory genes including many of those that are up-regulated early in dystrophic muscle. Although time course studies during early disease onset are limited, data from available studies has provided valuable insight into disease mechanisms. In conclusion, characterization of the early disease time course allows for the development of therapeutics that directly target aberrant pathways during critical disease stages and may ultimately result in highly effective treatments for ameliorating dystrophic muscle wasting [69].

In the second literature review (see Chapter 4), the central role of the immune response in dystrophic muscle lesion development was further illustrated [68]. Immune cell infiltration occurs prior to disease onset and plays a key role in muscle damage. The increase in MHC proteins on muscle fibers and conserved TCR rearrangements on T-cells is suggestive of an inflammatory response that stems from a highly coordinated disease process. Both pro-inflammatory and anti-inflammatory macrophage populations are present in dystrophic muscle. The balance of these cell populations is responsible for either triggering fiber lysis or regeneration. Specifically, cytokines and chemokines orchestrate interactions between macrophages and other immune cells. Pro-inflammatory cytokine and chemokine expression is up-regulated prior to disease onset in dystrophic mice and is indicative of a detrimental inflammatory process. Expression of these genes is regulated by

NF-κB activation which is also elevated in dystrophic muscle prior to disease onset. NF-κB activity has been shown to drive macrophage induced muscle wasting and suppress regeneration in dystrophic muscle. Therefore, blockade of NF-κB is an excellent target for therapies intended to ameliorate DMD. Treatment options, like GTE and EGCG, are reported to decrease NF-κB activation and have the added benefit of producing minimal side effects that are observed with traditional therapies. In conclusion, immune cells are key inducers of muscle lesion formation and are regulated by signaling cascades, including NF-κB activation, which are altered prior to disease onset. Since NF-κB activity plays an important role in dystrophic muscle wasting and can be blunted by low risk therapeutics (i.e. GTE and EGCG), it offers a promising treatment target for DMD patients [68].

On the basis of the conclusions from these two literature reviews, NF-κB was chosen as a viable target for blunting dystrophic muscle pathology associated with inflammatory processes. Because GTE and EGCG have shown substantial promise in reducing muscle pathology and are reported to inhibit NF-κB activity, they were selected as the therapeutics to test in these studies reported herein. NF-κB has been implicated to play a role in the overall dystrophic muscle pathology time course, but also specifically through altering macrophage activity and muscle regeneration. In the past, the importance of comparing and examining time course studies has been overlooked. Therefore, time course studies detailing serum CK, muscle histopathology, macrophage infiltration and NF-κB staining were performed first for GTE- and then for EGCG-treated *mdx* mice during critical disease stages.

For Specific Aim 1 (see Chapter 5), the overarching hypothesis tested was that GTE can decrease muscle pathology and inflammation in *mdx* mice by decreasing NF-κB

activation. To determine the early disease time course, muscle histopathology was quantified for *mdx* mice between ages 14-42 days and compared to C57BL/6J mice. Characterizing the early disease time course was important for identifying specific disease stages. Ages 28 and 42 days were selected as critical time points in degenerative and regenerative disease stages at which treatments with GTE should be evaluated. Diets containing GTE extract (0.25% and 0.5%) were provided to *mdx* pups and breeder pairs as an early intervention before disease onset which occurs at age 21 days. The GTE treatments significantly decreased serum creatine kinase (CK) by 85%, increased normal fiber morphology by 32 %, and decreased regenerating fibers by 21% in *mdx* mice age 42 days; however, no changes were observed at age 28 days. Macrophage infiltration of TA muscles was not altered at age 42 days. However, NF-κB in the centralized nuclei of regenerating fibers was significantly reduced at this age by 34%. This was the foremost finding because these data suggested that GTE treatments decrease muscle pathology by modulating NF-κB activity in regenerating muscle fibers.

For Specific Aim 2 (see Chapter 6), the overarching hypothesis tested was that EGCG, the primary polyphenol of GTE, decreases muscle pathology and inflammation in *mdx* mice by decreasing NF-κB activation. A purified AIN-93G diet containing 0.01% EGCG was provided to weaned mice beginning at age 18 days. As in the previous study with GTE treatment, the effectiveness of EGCG treatment was evaluated at age 28 and 42 days. Serum (CK) was not decreased in EGCG treated *mdx* mice; however, normal fiber morphology was significantly increased over ages 28 and 42 days by 20%. The primary histopathological change was a 21% decrease in regenerating fibers at age 42 days. As was observed with GTE, macrophage infiltration was not decreased by EGCG treatments. NF-

κB staining was significantly decreased by 21% in centralized nuclei of regenerating fibers. Although serum CK was not decreased, these data suggested that EGCG is the primary polyphenol in GTE that decreases muscle pathology by modulating NF-κB activity in regenerating muscle fibers.

GTE and EGCG were previously reported to improve muscle pathology and muscle function in *mdx* mice primarily through their antioxidant potential [23,26,58]. Although these changes were noted, specific histopathological features of muscle fibers were not characterized and other potential mechanisms were not assessed (e.g. NF-κB modulation). The data from these two studies herein confirm both GTE and EGCG reduce muscle pathology. An increase in normal fiber morphology was observed in *mdx* mice for both treatment groups with the primary histopathological change being a decrease in regenerating fibers at age 42 days. NF-κB staining in the centralized nuclei of regenerating fibers was similarly decreased in GTE and EGCG treated *mdx* mice at this age. Therefore, the beneficial effects of GTE appear to stem from EGCG; however, further tests should be performed on the other polyphenol components of GTE to confirm this finding. The decrease in regenerating fibers indicates an improvement in muscle regeneration, due to decreased NF-κB activity, resulting in a greater number of morphologically normal fibers. Prior to this study, this striking benefit of GTE and EGCG supplementation had not been identified and indicates a novel mechanism by which these treatments may improve DMD muscle wasting. Although serum CK was decreased by GTE, there was no decrease by EGCG. This difference likely reflects the different feeding strategies employed in these two studies because the duration of the EGCG was shorter than the GTE treatment. Neither GTE nor EGCG reduced overall macrophage infiltration; however, these treatments may

potentially alter the phenotype of these cells. Two phenotypically distinct populations of macrophages have been observed in *mdx* muscle tissue: one population is pro-inflammatory and the other is anti-inflammatory [207]. Presumably, GTE and EGCG could modulate a shift towards the anti-inflammatory population. GTE and EGCG's ability to alter NF-κB activity appears to be one mechanism by which these treatments improve muscle pathology in *mdx* mice [36,220]. In conclusion, GTE and EGCG reduce muscle pathology potentially by altering NF-κB activity in regenerating muscle fibers.

7.2 Future research

Multiple studies, including those reported herein, indicate that GTE and EGCG are effective for decreasing muscle wasting and improving muscle function [23,26,58,136]. As first identified here, regulation of NF-κB appears to play a key role in the improvements associated with these treatments. Although GTE and EGCG provide promising new treatments for DMD, our understanding of the mechanisms through which these treatments decrease muscle pathology is limited. Further research to elucidate how GTE and EGCG regulate NF-κB activity and ultimately muscle pathology would strengthen support for the use of these treatments in DMD. Two new potential pathways have been identified that may underscore GTE and EGCG ability to decrease muscle wasting. The first possibility is that GTE and EGCG alter NF-κB activity in regenerating fibers, contributing to an improvement in muscle regeneration. The second possibility is that GTE and EGCG alter NF-κB activity in macrophages, thereby inducing a shift to an anti-inflammatory macrophage population. Additionally, the pathway by which GTE and EGCG alter IKK activation of NF-κB is still unclear. Some studies suggest that EGCG may directly regulate IKK activity [36,220]; however, EGCG may indirectly exert its effects by reducing ROS [23,26,58].

Reduction of ROS by a variety of antioxidants appears to result in decreased activation of NF-κB in dystrophic muscle [105,126,127,180,214]. These data indicate that there may be specific pathways by which ROS ultimately activate NF-κB. This is a very intriguing and novel pathway which may explain how formation of ROS induces inflammatory signaling that results in tissue damage. Research defining the mechanism through which ROS activate the IKK/NF-κB pathway will undoubtedly lead to new therapeutic strategies for the treatment of many diseases, including DMD.

References

1. Abu-Ghazaleh RI, Gleich GJ, Prendergast FG. Interaction of eosinophil granule major basic protein with synthetic lipid bilayers: a mechanism for toxicity. J Membr Biol 1992;128:153-164.

2. Acharyya S, Villalta S, Bakkar N, Bupha-Intr T, Janssen P, Carathers M, Li Z, Beg A, Ghosh S, Sahenk Z, Weinstein M, Gardner K, Rafael-Fortney J, Karin M, Tidball J, Baldwin A, Guttridge D. Interplay of IKK/NF-kappaB signaling in macrophages and myofibers promotes muscle degeneration in Duchenne muscular dystrophy. J Clin Invest 2007;117:889-901.

3. Adams RD, Denny-Brown D, Pearson CM. Disease of muscle: a study in pathology. New York: Hoeber medical books, Harper and Brothers; 1962. 135-324 p.

4. Akhurst RJ. TGF-beta antagonists: why suppress a tumor suppressor? J Clin Invest 2002;109:1533-1536.

5. Alfieri CM, Evans-Anderson HJ, Yutzey KE. Developmental regulation of the mouse IGF-I exon 1 promoter region by calcineurin activation of NFAT in skeletal muscle. Am J Physiol Cell Physiol 2007;292:C1887-1894.

6. Allen DG, Whitehead NP, Yeung EW. Mechanisms of stretch-induced muscle damage in normal and dystrophic muscle: role of ionic changes. J Physiol 2005;567:723-735.

7. Anderson JE, McIntosh LM, Poettcker R. Deflazacort but not prednisone improves both muscle repair and fiber growth in diaphragm and limb muscle in vivo in the mdx dystrophic mouse. Muscle Nerve 1996;19:1576-1585.

8. Andreetta F, Bernasconi P, Baggi F, Ferro P, Oliva L, Arnoldi E, Cornelio F, Mantegazza R, Confalonieri P. Immunomodulation of TGF-beta1 in mdx mouse inhibits connective tissue proliferation in diaphragm but increases inflammatory response: implications for antifibrotic therapy. J Neuroimmunol 2006;175:77-86.

9. Angelini C. The role of corticosteroids in muscular dystrophy: a critical appraisal. Muscle Nerve 2007;36:424-435.

10. Appleyard S, Dunn M, Dubowitz V, Rose M. Increased expression of HLA ABC class I antigens by muscle fibres in Duchenne muscular dystrophy, inflammatory myopathy, and other neuromuscular disorders. Lancet 1985;1:361-363.

11. Arahata K, Engel A. Monoclonal antibody analysis of mononuclear cells in myopathies. I: Quantitation of subsets according to diagnosis and sites of accumulation and demonstration and counts of muscle fibers invaded by T cells. Ann Neurol 1984;16:193-208.

12. Auphan N, DiDonato JA, Rosette C, Helmberg A, Karin M. Immunosuppression by glucocorticoids: inhibition of NF-kappa B activity through induction of I kappa B synthesis. Science 1995;270:286-290.

13. Balaban B, Matthews DJ, Clayton GH, Carry T. Corticosteroid treatment and functional improvement in Duchenne muscular dystrophy: long-term effect. Am J Phys Med Rehabil 2005;84:843-850.

14. Bansal D, Miyake K, Vogel SS, Groh S, Chen CC, Williamson R, McNeil PL, Campbell KP. Defective membrane repair in dysferlin-deficient muscular dystrophy. Nature 2003;423:168-172.

15. Barnes PJ. Anti-inflammatory actions of glucocorticoids: molecular mechanisms. Clin Sci (Lond) 1998;94:557-572.

16. Barry FP, Murphy JM. Mesenchymal stem cells: clinical applications and biological characterization. Int J Biochem Cell Biol 2004;36:568-584.

17. Bell CD, Conen PE. Histopathological changes in Duchenne muscular dystrophy. J Neurol Sci 1968;7:529-544.

18. Beyth S, Borovsky Z, Mevorach D, Liebergall M, Gazit Z, Aslan H, Galun E, Rachmilewitz J. Human mesenchymal stem cells alter antigen-presenting cell maturation and induce T-cell unresponsiveness. Blood 2005;105:2214-2219.

19. Blake DJ, Weir A, Newey SE, Davies KE. Function and genetics of dystrophin and dystrophin-related proteins in muscle. Physiol Rev 2002;82:291-329.

20. Bradley W, Hudgson P, Larson P, Papapetropoulos T, Jenkison M. Structural changes in the early stages of Duchenne muscular dystrophy. J Neurol Neurosurg Psychiatry 1972;35:451-455.

21. Brooke M, Fenichel G, Griggs R, Mendell J, Moxley R, Miller J, Province M. Clinical investigation in Duchenne dystrophy: 2. Determination of the "power" of therapeutic trials based on the natural history. Muscle Nerve 1983;6:91-103.

22. Broussard SR, McCusker RH, Novakofski JE, Strle K, Shen WH, Johnson RW, Dantzer R, Kelley KW. IL-1beta impairs insulin-like growth factor i-induced differentiation and downstream activation signals of the insulin-like growth factor i receptor in myoblasts. J Immunol 2004;172:7713-7720.

23. Buetler TM, Renard M, Offord EA, Schneider H, Ruegg UT. Green tea extract decreases muscle necrosis in mdx mice and protects against reactive oxygen species. Am J Clin Nutr 2002;75:749-753.

24. Bulfield G, Siller WG, Wight PA, Moore KJ. X chromosome-linked muscular dystrophy (mdx) in the mouse. Proc Natl Acad Sci U S A 1984;81:1189-1192.

25. Cai B, Spencer MJ, Nakamura G, Tseng-Ong L, Tidball JG. Eosinophilia of dystrophin-deficient muscle is promoted by perforin-mediated cytotoxicity by T cell effectors. Am J Pathol 2000;156:1789-1796.

26. Call JA, Voelker KA, Wolff AV, McMillan RP, Evans NP, Hulver MW, Talmadge RJ, Grange RW. Endurance capacity in maturing mdx mice is markedly enhanced by combined voluntary wheel running and green tea extract. J Appl Physiol 2008;105:923-932.

27. Campbell KP. Three muscular dystrophies: loss of cytoskeleton-extracellular matrix linkage. Cell 1995;80:675-679.

28. Carnwath JW, Shotton DM. Muscular dystrophy in the mdx mouse: histopathology of the soleus and extensor digitorum longus muscles. J Neurosci 1987;80:39-54.

29. Chakkalakal JV, Stocksley MA, Harrison MA, Angus LM, Deschenes-Furry J, St-Pierre S, Megeney LA, Chin ER, Michel RN, Jasmin BJ. Expression of utrophin A mRNA correlates with the oxidative capacity of skeletal muscle fiber types and is regulated by calcineurin/NFAT signaling. Proc Natl Acad Sci U S A 2003;100:7791-7796.

30. Chakkalakal JV, Harrison M-A, Carbonetto S, Chin E, Michel RN, Jasmin BJ. Stimulation of calcineurin signaling attenuates the dystrophic pathology in mdx mice. Hum Mol Genet 2004;13:379-388.

31. Chakkalakal JV, Michel SA, Chin ER, Michel RN, Jasmin BJ. Targeted inhibition of Ca2+/calmodulin signaling exacerbates the dystrophic phenotype in mdx mouse muscle. Hum Mol Genet 2006;15:1423-1435.

32. Chamberlain JS, Metzger J, Reyes M, Townsend D, Faulkner JA. Dystrophin-deficient mdx mice display a reduced life span and are susceptible to spontaneous rhabdomyosarcoma. FASEB J 2007;21:2195-2204.

33. Chang CJ, Yen ML, Chen YC, Chien CC, Huang HI, Bai CH, Yen BL. Placenta-derived multipotent cells exhibit immunosuppressive properties that are enhanced in the presence of interferon-gamma. Stem Cells 2006;24:2466-2477.

34. Chang FY, Lu CL. Treatment of irritable bowel syndrome using complementary and alternative medicine. J Chin Med Assoc 2009;72:294-300.

35. Chazaud B, Sonnet C, Lafuste P, Bassez G, Rimaniol AC, Poron F, Authier FJ, Dreyfus PA, Gherardi RK. Satellite cells attract monocytes and use macrophages as a support to escape apoptosis and enhance muscle growth. J Cell Biol 2003;163:1133-1143.

36. Chen PC, Wheeler DS, Malhotra V, Odoms K, Denenberg AG, Wong HR. A green tea-derived polyphenol, epigallocatechin-3-gallate, inhibits IkappaB kinase activation and IL-8 gene expression in respiratory epithelium. Inflammation 2002;26:233-241.

37. Chen YW, Nagaraju K, Bakay M, McIntyre O, Rawat R, Shi R, Hoffman EP. Early onset of inflammation and later involvement of TGFbeta in Duchenne muscular dystrophy. Neurology 2005;65:826-834.

38. Chin ER, Olson EN, Richardson JA, Yang Q, Humphries C, Shelton JM, Wu H, Zhu W, Bassel-Duby R, Williams RS. A calcineurin-dependent transcriptional pathway controls skeletal muscle fiber type. Genes Dev 1998;12:2499-2509.

39. Chu KO, Wang CC, Chu CY, Chan KP, Rogers MS, Choy KW, Pang CP. Pharmacokinetic studies of green tea catechins in maternal plasma and fetuses in rats. J Pharm Sci 2006;95:1372-1381.

40. Chu KO, Wang CC, Chu CY, Choy KW, Pang CP, Rogers MS. Uptake and distribution of catechins in fetal organs following in utero exposure in rats. Hum Reprod 2007;22:280-287.

41. Collins CA, Morgan JE. Duchenne's muscular dystrophy: animal models used to investigate pathogenesis and develop therapeutic strategies. Int J Exp Pathol 2003;84:165-172.

42. Connolly AM, Schierbecker J, Renna R, Florence J. High dose weekly oral prednisone improves strength in boys with Duchenne muscular dystrophy. Neuromuscul Disord 2002;12:917-925.

43. Cooney RN, Maish GO, 3rd, Gilpin T, Shumate ML, Lang CH, Vary TC. Mechanism of IL-1 induced inhibition of protein synthesis in skeletal muscle. Shock 1999;11:235-241.

44. Coulton GR, Curtin NA, Morgan JE, Partridge TA. The mdx mouse skeletal muscle myopathy: II. Contractile properties. Neuropathol Appl Neurobiol 1988;14:299-314.

45. Coulton GR, Morgan JE, Partridge TA, Sloper JC. The mdx mouse skeletal muscle myopathy: I. A histological, morphometric and biochemical investigation. Neuropathol Appl Neurobiol 1988;14:53-70.

46. Couteaux R, Mira JC, d'Albis A. Regeneration of muscles after cardiotoxin injury. I. Cytological aspects. Biol Cell 1988;62:171-182.

47. Crabtree GR. Calcium, calcineurin, and the control of transcription. J Biol Chem 2001;276:2313-2316.

48. Dangain J, Vrbova G. Muscle development in mdx mutant mice. Muscle Nerve 1984;7:700-704.

49. Davis RJ. Transcriptional regulation by MAP kinases. Mol Reprod Dev 1995;42:459-467.

50. De Bosscher K, Van Craenenbroeck K, Meijer OC, Haegeman G. Selective transrepression versus transactivation mechanisms by glucocorticoid receptor modulators in stress and immune systems. Eur J Pharmacol 2008;583:290-302.

51. De Luca A, Nico B, Liantonio A, Didonna MP, Fraysse B, Pierno S, Burdi R, Mangieri D, Rolland JF, Camerino C, Zallone A, Confalonieri P, Andreetta F, Arnoldi E, Courdier-Fruh I, Magyar JP, Frigeri A, Pisoni M, Svelto M, Conte Camerino D. A multidisciplinary evaluation of the effectiveness of cyclosporine a in dystrophic mdx mice. Am J Pathol 2005;166:477-489.

52. Deconinck AE, Rafael JA, Skinner JA, Brown SC, Potter AC, Metzinger L, Watt DJ, Dickson JG, Tinsley JM, Davies KE. Utrophin-dystrophin-deficient mice as a model for Duchenne muscular dystrophy. Cell 1997;90:717-727.

53. Dellorusso C, Crawford RW, Chamberlain JS, Brooks SV. Tibialis anterior muscles in mdx mice are highly susceptible to contraction-induced injury. J Muscle Res Cell Motil 2001;22:467-475.

54. Dennis RA, Trappe TA, Simpson P, Carroll C, Huang BE, Nagarajan R, Bearden E, Gurley C, Duff GW, Evans WJ, Kornman K, Peterson CA. Interleukin-1

polymorphisms are associated with the inflammatory response in human muscle to acute resistance exercise. J Physiol 2004;560:617-626.

55. DiMario JX, Uzman A, Strohman RC. Fiber regeneration is not persistent in dystrophic (mdx) mouse skeletal muscle. Dev Biol 1991;148:314-321.

56. Disatnik MH, Dhawan J, Yu Y, Beal MF, Whirl MM, Franco AA, Rando TA. Evidence of oxidative stress in mdx mouse muscle: studies of the pre-necrotic state. J Neurol Sci 1998;161:77-84.

57. Dogra C, Changotra H, Wergedal JE, Kumar A. Regulation of phosphatidylinositol 3-kinase (PI3K)/Akt and nuclear factor-kappa B signaling pathways in dystrophin-deficient skeletal muscle in response to mechanical stretch. J Cell Physiol 2006;208:575-585.

58. Dorchies OM, Wagner S, Vuadens O, Waldhauser K, Buetler TM, Kucera P, Ruegg UT. Green tea extract and its major polyphenol (-)-epigallocatechin gallate improve muscle function in a mouse model for Duchenne muscular dystrophy. Am J Physiol Cell Physiol 2006;290:C616-625.

59. Dudley RW, Khairallah M, Mohammed S, Lands L, Des Rosiers C, Petrof BJ. Dynamic responses of the glutathione system to acute oxidative stress in dystrophic mouse (mdx) muscles. Am J Physiol Regul Integr Comp Physiol 2006;291:R704-710.

60. Durbeej M, Campbell KP. Muscular dystrophies involving the dystrophin-glycoprotein complex: an overview of current mouse models. Curr Opin Genet Dev 2002;12:349-361.

61. Durham WJ, Arbogast S, Gerken E, Li YP, Reid MB. Progressive nuclear factor-kappaB activation resistant to inhibition by contraction and curcumin in mdx mice. Muscle Nerve 2006;34:298-303.

62. Emery AE. Muscle histology and creatine kinase levels in the foetus in Duchenne muscular dystrophy. Nature 1977;266:472-473.

63. Emery AE, Burt D, Dubowitz V, Rocker I, Donnai D, Harris R, Donnai P. Antenatal diagnosis of Duchenne muscular dystrophy. Lancet 1979;1:847-849.

64. Emery AE. The muscular dystrophies. Lancet 2002;359:687-695.

65. Emslie-Smith A, Arahata K, Engel A. Major histocompatibility complex class I antigen expression, immunolocalization of interferon subtypes, and T cell-mediated cytotoxicity in myopathies. Hum Pathol 1989;20:224-231.

66. Engel A, Arahata K. Mononuclear cells in myopathies: quantitation of functionally distinct subsets, recognition of antigen-specific cell-mediated cytotoxicity in some diseases, and implications for the pathogenesis of the different inflammatory myopathies. Hum Pathol 1986;17:704-721.

67. Engel AG, Franzinin-Armstrong C. Dystrophinopathies. In: Engel AG, Ozawa E, editors. Myology. 3 ed. Volume 2: McGraw-Hill; 2004. p 961-1026.

68. Evans NP, Misyak SA, Robertson JL, Bassaganya-Riera J, Grange RW. Immune-mediated mechanisms potentially regulate the disease time-course of duchenne muscular dystrophy and provide targets for therapeutic intervention. Pm R 2009;1:755-768.

69. Evans NP, Misyak SA, Robertson JL, Bassaganya-Riera J, Grange RW. Dysregulated intracellular signaling and inflammatory gene expression during initial disease onset in Duchenne muscular dystrophy. Am J Phys Med Rehabil 2009;88:502-522.

70. Farini A, Meregalli M, Belicchi M, Battistelli M, Parolini D, D'Antona G, Gavina M, Ottoboni L, Constantin G, Bottinelli R, Torrente Y. T and B lymphocyte depletion has a marked effect on the fibrosis of dystrophic skeletal muscles in the scid/mdx mouse. J Pathol 2007;213:229-238.

71. Feng WY. Metabolism of green tea catechins: an overview. Curr Drug Metab 2006;7:755-809.

72. Fischer GF, Mayr WR. Molecular genetics of the HLA complex. Wien Klin Wochenschr 2001;113:814-824.

73. Franco A, Jr., Lansman JB. Calcium entry through stretch-inactivated ion channels in mdx myotubes. Nature 1990;344:670-673.

74. Fujioka S, Niu J, Schmidt C, Sclabas GM, Peng B, Uwagawa T, Li Z, Evans DB, Abbruzzese JL, Chiao PJ. NF-kappaB and AP-1 connection: mechanism of NF-kappaB-dependent regulation of AP-1 activity. Mol Cell Biol 2004;24:7806-7819.

75. Galvagni F, Cantini M, Oliviero S. The utrophin gene is transcriptionally up-regulated in regenerating muscle. J Biol Chem 2002;277:19106-19113.

76. Geissinger HD, Rao PV, McDonald-Taylor CK. "mdx" mouse myopathy: histopathological, morphometric and histochemical observations on young mice. J Comp Pathol 1990;102:249-263.

77. Gilbert RK, Hawk WA. The incidence of necrosis of muscle fibers in Duchenne type muscular dystrophy. Am J Pathol 1963;43:107-122.

78. Gorospe J, Tharp M, Demitsu T, Hoffman E. Dystrophin-deficient myofibers are vulnerable to mast cell granule-induced necrosis. Neuromuscul Disord 1994;4:325-333.

79. Gorospe J, Tharp M, Hinckley J, Kornegay J, Hoffman E. A role for mast cells in the progression of Duchenne muscular dystrophy? Correlations in dystrophin-deficient humans, dogs, and mice. J Neurol Sci 1994;122:44-56.

80. Gorospe JRM, Nishikawa BK, Hoffman EP. Recruitment of mast cells to muscle after mild damage. J Neurol Sci 1996;135:10-17.

81. Gosselin LE, Williams JE, Deering M, Brazeau D, Koury S, Martinez DA. Localization and early time course of TGF-beta 1 mRNA expression in dystrophic muscle. Muscle Nerve 2004;30:645-653.

82. Grady R, Teng H, Nichol MC, Cunningham JC, Wilkinson RS, Sanes JR. Skeletal and cardiac myopathies in mice lacking utrophin and dystrophin: a model for Duchenne muscular dystrophy. Cell 1997;90:729-738.

83. Grange RW, Gainer TG, Marschner KM, Talmadge RJ, Stull JT. Fast-twitch skeletal muscles of dystrophic mouse pups are resistant to injury from acute mechanical stress. Am J Physiol Cell Physiol 2002;283:C1090-1101.

84. Grounds MD, Torrisi JO. Anti-TNFalpha (Remicade) therapy protects dystrophic skeletal muscle from necrosis. FASEB J 2004;18:676-682.

85. Grounds MD, Radley HG, Lynch GS, Nagaraju K, De Luca A. Towards developing standard operating procedures for pre-clinical testing in the mdx mouse model of Duchenne muscular dystrophy. Neurobiol Dis 2008;31:1-19.

86. Grundtman C, Salomonsson S, Dorph C, Bruton J, Andersson U, Lundberg IE. Immunolocalization of interleukin-1 receptors in the sarcolemma and nuclei of skeletal muscle in patients with idiopathic inflammatory myopathies. Arthritis Rheum 2007;56:674-687.

87. Gussoni E, Pavlath GK, Miller RG, Panzara MA, Powell M, Blau HM, Steinman L. Specific T cell receptor gene rearrangements at the site of muscle degeneration in Duchenne muscular dystrophy. J Immunol 1994;153:4798-4805.

88. Guttridge DC, Mayo MW, Madrid LV, Wang C-Y, Baldwin AS, Jr. NF-kappaB-induced loss of MyoD messenger RNA: Possible role in muscle decay and cachexia. Science 2000;289:2363-2366.

89. Hess J, Angel P, Schorpp-Kistner M. AP-1 subunits: quarrel and harmony among siblings. J Cell Sci 2004;117:5965-5973.

90. Hodgetts S, Radley H, Davies M, Grounds MD. Reduced necrosis of dystrophic muscle by depletion of host neutrophils, or blocking TNFalpha function with Etanercept in mdx mice. Neuromuscul Disord 2006;16:591-602.

91. Hussein MR, Hamed SA, Mostafa MG, Abu-Dief EE, Kamel NF, Kandil MR. The effects of glucocorticoid therapy on the inflammatory and dendritic cells in muscular dystrophies. Int J Exp Pathol 2006;87:451-461.

92. Hutter OF, Burton FL, Bovell DL. Mechanical properties of normal and mdx mouse sarcolemma: bearing on function of dystrophin. J Muscle Res Cell Motil 1991;12:585-589.

93. Kalliolias GD, Liossis SN. The future of the IL-1 receptor antagonist anakinra: from rheumatoid arthritis to adult-onset Still's disease and systemic-onset juvenile idiopathic arthritis. Expert Opin Investig Drugs 2008;17:349-359.

94. Karin M, Ben-Neriah Y. Phosphorylation meets ubiquitination: the control of NF-kappaB activity. Annu Rev Immunol 2000;18:621-663.

95. Karin M, Chang L. AP-1--glucocorticoid receptor crosstalk taken to a higher level. J Endocrinol 2001;169:447-451.

96. Karin M, Lin A. NF-kappaB at the crossroads of life and death. Nat Immunol 2002;3:221-227.

97. Karin M, Gallagher E. From JNK to pay dirt: jun kinases, their biochemistry, physiology and clinical importance. IUBMB Life 2005;57:283-295.

98. Karpati G, Pouliot Y, Carpenter S. Expression of immunoreactive major histocompatibility complex products in human skeletal muscles. Ann Neurol 1988;23:64-72.

99. Keeling RM, Golumbek PT, Streif EM, Connolly AM. Weekly oral prednisolone improves survival and strength in male mdx mice. Muscle Nerve 2007;35:43-48.

100. Kolodziejczyk SM, Walsh GS, Balazsi K, Seale P, Sandoz J, Hierlihy AM, Rudnicki MA, Chamberlain JS, Miller FD, Megeney LA. Activation of JNK1 contributes to dystrophic muscle pathogenesis. Curr Biol 2001;11:1278-1282.

101. Kometani K, Tsugeno H, Yamada K. Mechanical and energetic properties of dystrophic (mdx) mouse muscle. Jpn J Physiol 1990;40:541-549.

102. Kristian T, Siesjo BK. Calcium in ischemic cell death. Stroke 1998;29:705-718.

103. Kroegel C, Costabel U, Matthys H. Mechanism of membrane damage mediated by eosinophil major basic protein. Lancet 1987;1:1380-1381.

104. Kuklina EM, Shirshev SV. Role of transcription factor NFAT in the immune response. Biochemistry (Mosc) 2001;66:467-475.

105. Kumar A, Boriek AM. Mechanical stress activates the nuclear factor-kappaB pathway in skeletal muscle fibers: a possible role in Duchenne muscular dystrophy. FASEB J 2003;17:386-396.

106. Kumar A, Khandelwal N, Malya R, Reid MB, Boriek AM. Loss of dystrophin causes aberrant mechanotransduction in skeletal muscle fibers. FASEB J 2004;18:102-113.

107. Lagrota-Candido J, Canella I, Savino W, Quirico-Santos T. Expression of extracellular matrix ligands and receptors in the muscular tissue and draining lymph nodes of mdx dystrophic mice. Clin Immunol 1999;93:143-151.

108. Le Blanc K, Ringden O. Mesenchymal stem cells: properties and role in clinical bone marrow transplantation. Curr Opin Immunol 2006;18:586-591.

109. Li Y, Reid M. Effect of tumor necrosis factor-alpha on skeletal muscle metabolism. Curr Opin Rheumatol 2001;13:483-487.

110. Liu HS, Chen YH, Hung PF, Kao YH. Inhibitory effect of green tea (-)-epigallocatechin gallate on resistin gene expression in 3T3-L1 adipocytes depends on the ERK pathway. Am J Physiol Endocrinol Metab 2006;290:E273-281.

111. Louboutin JP, Fichter-Gagnepain V, Thaon E, Fardeau M. Morphometric analysis of mdx diaphragm muscle fibres. Comparison with hindlimb muscles. Neuromuscul Disord 1993;3:463-469.

112. Lundberg I, Brengman JM, Engel AG. Analysis of cytokine expression in muscle in inflammatory myopathies, Duchenne dystrophy, and non-weak controls. J Neuroimmunol 1995;63:9-16.

113. Lundberg I, Ulfgren AK, Nyberg P, Andersson U, Klareskog L. Cytokine production in muscle tissue of patients with idiopathic inflammatory myopathies. Arthritis Rheum 1997;40:865-874.

114. Macian F, Lopez-Rodriguez C, Rao A. Partners in transcription: NFAT and AP-1. Oncogene 2001;20:2476-2489.

115. Mahmmoud YA. Curcumin modulation of Na,K-ATPase: phosphoenzyme accumulation, decreased K+ occlusion, and inhibition of hydrolytic activity. Br J Pharmacol 2005;145:236-245.

116. Mahoney MJ, Haseltine FP, Hobbins JC, Banker BQ, Caskey CT, Golbus MS. Prenatal diagnosis of Duchenne's muscular dystrophy. N Engl J Med 1977;297:968-973.

117. Mainardi T, Kapoor S, Bielory L. Complementary and alternative medicine: herbs, phytochemicals and vitamins and their immunologic effects. J Allergy Clin Immunol 2009;123:283-294; quiz 295-286.

118. Maitra B, Szekely E, Gjini K, Laughlin MJ, Dennis J, Haynesworth SE, Koc ON. Human mesenchymal stem cells support unrelated donor hematopoietic stem cells and suppress T-cell activation. Bone Marrow Transplant 2004;33:597-604.

119. Mantegazza R, Andreetta F, Bernasconi P, Baggi F, Oksenberg J, Simoncini O, Mora M, Cornelio F, Steinman L. Analysis of T cell receptor repertoire of muscle-infiltrating T lymphocytes in polymyositis. Restricted V alpha/beta rearrangements may indicate antigen-driven selection. J Clin Invest 1993;91:2880-2886.

120. Marx J. How the glucocorticoids suppress immunity. Science 1995;270:232-233.

121. McArdle A, Edwards R, Jackson M. Time course of changes in plasma membrane permeability in the dystrophin-deficient mdx mouse. Muscle Nerve 1994;17:1378-1384.

122. McArdle A, Edwards RHT, Jackson MJ. How does dystrophin deficiency lead to muscle degeneration? -- Evidence from the mdx mouse. Neuromuscul Disord 1995;5:445-456.

123. McDouall R, Dunn M, Dubowitz V. Expression of class I and class II MHC antigens in neuromuscular diseases. J Neurol Sci 1989;89:213-226.

124. McDouall R, Dunn M, Dubowitz V. Nature of the mononuclear infiltrate and the mechanism of muscle damage in juvenile dermatomyositis and Duchenne muscular dystrophy. J Neurol Sci 1990;99:199-217.

125. Merlini L, Cicognani A, Malaspina E, Gennari M, Gnudi S, Talim B, Franzoni E. Early prednisone treatment in Duchenne muscular dystrophy. Muscle Nerve 2003;27:222-227.

126. Messina S, Altavilla D, Aguennouz M, Seminara P, Minutoli L, Monici MC, Bitto A, Mazzeo A, Marini H, Squadrito F, Vita G. Lipid peroxidation inhibition blunts nuclear factor-kappaB activation, reduces skeletal muscle degeneration, and enhances muscle function in mdx mice. Am J Pathol 2006;168:918-926.

127. Messina S, Bitto A, Aguennouz Mh, Minutoli L, Monici MC, Altavilla D, Squadrito F, Vita G. Nuclear factor kappa-B blockade reduces skeletal muscle degeneration and enhances muscle function in mdx mice. Exp Neurol 2006;198:234-241.

128. Minetti C, Ricci E, Bonilla E. Progressive depletion of fast alpha-actinin-positive muscle fibers in Duchenne muscular dystrophy. Neurology 1991;41:1977-1981.

129. Mirolo M, Fabbri M, Sironi M, Vecchi A, Guglielmotti A, Mangano G, Biondi G, Locati M, Mantovani A. Impact of the anti-inflammatory agent bindarit on the chemokinome: selective inhibition of the monocyte chemotactic proteins. Eur Cytokine Netw 2008;19:119-122.

130. Monici MC, Aguennouz M, Mazzeo A, Messina C, Vita G. Activation of nuclear factor-kappaB in inflammatory myopathies and Duchenne muscular dystrophy. Neurology 2003;60:993-997.

131. Morioka S, Goto K, Kojima A, Naito T, Matsuba Y, Akema T, Fujiya H, Sugiura T, Ohira Y, Beppu M, Aoki H, Yoshioka T. Functional overloading facilitates the regeneration of injured soleus muscles in mice. J Physiol Sci 2008;58:397-404.

132. Morrison J, Lu Q, Pastoret C, Partridge T, Bou-Gharios G. T-cell-dependent fibrosis in the mdx dystrophic mouse. Lab Invest 2000;80:881-891.

133. Morrison J, Palmer DB, Cobbold S, Partridge T, Bou-Gharios G. Effects of T-lymphocyte depletion on muscle fibrosis in the mdx mouse. Am J Pathol 2005;166:1701-1710.

134. Mourkioti F, Rosenthal N. IGF-1, inflammation and stem cells: interactions during muscle regeneration. Trends Immunol 2005;26:535-542.

135. Nahas R, Moher M. Complementary and alternative medicine for the treatment of type 2 diabetes. Can Fam Physician 2009;55:591-596.

136. Nakae Y, Hirasaka K, Goto J, Nikawa T, Shono M, Yoshida M, Stoward PJ. Subcutaneous injection, from birth, of epigallocatechin-3-gallate, a component of green tea, limits the onset of muscular dystrophy in mdx mice: a quantitative histological, immunohistochemical and electrophysiological study. Histochem Cell Biol 2008;129:489-501.

137. Nakamura A, Yoshida K, Ueda H, Takeda Si, Ikeda S-i. Up-regulation of mitogen activated protein kinases in mdx skeletal muscle following chronic treadmill exercise. Biochim Biophys Acta 2005;1740:326-331.

138. Nowak KJ, Davies KE. Duchenne muscular dystrophy and dystrophin: pathogenesis and opportunities for treatment. EMBO Rep 2004;5:872-876.

139. Oak SA, Zhou YW, Jarrett HW. Skeletal muscle signaling pathway through the dystrophin glycoprotein complex and Rac1. J Biol Chem 2003;278:39287-39295.

140. Oberc M, Engel W. Ultrastructural localization of calcium in normal and abnormal skeletal muscle. Lab Invest 1977;36:566-577.

141. Olsen SA. A review of complementary and alternative medicine (CAM) by people with multiple sclerosis. Occup Ther Int 2009;16:57-70.

142. Olson EN, Williams RS. Calcineurin signaling and muscle remodeling. Cell 2000;101:689-692.

143. Ortega-Perez I, Cano E, Were F, Villar M, Vazquez J, Redondo JM. c-Jun N-terminal kinase (JNK) positively regulates NFATc2 transactivation through phosphorylation within the N-terminal regulatory domain. J Biol Chem 2005;280:20867-20878.

144. Pahl HL. Activators and target genes of Rel/NF-kappaB transcription factors. Oncogene 1999;18:6853-6866.

145. Pan Y, Chen C, Shen Y, Zhu CH, Wang G, Wang XC, Chen HQ, Zhu MS. Curcumin alleviates dystrophic muscle pathology in mdx mice. Mol Cells 2008;25:531-537.

146. Pasternak C, Wong S, Elson EL. Mechanical function of dystrophin in muscle cells. J Cell Biol 1995;128:355-361.

147. Pastoret C, Sebille A. Time course study of the isometric contractile properties of mdx mouse striated muscles. J Muscle Res Cell Motil 1993;14:423-431.

148. Pearce GW, Walton JN. Progressive muscular dystrophy: the histopathological changes in skeletal muscle obtained by biopsy. J Pathol Bacteriol 1962;83:535-550.

149. Perkins KJ, Davies KE. Ets, Ap-1 and GATA factor families regulate the utrophin B promoter: potential regulatory mechanisms for endothelial-specific expression. FEBS Lett 2003;538:168-172.

150. Pescatori M, Broccolini A, Minetti C, Bertini E, Bruno C, D'Amico A, Bernardini C, Mirabella M, Silvestri G, Giglio V, Modoni A, Pedemonte M, Tasca G, Galluzzi G, Mercuri E, Tonali PA, Ricci E. Gene expression profiling in the early phases of DMD: a constant molecular signature characterizes DMD muscle from early postnatal life throughout disease progression. FASEB J 2007;21:1210-1226.

151. Peter AK, Crosbie RH. Hypertrophic response of Duchenne and limb-girdle muscular dystrophies is associated with activation of Akt pathway. Exp Cell Res 2006;312:2580-2591.

152. Petrof BJ, Shrager JB, Stedman HH, Kelly AM, Sweeney HL. Dystrophin protects the sarcolemma from stresses developed during muscle contraction. PNAS 1993;90:3710-3714.

153. Porreca E, Guglielmi MD, Uncini A, Di Gregorio P, Angelini A, Di Febbo C, Pierdomenico SD, Baccante G, Cuccurullo F. Haemostatic abnormalities, cardiac involvement and serum tumor necrosis factor levels in X-linked dystrophic patients. Thromb Haemost 1999;81:543-546.

154. Porter JD, Khanna S, Kaminski HJ, Rao JS, Merriam AP, Richmonds CR, Leahy P, Li J, Guo W, Andrade FH. A chronic inflammatory response dominates the skeletal muscle molecular signature in dystrophin-deficient mdx mice. Hum Mol Genet 2002;11:263-272.

155. Porter JD, Guo W, Merriam AP, Khanna S, Cheng G, Zhou X, Andrade FH, Richmonds C, Kaminski HJ. Persistent over-expression of specific CC class

chemokines correlates with macrophage and T-cell recruitment in mdx skeletal muscle. Neuromuscul Disord 2003;13:223-235.

156. Porter JD, Merriam AP, Khanna S, Andrade FH, Richmonds CR, Leahy P, Cheng G, Karathanasis P, Zhou X, Kusner LL, Adams ME, Willem M, Mayer U, Kaminski HJ. Constitutive properties, not molecular adaptations, mediate extraocular muscle sparing in dystrophic mdx mice. FASEB J 2003:893-895.

157. Porter JD, Merriam AP, Leahy P, Gong B, Khanna S. Dissection of temporal gene expression signatures of affected and spared muscle groups in dystrophin-deficient (mdx) mice. Hum Mol Genet 2003;12:1813-1821.

158. Porter JD, Merriam AP, Leahy P, Gong B, Feuerman J, Cheng G, Khanna S. Temporal gene expression profiling of dystrophin-deficient (mdx) mouse diaphragm identifies conserved and muscle group-specific mechanisms in the pathogenesis of muscular dystrophy. Hum Mol Genet 2004;13:257-269.

159. Pradhan S, Ghosh D, Srivastava NK, Kumar A, Mittal B, Pandey CM, Singh U. Prednisolone in Duchenne muscular dystrophy with imminent loss of ambulation. J Neurol 2006;253:1309-1316.

160. Qin J, Xie LP, Zheng XY, Wang YB, Bai Y, Shen HF, Li LC, Dahiya R. A component of green tea, (-)-epigallocatechin-3-gallate, promotes apoptosis in T24 human bladder cancer cells via modulation of the PI3K/Akt pathway and Bcl-2 family proteins. Biochem Biophys Res Commun 2007;354:852-857.

161. Radley HG, Grounds MD. Cromolyn administration (to block mast cell degranulation) reduces necrosis of dystrophic muscle in mdx mice. Neurobiol Dis 2006;23:387-397.

162. Radley HG, De Luca A, Lynch GS, Grounds MD. Duchenne muscular dystrophy: focus on pharmaceutical and nutritional interventions. Int J Biochem Cell Biol 2007;39:469-477.

163. Ramji DP, Foka P. CCAAT/enhancer-binding proteins: structure, function and regulation. Biochem J 2002;365:561-575.

164. Rando TA. The dystrophin-glycoprotein complex, cellular signaling, and the regulation of cell survival in the muscular dystrophies. Muscle Nerve 2001;24:1575-1594.

165. Rao A, Luo C, Hogan PG. Transcription factors of the NFAT family: regulation and function. Annu Rev Immunol 1997;15:707-747.

166. Reeves PG. Components of the AIN-93 diets as improvements in the AIN-76A diet. J Nutr 1997;127:838S-841S.

167. Reid M, Li Y. Tumor necrosis factor-alpha and muscle wasting: a cellular perspective. Respir Res 2001;2:269-272.

168. Ren G, Zhang L, Zhao X, Xu G, Zhang Y, Roberts AI, Zhao RC, Shi Y. Mesenchymal stem cell-mediated immunosuppression occurs via concerted action of chemokines and nitric oxide. Cell Stem Cell 2008;2:141-150.

169. Rezvani M, Cafarelli E, Hood DA. Performance and excitability of mdx mouse muscle at 2, 5, and 13 wk of age. J Appl Physiol 1995;78:961-967.

170. Sah JF, Balasubramanian S, Eckert RL, Rorke EA. Epigallocatechin-3-gallate inhibits epidermal growth factor receptor signaling pathway. Evidence for direct inhibition of ERK1/2 and AKT kinases. J Biol Chem 2004;279:12755-12762.

171. Salvini TF, Morini CC, Selistre de Araujo HS, Ownby CL. Long-term regeneration of fast and slow murine skeletal muscles after induced injury by ACL myotoxin isolated from Agkistrodon contortrix laticinctus (broad-banded copperhead) venom. Anat Rec 1999;254:521-533.

172. Samdup DZ, Smith RG, Il Song S. The use of complementary and alternative medicine in children with chronic medical conditions. Am J Phys Med Rehabil 2006;85:842-846.

173. Sasaki CY, Barberi TJ, Ghosh P, Longo DL. Phosphorylation of RelA/p65 on serine 536 defines an IkappaBalpha-independent NF-kappaB pathway. J Biol Chem 2005;280:34538-34547.

174. Sen CK, Roy S. Relief from a heavy heart: redox-sensitive NF-kappaB as a therapeutic target in managing cardiac hypertrophy. Am J Physiol Heart Circ Physiol 2005;289:H17-19.

175. Sen P, Chakraborty PK, Raha S. Tea polyphenol epigallocatechin 3-gallate impedes the anti-apoptotic effects of low-grade repetitive stress through inhibition of Akt and NFkappaB survival pathways. FEBS Lett 2006;580:278-284.

176. Serfling E, Berberich-Siebelt F, Avots A, Chuvpilo S, Klein-Hessling S, Jha MK, Kondo E, Pagel P, Schulze-Luehrmann J, Palmetshofer A. NFAT and NF-kappaB factors-the distant relatives. Int J Biochem Cell Biol 2004;36:1166-1170.

177. Shaulian E, Karin M. AP-1 in cell proliferation and survival. Oncogene 2001;20:2390-2400.

178. Shireman PK, Contreras-Shannon V, Reyes-Reyna SM, Robinson SC, McManus LM. MCP-1 parallels inflammatory and regenerative responses in ischemic muscle. J Surg Res 2006;134:145-157.

179. Shireman PK, Contreras-Shannon V, Ochoa O, Karia BP, Michalek JE, McManus LM. MCP-1 deficiency causes altered inflammation with impaired skeletal muscle regeneration. J Leukoc Biol 2007;81:775-785.

180. Siegel AL, Bledsoe C, Lavin J, Gatti F, Berge J, Millman G, Turin E, Winders WT, Rutter J, Palmeiri B, Carlson CG. Treatment with inhibitors of the NF-kappaB pathway improves whole body tension development in the mdx mouse. Neuromuscul Disord 2009;19:131-139.

181. Spence HJ, Yun-Ju C, Steven JW. Muscular dystrophies, the cytoskeleton and cell adhesion. Bioessays 2002;24:542-552.

182. Spencer MJ, Croall DE, Tidball JG. Calpains are activated in necrotic fibers from mdx dystrophic mice. J Biol Chem 1995;270:10909-10914.

183. Spencer MJ, Tidball JG. Calpain translocation during muscle fiber necrosis and regeneration in dystrophin-deficient mice. Exp Cell Res 1996;226:264-272.

184. Spencer MJ, Walsh CM, Dorshkind KA, Rodriguez EM, Tidball JG. Myonuclear apoptosis in dystrophic mdx muscle occurs by perforin-mediated cytotoxicity. J Clin Invest 1997;99:2745-2751.

185. Spencer MJ, Marino MW, Winckler WM. Altered pathological progression of diaphragm and quadriceps muscle in TNF-deficient, dystrophin-deficient mice. Neuromuscul Disord 2000;10:612-619.

186. Spencer MJ, Montecino-Rodriguez E, Dorshkind K, Tidball JG. Helper (CD4+) and cytotoxic (CD8+) T cells promote the pathology of dystrophin-deficient muscle. Clin Immunol 2001;98:235-243.

187. Spencer MJ, Tidball JG. Do immune cells promote the pathology of dystrophin-deficient myopathies? Neuromuscul Disord 2001;11:556-564.

188. Spuler S, Engel AG. Unexpected sarcolemmal complement membrane attack complex deposits on nonnecrotic muscle fibers in muscular dystrophies. Neurology 1998;50:41-46.

189. St-Pierre SJ, Chakkalakal JV, Kolodziejczyk SM, Knudson JC, Jasmin BJ, Megeney LA. Glucocorticoid treatment alleviates dystrophic myofiber pathology by activation of the calcineurin/NF-AT pathway. FASEB J 2004;18:1937-1939.

190. Stein B, Baldwin AS, Jr., Ballard DW, Greene WC, Angel P, Herrlich P. Cross-coupling of the NF-kappa B p65 and Fos/Jun transcription factors produces potentiated biological function. EMBO J 1993;12:3879-3891.

191. Stengel-Rutkowski L, Scheuerbrandt G, Beckmann R, Pongratz D. Prenatal diagnosis of Duchenne's muscular dystrophy. Lancet 1977;1:1359-1360.

192. Straub V, Campbell KP. Muscular dystrophies and the dystrophin-glycoprotein complex. Curr Opin Neurol 1997;10:168-175.

193. Stupka N, Gregorevic P, Plant DR, Lynch GS. The calcineurin signal transduction pathway is essential for successful muscle regeneration in mdx dystrophic mice. Acta Neuropathol 2004;107:299-310.

194. Stupka N, Plant DR, Schertzer JD, Emerson TM, Bassel-Duby R, Olson EN, Lynch GS. Activated calcineurin ameliorates contraction-induced injury to skeletal muscles of mdx dystrophic mice. J Physiol 2006;575:645-656.

195. Summan M, Warren GL, Mercer RR, Chapman R, Hulderman T, Van Rooijen N, Simeonova PP. Macrophages and skeletal muscle regeneration: a clodronate-containing liposome depletion study. Am J Physiol Regul Integr Comp Physiol 2006;290:R1488-1495.

196. Tews DS, Goebel HH. Cytokine expression profile in idiopathic inflammatory myopathies. J Neuropathol Exp Neurol 1996;55:342-347.

197. Tidball JG, Wehling-Henricks M. Evolving therapeutic strategies for Duchenne muscular dystrophy: targeting downstream events. Pediatr Res 2004;56:831-841.

198. Tidball JG. Inflammatory processes in muscle injury and repair. Am J Physiol Regul Integr Comp Physiol 2005;288:R345-353.

199. Tidball JG, Wehling-Henricks M. Damage and inflammation in muscular dystrophy: potential implications and relationships with autoimmune myositis. Curr Opin Rheumatol 2005;17:707-713.

200. Tidball JG, Wehling-Henricks M. The role of free radicals in the pathophysiology of muscular dystrophy. J Appl Physiol 2007;102:1677-1686.

201. Totsuka T, Watanabe K, Uramoto I, Sakuma K, Mizutani T. Muscular dystrophy: centronucleation may reflect a compensatory activation of defective myonuclei. J Biomed Sci 1998;5:54-61.

202. Tseng BS, Zhao P, Pattison JS, Gordon SE, Granchelli JA, Madsen RW, Folk LC, Hoffman EP, Booth FW. Regenerated mdx mouse skeletal muscle shows differential mRNA expression. J Appl Physiol 2002;93:537-545.

203. Vacca A, Felli MP, Farina AR, Martinotti S, Maroder M, Screpanti I, Meco D, Petrangeli E, Frati L, Gulino A. Glucocorticoid receptor-mediated suppression of the interleukin 2 gene expression through impairment of the cooperativity between nuclear factor of activated T cells and AP-1 enhancer elements. J Exp Med 1992;175:637-646.

204. Valcic S, Muders A, Jacobsen NE, Liebler DC, Timmermann BN. Antioxidant chemistry of green tea catechins. Identification of products of the reaction of (-)-epigallocatechin gallate with peroxyl radicals. Chem Res Toxicol 1999;12:382-386.

205. Van Erp C, Irwin NG, Hoey AJ. Long-term administration of pirfenidone improves cardiac function in mdx mice. Muscle Nerve 2006;34:327-334.

206. Vandebrouck A, Sabourin J, Rivet J, Balghi H, Sebille S, Kitzis A, Raymond G, Cognard C, Bourmeyster N, Constantin B. Regulation of capacitative calcium entries by alpha1-syntrophin: association of TRPC1 with dystrophin complex and the PDZ domain of alpha1-syntrophin. FASEB J 2007;21:608-617.

207. Villalta SA, Nguyen HX, Deng B, Gotoh T, Tidball JG. Shifts in macrophage phenotypes and macrophage competition for arginine metabolism affect the severity of muscle pathology in muscular dystrophy. Hum Mol Genet 2009;18:482-496.

208. Warren GL, O'Farrell L, Summan M, Hulderman T, Mishra D, Luster MI, Kuziel WA, Simeonova PP. Role of CC chemokines in skeletal muscle functional restoration after injury. Am J Physiol Cell Physiol 2004;286:C1031-1036.

209. Webster C, Silberstein L, Hays AP, Blau HM. Fast muscle fibers are preferentially affected in Duchenne muscular dystrophy. Cell 1988;52:503-513.

210. Wehling M, Spencer MJ, Tidball JG. A nitric oxide synthase transgene ameliorates muscular dystrophy in mdx mice. J Cell Biol 2001;155:123-132.

211. Weir AP, Burton EA, Harrod G, Davies KE. A- and B-utrophin have different expression patterns and are differentially up-regulated in mdx muscle. J Biol Chem 2002;277:45285-45290.

212. Weir AP, Morgan JE, Davies KE. A-utrophin up-regulation in mdx skeletal muscle is independent of regeneration. Neuromuscul Disord 2004;14:19-23.

213. Whitehead NP, Yeung EW, Allen DG. Muscle damage in mdx (dystrophic) mice: role of calcium and reactive oxygen species. Clin Exp Pharmacol Physiol 2006;33:657-662.

214. Whitehead NP, Pham C, Gervasio OL, Allen DG. N-Acetylcysteine ameliorates skeletal muscle pathophysiology in mdx mice. J Physiol 2008;586:2003-2014.

215. Williams LW, Burks AW, Steele RW. Complement: function and clinical relevance. Ann Allergy 1988;60:293-300.

216. Wisniewska M, Stanczyk M, Grzelakowska-Sztabert B, Kaminska B. Nuclear factor of activated T cells (NFAT) is a possible target for dexamethasone in thymocyte apoptosis. Cell Biol Int 1997;21:127-132.

217. Wisniewska M, Pyrzynska B, Kaminska B. Impaired AP-1 dimers and NFAT complex formation in immature thymocytes during in vivo glucocorticoid-induced apoptosis. Cell Biol Int 2004;28:773-780.

218. Wolff AV, Niday AK, Voelker KA, Call JA, Evans NP, Granata KP, Grange RW. Passive mechanical properties of maturing extensor digitorum longus are not affected by lack of dystrophin. Muscle Nerve 2006;34:304-312.

219. Wullaert A, Heyninck K, Beyaert R. Mechanisms of crosstalk between TNF-induced NF-kappaB and JNK activation in hepatocytes. Biochem Pharmacol 2006;72:1090-1101.

220. Yang F, Oz HS, Barve S, de Villiers WJ, McClain CJ, Varilek GW. The green tea polyphenol (-)-epigallocatechin-3-gallate blocks nuclear factor-kappa B activation by inhibiting I kappa B kinase activity in the intestinal epithelial cell line IEC-6. Mol Pharmacol 2001;60:528-533.

221. Yeung EW, Whitehead NP, Suchyna TM, Gottlieb PA, Sachs F, Allen DG. Effects of stretch-activated channel blockers on [Ca2+]i and muscle damage in the mdx mouse. J Physiol 2005;562:367-380.

222. Yoshida M, Yonetani A, Shirasaki T, Wada K. Dietary NaCl supplementation prevents muscle necrosis in a mouse model of Duchenne muscular dystrophy. Am J Physiol Regul Integr Comp Physiol 2006;290:R449-455.

223. Zhang Q, Kelly AP, Wang L, French SW, Tang X, Duong HS, Messadi DV, Le AD. Green tea extract and (-)-epigallocatechin-3-gallate inhibit mast cell-stimulated type I collagen expression in keloid fibroblasts via blocking PI-3K/AkT signaling pathways. J Invest Dermatol 2006;126:2607-2613.

224. Zhou L, Porter JD, Cheng G, Gong B, Hatala DA, Merriam AP, Zhou X, Rafael JA, Kaminski HJ. Temporal and spatial mRNA expression patterns of TGF-beta1, 2, 3 and TbetaRI, II, III in skeletal muscles of mdx mice. Neuromuscul Disord 2006;16:32-38.

Appendix A: Methods

H&E staining procedure for paraffin embedded and frozen tissues

1. Deparaffinize/Re-hydrate (For frozen sections skip to step 2).
    a. 2X5 minutes: xylene bath
    b. 2X3 minutes: 100% ethanol bath
    c. 2X3 minutes: 95% ethanol bath
    d. 2X3 minutes: 70% ethanol bath
    e. 3 minutes: ddH_2O
2. 3 minutes: hematoxylin (Hematoxylin Gill 2x: Protocol, CAT#245-654)
3. Wash under running tap water.
4. 4 dips: 1% acid alcohol (1% HCl, 70% EtOH)
5. 3 minutes: "blue" sections in 0.1% sodium bicarbonate
6. Wash under running tap water.
7. 3 minutes: eosin (Eosin Y: Protocol, CAT# 245-658)
8. Wash under running tap water.
9. Dehydrate/clear
    a. 3 minutes: ddH_2O
    b. 2X3 minutes: 70% ethanol bath
    c. 2X3 minutes: 95% ethanol bath
    d. 2X3 minutes: 100% ethanol bath
    e. 2X5 minutes: xylene bath
10. Add 2-3 drops of Mounting Medium Xylene (Protocol, CAT#245-691).
11. Coverslip carefully.

Quantification of histopathological features

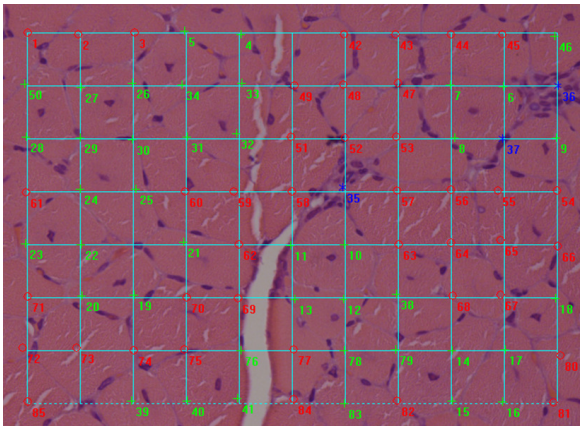

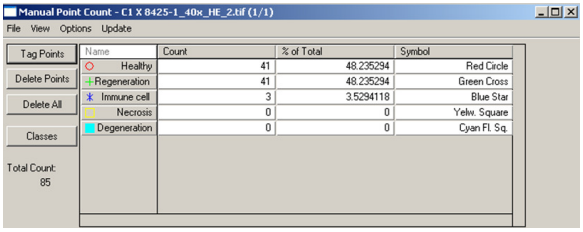

1. Use battlement technique to systematically select ~10-15 fields from the tibialis anterior cross section. Battlement technique: Select initial field from the periphery of muscle cross section and acquire an image. Move up two fields and acquire an image. Move right two fields and acquire an image. Move down two fields and acquire and image. Continue this process for the entire cross section.
2. Acquire pictures of fields with Image-Pro Plus (Media Cubernetics, Inc. Silver Spring, MD).
    a. Set auto exposure and white balance with the acquisition menu and set picture resolution to 1360X1024.
    b. Save pictures under the appropriate folder with the corresponding file name (mouse ID_age_genotype_treatment_magnification_field#).
3. Superimpose the 10X7 grid mask over the image. Identify and count histopathological features with the manual tag function.
4. Export the data to excel and save tag file as before.
5. For each sample, calculate the field averages of each histopathological feature in excel.

Immunohistochemical (IHC) staining and quantification

1. Section tibialis anterior muscles at 10 micrometers in cross section and transfer to positively charged slides.
2. Let slides dry at room temperature for 30 minutes.
3. Store at -80°C.
4. Before staining, warm slides at room temperature for 30 minutes and fix in 2% formalin for 5 minutes.
5. Rinse in PBS 2X5 minutes
6. For sections to be stained with anti-NF-κB-p65.
    a. Permeabilize in 1% Triton X-100 for 5 minutes.
    b. Rinse in PBS 2X5 minutes.
7. Circle tissue with PAP pen.
8. Wash in PBS and blot slides dry.
9. Follow blocking steps in cell and tissue staining kit (R&D systems).
10. Cover tissue with primary antibody (anti-F4/80 1:500, Serotec; anti-NF-κB-p65 1:100, Abcam) and incubate overnight at 4°C.
11. Follow secondary detection steps in cell and tissue staining kit (R&D systems).
12. Counter stain, anti-F4/80 slides, with hematoxylin for 5 seconds.
    a. Rinse in tap water.
    b. Blue in 0.1% sodium bicarbonate.
13. Mount and coverslip.
14. Count features at 400X with tally counter.

Appendix B: Specific Aim 1 Raw Data

Histopathology (percent area of fields) for C57BL/6J and *mdx* mice ages 14, 21, 28, 35, and 42 days

Mouse	Genotype	Age (days)	Normal	Regeneration	Immune Cell	Necrosis	Degeneration
7748a-1	C57BL/6J	14	99.7	0.3	0.0	0.0	0.0
7748a-2	C57BL/6J	14	100.0	0.0	0.0	0.0	0.0
7748a-3	C57BL/6J	14	99.7	0.3	0.0	0.0	0.0
8441-1	C57BL/6J	21	100.0	0.0	0.0	0.0	0.0
8441-5	C57BL/6J	21	99.7	0.0	0.0	0.0	0.3
8441-4	C57BL/6J	21	99.6	0.0	0.4	0.0	0.0
7770-1	C57BL/6J	28	97.7	2.3	0.0	0.0	0.0
8878-1	C57BL/6J	28	99.2	0.8	0.0	0.0	0.0
8878-2	C57BL/6J	28	99.5	0.5	0.0	0.0	0.0
1103-3	C57BL/6J	35	100.0	0.0	0.0	0.0	0.0
1102-2	C57BL/6J	35	100.0	0.0	0.0	0.0	0.0
1102-1	C57BL/6J	35	100.0	0.0	0.0	0.0	0.0
1188-1	C57BL/6J	42	99.7	0.3	0.0	0.0	0.0
1188-3	C57BL/6J	42	99.9	0.1	0.0	0.0	0.0
1185-1	C57BL/6J	42	99.6	0.4	0.0	0.0	0.0
1188-2	C57BL/6J	42	100.0	0.0	0.0	0.0	0.0
7241a-1	mdx	14	99.6	0.4	0.0	0.0	0.0
7241a-4	mdx	14	99.8	0.2	0.0	0.0	0.0
7241a-3	mdx	14	98.9	0.0	1.1	0.0	0.0
7200a-1	mdx	21	91.5	1.3	2.4	0.0	4.7
7200a-3	mdx	21	95.8	0.0	1.9	1.3	1.0
7241a-1	mdx	21	94.2	0.6	2.3	0.0	3.0
7241a-2	mdx	21	92.9	0.4	0.9	0.4	5.3
7271-2	mdx	28	76.5	16.6	6.9	0.0	0.0
7773-2	mdx	28	62.6	35.6	0.6	1.2	0.0
7773-3	mdx	28	67.2	22.8	7.0	3.0	0.0
8841-1	mdx	28	62.7	37.3	0.0	0.0	0.0
8425-1	mdx	35	42.1	56.8	1.1	0.0	0.0
8425-2	mdx	35	47.0	52.6	0.4	0.0	0.0
8425-3	mdx	35	54.7	45.1	0.2	0.0	0.0
1251-2	mdx	42	47.0	48.7	1.9	0.0	2.3
1251-3	mdx	42	33.4	66.2	0.5	0.0	0.0
1294-1	mdx	42	36.0	62.9	0.4	0.0	0.6
1294-3	mdx	42	35.6	64.4	0.0	0.0	0.0

Body mass for control and GTE treated *mdx* mice ages 28 and 42 days

Mouse	Age (days)	Treatment	Body Mass (g)
7271-1	28	Control	8.9
7271-2	28	Control	11.0
7255-1	28	Control	12.9
7255-2	28	Control	12.5
7773-1	28	Control	15.5
7773-2	28	Control	14.3
7773-3	28	Control	13.3
8841-1	28	Control	15.2
8871-1	28	Control	11.7
8871-2	28	Control	16.8
8871-3	28	Control	15.9
1315-1	28	Control	13.3
1315-2	28	Control	13.2
1315-3	28	Control	13.2
1294-1	42	Control	21.1
1294-2	42	Control	24.3
1294-3	42	Control	21.4
1251-1	42	Control	21
1251-2	42	Control	21.6
1251-3	42	Control	20.2
1172-2	28	0.25% GTE	15.6
1172-3	28	0.25% GTE	17.4
1548-1	28	0.25% GTE	14.8
1288-1	42	0.25% GTE	22.9
1288-2	42	0.25% GTE	21.7
1326-1	42	0.25% GTE	19.6
1326-2	42	0.25% GTE	22.9
1166-1	28	0.5% GTE	12.9
1166-3	28	0.5% GTE	17.4
1160-1	28	0.5% GTE	9.3
1160-2	28	0.5% GTE	15.9
1160-3	28	0.5% GTE	13.7
1225-1	42	0.5% GTE	24.3
1225-2	42	0.5% GTE	25.5
1225-3	42	0.5% GTE	24.7
1224-1	42	0.5% GTE	17.8
1224-2	42	0.5% GTE	22.2
1224-3	42	0.5% GTE	21

Serum CK for control and GTE treated *mdx* mice ages 28 and 42 days

Mouse	Age (days)	Treatment	Serum CK (U/L)
8871-3	28	Control	776
8871-1	28	Control	9095
8871-2	28	Control	14328
1315-1	28	Control	1887
1315-2	28	Control	2217
1315-3	28	Control	4002
1294-1	42	Control	5466
1294-2	42	Control	4842
1294-3	42	Control	5982
1251-1	42	Control	5289
1251-2	42	Control	13101
1251-3	42	Control	12699
1172-1	28	0.25% GTE	1942
1172-2	28	0.25% GTE	1384
1172-3	28	0.25% GTE	1768
1172-4	28	0.25% GTE	3269
1288-1	42	0.25% GTE	1545
1288-2	42	0.25% GTE	644
1288-3	42	0.25% GTE	1483
1288-4	42	0.25% GTE	853
1326-1	42	0.25% GTE	1433
1326-2	42	0.25% GTE	2115
1166-2	28	0.5% GTE	4664
1166-3	28	0.5% GTE	4439
1160-2	28	0.5% GTE	2288
1160-3	28	0.5% GTE	6656
1225-1	42	0.5% GTE	1022
1225-2	42	0.5% GTE	780
1225-3	42	0.5% GTE	1732
1224-1	42	0.5% GTE	1120
1224-2	42	0.5% GTE	1672
1224-3	42	0.5% GTE	840

Histopathology (percent area of fields) for control and GTE treated *mdx* mice ages 28 and 42 days

Mouse	Age (days)	Treatment	Normal	Regeneration	Immune Cell	Necrosis	Degeneration
7271-2	28	Control	76.5	16.6	6.9	0.0	0.0
7773-2	28	Control	62.6	35.6	0.6	1.2	0.0
7773-3	28	Control	67.2	22.8	7.0	3.0	0.0
8841-1	28	Control	62.7	37.3	0.0	0.0	0.0
1251-2	42	Control	47.0	48.7	1.9	0.0	2.3
1251-3	42	Control	33.4	66.2	0.5	0.0	0.0
1294-1	42	Control	36.0	62.9	0.4	0.0	0.6
1294-3	42	Control	35.6	64.4	0.0	0.0	0.0
1172-1	28	0.25% GTE	70.7	28.6	0.6	0.0	0.0
1172-2	28	0.25% GTE	68.8	27.5	3.7	0.0	0.0
1172-3	28	0.25% GTE	69.9	27.1	3.0	0.0	0.0
1172-4	28	0.25% GTE	60.9	28.0	10.8	0.2	0.2
1288-1	42	0.25% GTE	51.7	46.6	1.8	0.0	0.0
1288-2	42	0.25% GTE	43.6	55.3	0.8	0.0	0.4
1288-3	42	0.25% GTE	52.5	47.1	0.4	0.0	0.0
1288-4	42	0.25% GTE	55.0	44.2	0.8	0.0	0.0
1326-1	42	0.25% GTE	52.2	46.0	1.1	0.5	0.2
1326-2	42	0.25% GTE	46.7	51.8	0.9	0.2	0.3
1166-1	28	0.5% GTE	60.1	31.2	6.4	0.0	2.4
1166-2	28	0.5% GTE	68.3	26.3	0.8	0.0	4.6
1166-3	28	0.5% GTE	63.6	35.1	0.6	0.0	0.7
1160-1	28	0.5% GTE	83.3	15.5	0.7	0.0	0.5
1160-2	28	0.5% GTE	68.2	30.7	0.6	0.0	0.6
1160-3	28	0.5% GTE	60.1	30.2	1.4	0.0	8.3
1224-1	42	0.5% GTE	49.9	48.4	0.3	0.3	1.2
1224-2	42	0.5% GTE	45.8	52.4	0.7	0.5	0.7
1224-3	42	0.5% GTE	39.3	59.9	0.8	0.0	0.0
1225-1	42	0.5% GTE	44.8	53.4	0.2	0.5	1.1
1225-2	42	0.5% GTE	56.9	42.5	0.1	0.1	0.4
1225-3	42	0.5% GTE	49.0	45.2	0.5	0.9	4.4

Macrophage infiltration for control and GTE treated *mdx* mice age 42 days

Mouse	Treatment	Macrophage/mm^2
1610-1	Control	189
1610-2	Control	122
1611-1	Control	75
1618-1	Control	113
1288-1	0.25% GTE	92
1288-3	0.25% GTE	49
1288-4	0.25% GTE	90
1326-1	0.25% GTE	162
1326-2	0.25% GTE	95
1224-1	0.5% GTE	153
1224-2	0.5% GTE	98
1224-3	0.5% GTE	157
1225-2	0.5% GTE	87
1225-3	0.5% GTE	93

Necrotic fibers with NF-κB staining in control and GTE treated *mdx* mice age 42 days

Mouse	Treatment	Necrotic Fibers/mm^2
1610-1	Control	5.7
1610-2	Control	4.2
1618-1	Control	5.1
1288-1	0.25% GTE	6.3
1288-3	0.25% GTE	2.6
1288-4	0.25% GTE	4.2
1326-2	0.25% GTE	3.7
1224-1	0.5% GTE	15.0
1224-2	0.5% GTE	0.7
1224-3	0.5% GTE	4.7
1225-2	0.5% GTE	1.3
1225-3	0.5% GTE	6.2

Centralized nuclei with NF-κB staining in control and GTE treated *mdx* mice age 42 days

Mouse	Treatment	% Dark Staining Centralized Nuclei
1610-1	Control	39.5
1610-2	Control	39.2
1611-1	Control	50.0
1618-1	Control	45.5
1288-1	0.25% GTE	25.4
1288-3	0.25% GTE	34.6
1288-4	0.25% GTE	25.4
1326-2	0.25% GTE	29.4
1224-1	0.5% GTE	33.1
1224-2	0.5% GTE	26.9
1224-3	0.5% GTE	22.6
1225-2	0.5% GTE	35.1
1225-3	0.5% GTE	31.6

Appendix C: Specific Aim 1 Statistical Analyses

Normal fiber morphology for 14-42 day C57BL/6J and *mdx*

Analysis of Variance

Source	DF	Sum of Squares	Mean Square	F Ratio
Model	9	18466.798	2051.87	147.5651
Error	24	333.716	13.90	**Prob > F**
C. Total	33	18800.513		<.0001*

Effect Tests

Source	Nparm	DF	Sum of Squares	F Ratio	Prob > F
Genotype	1	1	7695.0220	553.4067	<.0001*
Age (days)	4	4	4992.0549	89.7540	<.0001*
Genotype*Age (days)	4	4	5026.1831	90.3676	<.0001*

Degeneration for 14-42 day C57BL/6J and *mdx*

Analysis of Variance

Source	DF	Sum of Squares	Mean Square	F Ratio
Model	9	42.466097	4.71846	7.5875
Error	24	14.924849	0.62187	**Prob > F**
C. Total	33	57.390947		<.0001*

Effect Tests

Source	Nparm	DF	Sum of Squares	F Ratio	Prob > F
Genotype	1	1	5.684780	9.1414	0.0059*
Age (days)	4	4	16.513786	6.6388	0.0010*
Genotype*Age (days)	4	4	14.461224	5.8136	0.0020*

Immune Cell for 14-42 day C57BL/6J and *mdx*

Analysis of Variance

Source	DF	Sum of Squares	Mean Square	F Ratio
Model	9	46.933778	5.21486	2.5544
Error	24	48.996412	2.04152	**Prob > F**
C. Total	33	95.930190		0.0322*

Effect Tests

Source	Nparm	DF	Sum of Squares	F Ratio	Prob > F
Genotype	1	1	16.197325	7.9340	0.0096*
Age (days)	4	4	12.773116	1.5642	0.2160
Genotype*Age (days)	4	4	12.344246	1.5117	0.2303

Necrotic fibers for 14-42 day C57BL/6J and *mdx*

Analysis of Variance

Source	DF	Sum of Squares	Mean Square	F Ratio
Model	9	4.178466	0.464274	1.5490
Error	24	7.193337	0.299722	**Prob > F**
C. Total	33	11.371803		0.1876

Regeneration for 14-42 day C57BL/6J and *mdx*

Analysis of Variance

Source	DF	Sum of Squares	Mean Square	F Ratio
Model	9	17923.039	1991.45	84.4741
Error	24	565.792	23.57	**Prob > F**
C. Total	33	18488.831		<.0001*

Effect Tests

Source	Nparm	DF	Sum of Squares	F Ratio	Prob > F
Genotype	1	1	6471.8047	274.5238	<.0001*
Age (days)	4	4	5379.5984	57.0485	<.0001*
Genotype*Age (days)	4	4	5379.3641	57.0461	<.0001*

Body mass for 28 day control and GTE treated *mdx* mice

Analysis of Variance

Source	DF	Sum of Squares	Mean Square	F Ratio	Prob > F
Treatment	2	15.76705	7.88352	1.5237	0.2434
Error	19	98.30795	5.17410		
C. Total	21	114.07500			

Body mass for 42 day control and GTE treated *mdx* mice

Analysis of Variance

Source	DF	Sum of Squares	Mean Square	F Ratio	Prob > F
Treatment	2	3.201667	1.60083	0.3549	0.7078
Error	13	58.635833	4.51045		
C. Total	15	61.837500			

Serum CK for 28 and 42 day control and GTE treated *mdx* mice

Analysis of Variance

Source	DF	Sum of Squares	Mean Square	F Ratio
Model	5	206340059	41268012	4.6885
Error	26	228849895	8801919	**Prob > F**
C. Total	31	435189953		0.0035*

Effect Tests

Source	Nparm	DF	Sum of Squares	F Ratio	Prob > F
Treatment	2	2	146223292	8.3063	0.0016*
Age	1	1	2060172	0.2341	0.6326
Treatment*Age	2	2	46052924	2.6161	0.0922

Dunnett's test for 28 day serum CK

Means Comparisons

Comparisons with a control using Dunnett's Method

Control Group = Control

|d|	Alpha
2.43642	0.05

Level	Abs(Dif)-LSD	p-Value
Control	-3780	1.0000
0.5% GTE	-3217	0.5579
0.25% GTE	-796	0.1008

Positive values show pairs of means that are significantly different.

Dunnett's test for 42 day serum CK

Means Comparisons

Comparisons with a control using Dunnett's Method

Control Group = Control

|d|	Alpha
2.43926	0.05

Level	Abs(Dif)-LSD	p-Value
Control	-3213	1.0000
0.25% GTE	3338	0.0003*
0.5% GTE	3489	0.0003*

Positive values show pairs of means that are significantly different.

Normal fiber morphology for 28 and 42 day control and untreated *mdx* mice

Analysis of Variance

Source	DF	Sum of Squares	Mean Square	F Ratio
Model	5	3716.3766	743.275	18.9241
Error	24	942.6381	39.277	**Prob > F**
C. Total	29	4659.0147		<.0001*

Effect Tests

Source	Nparm	DF	Sum of Squares	F Ratio	Prob > F
Treatment	2	2	187.8786	2.3917	0.1129
Age	1	1	3505.2125	89.2443	<.0001*
Treatment*Age	2	2	171.0912	2.1780	0.1351

Dunnett's test for 28 day normal fiber morphology

Means Comparisons

Comparisons with a control using Dunnett's Method

Control Group = Control

|d|	Alpha
2.52314	0.05

Level	Abs(Dif)-LSD	p-Value
0.25% GTE	-12.4	0.9957
0.5% GTE	-11.7	1.0000
Control	-12.8	1.0000

Positive values show pairs of means that are significantly different.

Dunnett's test for 42 day normal fiber morphology

Means Comparisons

Comparisons with a control using Dunnett's Method

Control Group = Control

|d|	Alpha
2.45876	0.05

Level	Abs(Dif)-LSD	p-Value
0.25% GTE	3.729	0.0067*
0.5% GTE	1.077	0.0282*
Control	-9.35	1.0000

Positive values show pairs of means that are significantly different.

Degeneration for 28 and 42 day control and untreated *mdx* mice

Analysis of Variance

Source	DF	Sum of Squares	Mean Square	F Ratio
Model	5	33.649997	6.73000	2.5071
Error	24	64.424434	2.68435	Prob > F
C. Total	29	98.074432		0.0581

Dunnett's test for 28 day degeneration

Means Comparisons

Comparisons with a control using Dunnett's Method

Control Group = Control

|d|	Alpha
2.52314	0.05

Level	Abs(Dif)-LSD	p-Value
0.5% GTE	-0.55	0.0997
0.25% GTE	-3.69	0.9994
Control	-3.73	1.0000

Positive values show pairs of means that are significantly different.

Dunnett's test for 42 day degeneration

Means Comparisons

Comparisons with a control using Dunnett's Method

Control Group = Control

|d|	Alpha
2.45876	0.05

Level	Abs(Dif)-LSD	p-Value
0.5% GTE	-1.22	0.6500
Control	-1.95	1.0000
0.25% GTE	-1.17	0.6108

Positive values show pairs of means that are significantly different.

Immune cell for 28 and 42 day control and GTE treated *mdx* mice

Analysis of Variance

Source	DF	Sum of Squares	Mean Square	F Ratio
Model	5	63.46480	12.6930	2.3246
Error	24	131.04600	5.4603	**Prob > F**
C. Total	29	194.51080		0.0742

Dunnett's test for 28 day immune cell

Means Comparisons

Comparisons with a control using Dunnett's Method

Control Group = Control

|d|	Alpha
2.52314	0.05

Level	Abs(Dif)-LSD	p-Value
0.25% GTE	-5.18	0.9035
Control	-6.07	1.0000
0.5% GTE	-3.65	0.6018

Positive values show pairs of means that are significantly different.

Dunnett's test for 42 day immune cell

Means Comparisons

Comparisons with a control using Dunnett's Method

Control Group = Control

|d|	Alpha
2.45876	0.05

Level	Abs(Dif)-LSD	p-Value
0.25% GTE	-0.55	0.6237
Control	-0.91	1.0000
0.5% GTE	-0.56	0.6303

Positive values show pairs of means that are significantly different.

Necrotic fibers for 28 and 42 day control and GTE treated *mdx* mice

Analysis of Variance

Source	DF	Sum of Squares	Mean Square	F Ratio
Model	5	3.586722	0.717344	2.5621
Error	24	6.719508	0.279980	**Prob > F**
C. Total	29	10.306230		0.0540

Dunnett's test for 28 day necrotic fibers

Means Comparisons

Comparisons with a control using Dunnett's Method

Control Group = Control

|d|	Alpha
2.52314	0.05

Level	Abs(Dif)-LSD	p-Value
Control	-1.32	1.0000
0.25% GTE	-0.31	0.1348
0.5% GTE	-0.15	0.0856

Positive values show pairs of means that are significantly different.

Dunnett's test for 42 day necrotic fibers

Means Comparisons

Comparisons with a control using Dunnett's Method

Control Group = Control

|d|	Alpha
2.48780	0.05

Level	Abs(Dif)-LSD	p-Value
0.5% GTE	-0	0.0502
0.25% GTE	-0.17	0.5071
Control	-0.32	1.0000

Positive values show pairs of means that are significantly different.

Regeneration for 28 and 42 day control and GTE treated *mdx* mice

Analysis of Variance

Source	DF	Sum of Squares	Mean Square	F Ratio
Model	5	4738.7989	947.760	22.5596
Error	24	1008.2735	42.011	**Prob > F**
C. Total	29	5747.0724		<.0001*

Effect Tests

Source	Nparm	DF	Sum of Squares	F Ratio	Prob > F
Treatment	2	2	188.2018	2.2399	0.1283
Age	1	1	4536.4934	107.9825	<.0001*
Treatment*Age	2	2	178.2710	2.1217	0.1418

Dunnett's test for 28 day regeneration

Means Comparisons

Comparisons with a control using Dunnett's Method

Control Group = Control

|d|	Alpha
2.52314	0.05

Level	Abs(Dif)-LSD	p-Value
0.5% GTE	-11.3	0.9999
Control	-12.4	1.0000
0.25% GTE	-12.1	0.9971

Positive values show pairs of means that are significantly different.

Dunnett's test for 42 day regeneration

Means Comparisons

Comparisons with a control using Dunnett's Method

Control Group = Control

|d|	Alpha
2.45876	0.05

Level	Abs(Dif)-LSD	p-Value
Control	-10.5	1.0000
0.5% GTE	0.677	0.0363*
0.25% GTE	2.454	0.0155*

Positive values show pairs of means that are significantly different.

Macrophage infiltration for 42 day control and GTE treated *mdx* mice

Analysis of Variance

Source	DF	Sum of Squares	Mean Square	F Ratio	Prob > F
Genotype/Treatment	2	6121.569	3060.78	1.6319	0.2395
Error	11	20631.854	1875.62		
C. Total	13	26753.422			

NF-κB staining in necrotic fibers for 42 day control and GTE treated *mdx* mice

Analysis of Variance

Source	DF	Sum of Squares	Mean Square	F Ratio	Prob > F
Column 2	2	4.10908	2.0545	0.1316	0.8783
Error	9	140.50429	15.6116		
C. Total	11	144.61337			

NF-κB staining in regenerating fibers for 42 day control and GTE treated *mdx* mice

Analysis of Variance

Source	DF	Sum of Squares	Mean Square	F Ratio	Prob > F
Genotype/Treatment	2	562.24417	281.122	11.6680	0.0024*
Error	10	240.93323	24.093		
C. Total	12	803.17740			

Appendix D: Specific Aim 2 Raw Data

Food consumption (g/g bm/d) for control and EGCG treated C57BL/6J and *mdx* mice

Mouse	Genotype	Treatment	18-21	21-28	28-35	35-42
1596-1	C57BL/6J	AIN-93G	0.13	0.17	0.19	0.18
1596-2	C57BL/6J	AIN-93G	0.13	0.16	0.16	0.15
1596-3	C57BL/6J	AIN-93G	0.13	0.16	0.16	0.15
1597-1	C57BL/6J	AIN-93G	0.18	0.17	0.18	0.15
1642-1	C57BL/6J	AIN-93G	0.15	0.18	-	-
1642-2	C57BL/6J	AIN-93G	0.14	0.17	-	-
1643-1	C57BL/6J	AIN-93G	0.21	0.19	-	-
1648-1	C57BL/6J	AIN-93G	0.16	0.22	-	-
1612-1	C57BL/6J	EGCG	0.10	0.17	0.16	0.16
1612-2	C57BL/6J	EGCG	0.09	0.17	0.17	0.16
1612-3	C57BL/6J	EGCG	0.11	0.18	0.17	0.18
1613-1	C57BL/6J	EGCG	0.11	0.20	0.18	0.18
1650-1	C57BL/6J	EGCG	0.19	0.18	-	-
1650-2	C57BL/6J	EGCG	0.21	0.19	-	-
1650-3	C57BL/6J	EGCG	0.20	0.19	-	-
1651-1	C57BL/6J	EGCG	0.22	0.19	-	-
1651-2	C57BL/6J	EGCG	0.22	0.18	-	-
1542-1	mdx	AIN-93G	0.23	0.14	-	-
1542-2	mdx	AIN-93G	0.26	0.16	-	-
1544-1	mdx	AIN-93G	0.49	0.14	-	-
1582-1	mdx	AIN-93G	0.25	0.19	-	-
1582-2	mdx	AIN-93G	0.26	0.17	-	-
1584-1	mdx	AIN-93G	0.23	0.15	-	-
1584-2	mdx	AIN-93G	0.25	0.16	-	-
1608-1	mdx	AIN-93G	0.17	0.13	-	-
1608-2	mdx	AIN-93G	0.18	0.15	-	-
1588-1	mdx	AIN-93G	0.14	0.11	0.13	0.12
1588-2	mdx	AIN-93G	0.14	0.13	0.14	0.12
1588-3	mdx	AIN-93G	0.21	0.19	0.18	0.15
1589-1	mdx	AIN-93G	0.11	0.18	0.19	0.13
1593-1	mdx	AIN-93G	0.21	0.14	0.13	0.13
1593-2	mdx	AIN-93G	0.24	0.15	0.14	0.14
1593-3	mdx	AIN-93G	0.27	0.18	0.15	0.16
1545-1	mdx	EGCG	0.22	0.16	-	-
1545-2	mdx	EGCG	0.20	0.14	-	-
1545-3	mdx	EGCG	0.20	0.16	-	-
1583-1	mdx	EGCG	0.22	0.19	-	-
1583-2	mdx	EGCG	0.22	0.17	-	-
1585-1	mdx	EGCG	0.24	0.18	-	-
1585-2	mdx	EGCG	0.22	0.17	-	-
1606-1	mdx	EGCG	0.07	0.18	-	-
1606-2	mdx	EGCG	0.08	0.16	-	-
1606-3	mdx	EGCG	0.08	0.21	-	-
1603-1	mdx	EGCG	0.08	0.15	0.16	0.14
1603-2	mdx	EGCG	0.09	0.18	0.17	0.14
1604-1	mdx	EGCG	0.09	0.17	0.16	0.15
1604-2	mdx	EGCG	0.09	0.17	0.17	0.16
1609-2	mdx	EGCG	0.11	0.15	0.14	0.14
1609-3	mdx	EGCG	0.14	0.19	0.17	0.17

Body mass (g) for control and EGCG treated C57BL/6J and *mdx* mice

Mouse	Genotype	Treatment	21	28	35	42
1596-1	C57BL/6J	AIN-93G	10.8	13.4	15.4	16.8
1596-2	C57BL/6J	AIN-93G	10.7	14.3	18.2	19.4
1596-3	C57BL/6J	AIN-93G	10.9	14.3	18	20.2
1597-1	C57BL/6J	AIN-93G	11.1	17.1	21	21.2
1612-1	C57BL/6J	EGCG	9.3	13.8	17.5	18.1
1612-2	C57BL/6J	EGCG	10	14.2	16.9	18.2
1612-3	C57BL/6J	EGCG	9	13	16.2	16.1
1613-1	C57BL/6J	EGCG	8	13.5	17.5	18.5
1542-1	mdx	AIN-93G	11.3	18.2	-	-
1542-2	mdx	AIN-93G	9.9	15.9	-	-
1544-1	mdx	AIN-93G	11.3	13	-	-
1582-1	mdx	AIN-93G	10.8	15.4	-	-
1582-2	mdx	AIN-93G	10.6	17.2	-	-
1584-1	mdx	AIN-93G	11.8	21.1	-	-
1584-2	mdx	AIN-93G	11.1	20.4	-	-
1608-1	mdx	AIN-93G	15	18	-	-
1608-2	mdx	AIN-93G	13.6	15.5	-	-
1588-1	mdx	AIN-93G	15.1	22.3	25.1	28.6
1588-2	mdx	AIN-93G	14.6	19.3	24.6	27.1
1588-3	mdx	AIN-93G	10	13.1	18.8	21.8
1589-1	mdx	AIN-93G	12.9	16.3	21.3	24.5
1593-1	mdx	AIN-93G	12.8	18.2	19.8	21
1593-2	mdx	AIN-93G	11.4	16.9	18.7	20.6
1593-3	mdx	AIN-93G	10.1	14.5	16.8	18
1545-1	mdx	EGCG	9.2	13.9	-	-
1545-2	mdx	EGCG	9.9	15.8	-	-
1545-3	mdx	EGCG	10.2	14.7	-	-
1583-1	mdx	EGCG	10.4	14.9	-	-
1583-2	mdx	EGCG	10.6	16.6	-	-
1585-1	mdx	EGCG	9.5	16.9	-	-
1585-2	mdx	EGCG	10.6	17.9	-	-
1606-1	mdx	EGCG	9.8	13.8	-	-
1606-2	mdx	EGCG	9.3	15	-	-
1606-3	mdx	EGCG	8.5	11.7	-	-
1603-1	mdx	EGCG	9.8	18	24.5	26.4
1603-2	mdx	EGCG	8.8	15.1	23.2	26.5
1604-1	mdx	EGCG	9.8	15.3	18.5	21.1
1604-2	mdx	EGCG	9.7	15.7	17.7	19.3
1609-2	mdx	EGCG	12.8	16.6	19.4	21.7
1609-3	mdx	EGCG	9.5	13.1	16.3	17.4

Serum CK for control and EGCG treated C57BL/6J and *mdx* mice

Mouse	Genotype	Treatment	Age (days)	Serum CK (U/L)
1642-1	C57BL/6J	AIN-93G	28	252
1642-2	C57BL/6J	AIN-93G	28	116
1643-1	C57BL/6J	AIN-93G	28	201
1648-1	C57BL/6J	AIN-93G	28	217
1596-1	C57BL/6J	AIN-93G	42	1736
1596-2	C57BL/6J	AIN-93G	42	136
1596-3	C57BL/6J	AIN-93G	42	145
1597-1	C57BL/6J	AIN-93G	42	315
1650-1	C57BL/6J	EGCG	28	251
1650-2	C57BL/6J	EGCG	28	739
1650-3	C57BL/6J	EGCG	28	426
1651-1	C57BL/6J	EGCG	28	347
1651-2	C57BL/6J	EGCG	28	298
1612-1	C57BL/6J	EGCG	42	391
1612-2	C57BL/6J	EGCG	42	323
1613-1	C57BL/6J	EGCG	42	421
1542-1	mdx	AIN-93G	28	4911
1542-2	mdx	AIN-93G	28	8069
1582-1	mdx	AIN-93G	28	2811
1582-2	mdx	AIN-93G	28	3198
1584-1	mdx	AIN-93G	28	4318
1584-2	mdx	AIN-93G	28	4046
1608-1	mdx	AIN-93G	28	6502
1608-2	mdx	AIN-93G	28	4993
1542-1	mdx	AIN-93G	28	4911
1588-2	mdx	AIN-93G	42	5904
1588-3	mdx	AIN-93G	42	5471
1589-1	mdx	AIN-93G	42	6033
1593-1	mdx	AIN-93G	42	2410
1593-2	mdx	AIN-93G	42	2907
1593-3	mdx	AIN-93G	42	10093
1545-1	mdx	EGCG	28	2791
1545-2	mdx	EGCG	28	2986
1545-3	mdx	EGCG	28	4356
1583-1	mdx	EGCG	28	3376
1583-2	mdx	EGCG	28	2670
1585-1	mdx	EGCG	28	1574
1585-2	mdx	EGCG	28	2376
1606-1	mdx	EGCG	28	5308
1606-2	mdx	EGCG	28	5940
1606-3	mdx	EGCG	28	3260
1603-1	mdx	EGCG	42	4951
1603-2	mdx	EGCG	42	5537
1604-1	mdx	EGCG	42	2183
1604-2	mdx	EGCG	42	5882
1609-2	mdx	EGCG	42	8702
1609-3	mdx	EGCG	42	2539

Histopathology (percent area of fields) for control and EGCG treated C57BL/6J and *mdx* mice

Mouse	Genotype	Treatment	Age (days)	Normal	Regeneration	Immune Cell	Necrosis	Degeneration	Myotube
1642-1	C57BL/6J	AIN	28	99.7	0.0	0.3	0.0	0.0	0.0
1642-2	C57BL/6J	AIN	28	99.7	0.1	0.2	0.0	0.0	0.0
1643-1	C57BL/6J	AIN	28	99.2	0.7	0.1	0.0	0.0	0.0
1648-1	C57BL/6J	AIN	28	99.1	0.7	0.1	0.0	0.0	0.1
1596-1	C57BL/6J	AIN	42	99.4	0.0	0.0	0.0	0.0	0.6
1596-2	C57BL/6J	AIN	42	98.6	1.3	0.1	0.0	0.0	0.0
1596-3	C57BL/6J	AIN	42	100.0	0.0	0.0	0.0	0.0	0.0
1597-1	C57BL/6J	AIN	42	99.8	0.0	0.2	0.0	0.0	0.0
1650-1	C57BL/6J	EGCG	28	98.8	0.8	0.2	0.0	0.0	0.2
1650-2	C57BL/6J	EGCG	28	99.4	0.0	0.5	0.0	0.0	0.1
1650-3	C57BL/6J	EGCG	28	98.4	0.7	0.4	0.0	0.0	0.5
1651-1	C57BL/6J	EGCG	28	98.3	1.4	0.1	0.0	0.0	0.2
1651-2	C57BL/6J	EGCG	28	98.9	1.0	0.1	0.0	0.0	0.0
1612-1	C57BL/6J	EGCG	42	99.7	0.0	0.3	0.0	0.0	0.0
1612-2	C57BL/6J	EGCG	42	99.8	0.0	0.2	0.0	0.0	0.0
1612-3	C57BL/6J	EGCG	42	99.8	0.0	0.2	0.0	0.0	0.0
1613-1	C57BL/6J	EGCG	42	98.6	1.3	0.1	0.0	0.0	0.0
1542-1	mdx	AIN	28	55.6	27.3	14.5	0.0	0.0	2.6
1542-2	mdx	AIN	28	48.5	43.2	7.0	0.0	0.1	1.1
1544-1	mdx	AIN	28	52.2	9.5	17.8	0.0	0.6	19.8
1582-1	mdx	AIN	28	73.9	22.5	2.6	0.0	0.0	1.0
1582-2	mdx	AIN	28	44.0	48.3	4.9	0.0	0.0	2.7
1584-1	mdx	AIN	28	53.9	38.5	6.0	0.0	0.0	1.6
1584-2	mdx	AIN	28	61.4	32.5	4.2	0.0	0.0	1.9
1608-2	mdx	AIN	28	36.5	15.6	24.5	11.6	7.6	4.1
1608-1	mdx	AIN	28	54.7	37.0	2.9	0.2	0.6	4.6
1588-1	mdx	AIN	42	48.4	49.3	1.8	0.2	0.0	0.3
1588-2	mdx	AIN	42	39.9	56.9	2.4	0.4	0.0	0.5
1588-3	mdx	AIN	42	52.6	40.7	4.0	0.4	1.9	0.4
1589-1	mdx	AIN	42	49.8	47.0	2.6	0.0	0.0	0.5
1593-1	mdx	AIN	42	45.6	52.8	1.4	0.0	0.0	0.2
1593-2	mdx	AIN	42	38.1	58.7	2.5	0.0	0.0	0.8
1593-3	mdx	AIN	42	47.2	49.7	3.0	0.0	0.0	0.1
1545-1	mdx	EGCG	28	76.1	17.8	3.1	0.5	0.0	2.5
1545-2	mdx	EGCG	28	70.3	17.2	8.3	3.1	0.0	1.2
1545-3	mdx	EGCG	28	88.5	6.7	2.4	1.8	0.0	0.6
1583-1	mdx	EGCG	28	66.8	28.8	1.9	0.7	0.0	1.8
1583-2	mdx	EGCG	28	47.9	50.0	1.1	0.0	0.0	1.1
1585-1	mdx	EGCG	28	53.8	45.3	0.7	0.0	0.0	0.3
1585-2	mdx	EGCG	28	62.0	33.9	2.3	0.0	0.0	1.9
1606-1	mdx	EGCG	28	58.6	33.5	5.1	0.5	0.0	2.2
1606-2	mdx	EGCG	28	50.6	32.1	10.5	0.1	0.6	6.0
1606-3	mdx	EGCG	28	53.8	19.5	4.2	0.1	0.0	22.3
1603-2	mdx	EGCG	42	59.0	38.1	1.6	0.0	0.0	1.2
1603-1	mdx	EGCG	42	53.6	42.5	2.7	0.4	0.0	0.8
1604-1	mdx	EGCG	42	54.1	44.2	0.4	0.8	0.0	0.4
1604-2	mdx	EGCG	42	58.8	39.0	2.2	0.0	0.0	0.0
1609-2	mdx	EGCG	42	57.7	40.4	1.3	0.2	0.0	0.4
1609-3	mdx	EGCG	42	62.8	28.3	4.9	0.0	0.1	4.0

Macrophage infiltration for control and EGCG treated C57BL/6J and *mdx* mice

Mouse	Genotype	Treatment	Age (days)	Macrophages/mm^2
1642-1	C57BL/6J	AIN-93G	28	2
1642-2	C57BL/6J	AIN-93G	28	17
1643-1	C57BL/6J	AIN-93G	28	6
1648-1	C57BL/6J	AIN-93G	28	10
1596-1	C57BL/6J	AIN-93G	42	1
1596-2	C57BL/6J	AIN-93G	42	1
1596-3	C57BL/6J	AIN-93G	42	0
1597-1	C57BL/6J	AIN-93G	42	0
1650-1	C57BL/6J	EGCG	28	13
1650-2	C57BL/6J	EGCG	28	6
1650-3	C57BL/6J	EGCG	28	3
1651-1	C57BL/6J	EGCG	28	4
1612-1	C57BL/6J	EGCG	42	4
1612-2	C57BL/6J	EGCG	42	1
1612-3	C57BL/6J	EGCG	42	2
1613-1	C57BL/6J	EGCG	42	1
1542-1	mdx	AIN-93G	28	194
1542-2	mdx	AIN-93G	28	125
1544-1	mdx	AIN-93G	28	497
1582-1	mdx	AIN-93G	28	83
1582-2	mdx	AIN-93G	28	133
1584-1	mdx	AIN-93G	28	84
1584-2	mdx	AIN-93G	28	90
1608-1	mdx	AIN-93G	28	211
1608-2	mdx	AIN-93G	28	572
1588-1	mdx	AIN-93G	42	115
1588-2	mdx	AIN-93G	42	50
1588-3	mdx	AIN-93G	42	98
1589-1	mdx	AIN-93G	42	108
1593-1	mdx	AIN-93G	42	30
1593-2	mdx	AIN-93G	42	90
1593-3	mdx	AIN-93G	42	54
1545-1	mdx	EGCG	28	208
1545-2	mdx	EGCG	28	445
1545-3	mdx	EGCG	28	239
1583-1	mdx	EGCG	28	117
1583-2	mdx	EGCG	28	96
1585-1	mdx	EGCG	28	26
1585-2	mdx	EGCG	28	101
1606-1	mdx	EGCG	28	110
1606-2	mdx	EGCG	28	205
1603-1	mdx	EGCG	42	17
1603-2	mdx	EGCG	42	18
1604-1	mdx	EGCG	42	58
1604-2	mdx	EGCG	42	61
1609-2	mdx	EGCG	42	110
1609-3	mdx	EGCG	42	114

NF-κB staining in necrotic fibers for control and EGCG treated C57BL/6J and *mdx* mice

Mouse	Genotype	Treatment	Age (days)	Necrotic Fibers/mm^2
1642-1	C57BL/6J	AIN-93G	28	0.7
1642-2	C57BL/6J	AIN-93G	28	0.0
1643-1	C57BL/6J	AIN-93G	28	0.2
1648-1	C57BL/6J	AIN-93G	28	0.0
1596-1	C57BL/6J	AIN-93G	42	0.2
1596-2	C57BL/6J	AIN-93G	42	0.2
1596-3	C57BL/6J	AIN-93G	42	0.0
1597-1	C57BL/6J	AIN-93G	42	0.2
1650-1	C57BL/6J	EGCG	28	0.2
1650-2	C57BL/6J	EGCG	28	0.0
1650-3	C57BL/6J	EGCG	28	0.2
1651-1	C57BL/6J	EGCG	28	0.0
1612-1	C57BL/6J	EGCG	42	0.4
1612-2	C57BL/6J	EGCG	42	0.0
1612-3	C57BL/6J	EGCG	42	0.0
1613-1	C57BL/6J	EGCG	42	0.2
1542-1	mdx	AIN-93G	28	4.3
1582-1	mdx	AIN-93G	28	4.5
1582-2	mdx	AIN-93G	28	3.7
1584-1	mdx	AIN-93G	28	6.4
1584-2	mdx	AIN-93G	28	2.0
1608-2	mdx	AIN-93G	28	11.5
1588-1	mdx	AIN-93G	42	2.6
1588-2	mdx	AIN-93G	42	3.4
1588-3	mdx	AIN-93G	42	5.0
1589-1	mdx	AIN-93G	42	2.2
1593-1	mdx	AIN-93G	42	1.7
1593-2	mdx	AIN-93G	42	2.9
1593-3	mdx	AIN-93G	42	2.1
1545-1	mdx	EGCG	28	5.1
1545-2	mdx	EGCG	28	3.9
1545-3	mdx	EGCG	28	7.1
1583-1	mdx	EGCG	28	3.2
1583-2	mdx	EGCG	28	1.5
1585-1	mdx	EGCG	28	3.6
1585-2	mdx	EGCG	28	1.8
1606-1	mdx	EGCG	28	6.6
1606-2	mdx	EGCG	28	5.1
1603-1	mdx	EGCG	42	3.4
1603-2	mdx	EGCG	42	1.4
1604-1	mdx	EGCG	42	4.1
1604-2	mdx	EGCG	42	1.1
1609-2	mdx	EGCG	42	6.6
1609-3	mdx	EGCG	42	2.9

NF-κB staining in regenerating fibers for control and EGCG treated *mdx* mice

Mouse	Treatment	Age (days)	% Dark Staining Centralized Nuclei
1542-1	AIN-93G	28	47.6
1582-1	AIN-93G	28	50.7
1582-2	AIN-93G	28	50.0
1584-1	AIN-93G	28	49.5
1584-2	AIN-93G	28	49.5
1608-2	AIN-93G	28	52.3
1588-1	AIN-93G	42	45.8
1588-2	AIN-93G	42	40.6
1588-3	AIN-93G	42	45.0
1589-1	AIN-93G	42	46.8
1593-1	AIN-93G	42	40.4
1593-2	AIN-93G	42	39.4
1593-3	AIN-93G	42	40.0
1545-1	EGCG	28	45.1
1545-2	EGCG	28	48.0
1545-3	EGCG	28	54.8
1583-1	EGCG	28	47.7
1583-2	EGCG	28	47.7
1585-1	EGCG	28	52.0
1585-2	EGCG	28	41.8
1606-1	EGCG	28	42.7
1603-1	EGCG	42	29.6
1603-2	EGCG	42	38.3
1604-1	EGCG	42	37.0
1604-2	EGCG	42	26.8
1609-2	EGCG	42	27.8
1609-3	EGCG	42	36.2

Appendix E: Specific Aim 2 Statistical Analyses

Food consumption for control and EGCG treated C57BL/6J and *mdx* mice

All Between	F Test	Exact F	NumDF	DenDF	Prob>F
Genotype	0.03911634	0.66497783	1	17	0.4261
Treatment	0.06610662	1.12381254	1	17	0.3039
Genotype x Treatment	0.01916701	0.32583914	1	17	0.5756

All Within	F Test	Exact F	NumDF	DenDF	Prob>F
Time	1.76294258	8.81471288	3	15	0.0013
Time x Genotype	1.20207718	6.0103859	3	15	0.0067
Time x Treatment	6.43452028	32.1726014	3	15	<0.0001
Time x Genotype x Treatment	0.17417562	0.87087811	3	15	0.4779

Food consumption for 18-21 day control and EGCG treated *mdx* mice

Analysis of Variance

Source	DF	Sum of Squares	Mean Square	F Ratio	Prob > F
Treatment	1	0.05200313	0.052003	8.8923	0.0056*
Error	30	0.17544375	0.005848		
C. Total	31	0.22744688			

Food consumption for 21-28 day control and EGCG treated *mdx* mice

Analysis of Variance

Source	DF	Sum of Squares	Mean Square	F Ratio	Prob > F
Treatment	1	0.00211250	0.002112	4.9951	0.0330*
Error	30	0.01268750	0.000423		
C. Total	31	0.01480000			

Food consumption for 28-35 day control and EGCG treated *mdx* mice

Analysis of Variance

Source	DF	Sum of Squares	Mean Square	F Ratio	Prob > F
Treatment	1	0.00033864	0.000339	0.8935	0.3648
Error	11	0.00416905	0.000379		
C. Total	12	0.00450769			

Food consumption for 35-42 day control and EGCG treated *mdx* mice

Analysis of Variance

Source	DF	Sum of Squares	Mean Square	F Ratio	Prob > F
Treatment	1	0.00033864	0.000339	0.8935	0.3648
Error	11	0.00416905	0.000379		
C. Total	12	0.00450769			

Food consumption for 18-21 day C57BL/6J and *mdx* mice

Analysis of Variance

Source	DF	Sum of Squares	Mean Square	F Ratio	Prob > F
Genotype	1	0.00968806	0.009688	1.7570	0.1914
Error	47	0.25915276	0.005514		
C. Total	48	0.26884082			

Food consumption for 21-28 day C57BL/6J and *mdx* mice

Analysis of Variance

Source	DF	Sum of Squares	Mean Square	F Ratio	Prob > F
Genotype	1	0.00363241	0.003632	9.2312	0.0039*
Error	47	0.01849412	0.000393		
C. Total	48	0.02212653			

Food consumption for 28-35 day C57BL/6J and *mdx* mice

Analysis of Variance

Source	DF	Sum of Squares	Mean Square	F Ratio	Prob > F
Genotype	1	0.00112862	0.001129	3.9746	0.0607
Error	19	0.00539519	0.000284		
C. Total	20	0.00652381			

Food consumption for 35-42 day C57BL/6J and *mdx* mice

Analysis of Variance

Source	DF	Sum of Squares	Mean Square	F Ratio	Prob > F
Genotype	1	0.00227697	0.002277	10.2560	0.0047*
Error	19	0.00421827	0.000222		
C. Total	20	0.00649524			

Body mass for control and EGCG treated C57BL/6J and *mdx* mice

All Between	F Test	Exact F	NumDF	DenDF	Prob>F
Genotype	0.420627	7.15065908	1	17	0.0160
Treatment	0.13244082	2.25149387	1	17	0.1518
Genotype x Treatment	<0.0001	<0.0001	1	17	0.9993

All Within	F Test	Exact F	NumDF	DenDF	Prob>F
Time	18.4484472	92.2422358	3	15	<0.0001
Time x Genotype	0.97376762	4.8688381	3	15	0.0147
Time x Treatment	0.18606884	0.93034421	3	15	0.4503
Time x Genotype x Treatment	0.01775343	0.08876713	3	15	0.9651

Body mass for 21 day C57BL/6J and *mdx* mice

Analysis of Variance

Source	DF	Sum of Squares	Mean Square	F Ratio	Prob > F
Genotype	1	6.20156	6.20156	2.2301	0.1436
Error	38	105.67219	2.78085		
C. Total	39	111.87375			

Body mass for 28 day C57BL/6J and *mdx* mice

Analysis of Variance

Source	DF	Sum of Squares	Mean Square	F Ratio	Prob > F
Genotype	1	27.14256	27.1426	5.3754	0.0259*
Error	38	191.87719	5.0494		
C. Total	39	219.01975			

Body mass for 35 day C57BL/6J and *mdx* mice

Analysis of Variance

Source	DF	Sum of Squares	Mean Square	F Ratio	Prob > F
Genotype	1	38.11000	38.1100	5.4839	0.0302*
Error	19	132.03952	6.9494		
C. Total	20	170.14952			

Body mass for 42 day C57BL/6J and *mdx* mice

Analysis of Variance

Source	DF	Sum of Squares	Mean Square	F Ratio	Prob > F
Genotype	1	81.34718	81.3472	8.6484	0.0084*
Error	19	178.71567	9.4061		
C. Total	20	260.06286			

Serum CK for control and EGCG treated C57BL/6J and *mdx* mice

Analysis of Variance

Source	DF	Sum of Squares	Mean Square	F Ratio
Model	7	197972639	28281806	10.1482
Error	38	105901295	2786876.2	**Prob > F**
C. Total	45	303873934		<.0001*

Effect Tests

Source	Nparm	DF	Sum of Squares	F Ratio	Prob > F
Genotype	1	1	185544016	66.5778	<.0001*
Treatment	1	1	2233024	0.8013	0.3764
Genotype*Treatment	1	1	2285604	0.8201	0.3708
Age	1	1	3827648	1.3735	0.2485
Genotype*Age	1	1	1952776	0.7007	0.4078
Treatment*Age	1	1	137568	0.0494	0.8254
Genotype*Treatment*Age	1	1	1075984	0.3861	0.5381

Normal fiber morphology for control and EGCG treated C57BL/6J and *mdx* mice

Analysis of Variance

Source	DF	Sum of Squares	Mean Square	F Ratio
Model	7	22466.540	3209.51	51.0365
Error	41	2578.348	62.89	**Prob > F**
C. Total	48	25044.888		<.0001*

Effect Tests

Source	Nparm	DF	Sum of Squares	F Ratio	Prob > F
Genotype	1	1	21358.089	339.6290	<.0001*
Treatment	1	1	285.650	4.5423	0.0391*
Genotype*Treatment	1	1	322.748	5.1322	0.0288*
Age	1	1	95.737	1.5224	0.2243
Genotype*Age	1	1	122.513	1.9482	0.1703
Treatment*Age	1	1	6.084	0.0968	0.7573
Genotype*Treatment*Age	1	1	1.749	0.0278	0.8684

Regeneration for 28 day control and EGCG treated C57BL/6J and *mdx* mice

Analysis of Variance

Source	DF	Sum of Squares	Mean Square	F Ratio
Model	3	5093.5904	1697.86	13.8867
Error	24	2934.3790	122.27	**Prob > F**
C. Total	27	8027.9695		<.0001*

Effect Tests

Source	Nparm	DF	Sum of Squares	F Ratio	Prob > F
Genotype	1	1	5052.9253	41.3274	<.0001*
Treatment	1	1	4.0316	0.0330	0.8574
Genotype*Treatment	1	1	8.8424	0.0723	0.7903

Regeneration for 42 day control and EGCG treated C57BL/6J and *mdx* mice

Analysis of Variance

Source	DF	Sum of Squares	Mean Square	F Ratio
Model	3	10429.987	3476.66	154.7298
Error	17	381.977	22.47	**Prob > F**
C. Total	20	10811.965		<.0001*

Effect Tests

Source	Nparm	DF	Sum of Squares	F Ratio	Prob > F
Genotype	1	1	9741.0850	433.5296	<.0001*
Treatment	1	1	176.9066	7.8733	0.0122*
Genotype*Treatment	1	1	177.3259	7.8919	0.0121*

Immune cell for 28 day control and EGCG treated C57BL/6J and *mdx* mice

Analysis of Variance

Source	DF	Sum of Squares	Mean Square	F Ratio
Model	3	382.94149	127.647	5.3702
Error	24	570.46384	23.769	**Prob > F**
C. Total	27	953.40533		0.0057*

Effect Tests

Source	Nparm	DF	Sum of Squares	F Ratio	Prob > F
Genotype	1	1	251.78888	10.5930	0.0034*
Treatment	1	1	43.17568	1.8164	0.1903
Genotype*Treatment	1	1	46.49883	1.9563	0.1747

Immune cell for 42 day control and EGCG treated C57BL/6J and *mdx* mice

Analysis of Variance

Source	DF	Sum of Squares	Mean Square	F Ratio
Model	3	25.321762	8.44059	9.0324
Error	17	15.886154	0.93448	**Prob > F**
C. Total	20	41.207916		0.0008*

Effect Tests

Source	Nparm	DF	Sum of Squares	F Ratio	Prob > F
Genotype	1	1	24.626382	26.3530	<.0001*
Treatment	1	1	0.055882	0.0598	0.8097
Genotype*Treatment	1	1	0.233628	0.2500	0.6235

Necrotic fibers for 28 day control and EGCG treated C57BL/6J and *mdx* mice

Analysis of Variance

Source	DF	Sum of Squares	Mean Square	F Ratio
Model	3	7.81851	2.60617	0.4880
Error	24	128.17855	5.34077	**Prob > F**
C. Total	27	135.99705		0.6939

Necrotic fibers for 42 day control and EGCG treated C57BL/6J and *mdx* mice

Analysis of Variance

Source	DF	Sum of Squares	Mean Square	F Ratio
Model	3	0.20805424	0.069351	1.6449
Error	17	0.71675345	0.042162	**Prob > F**
C. Total	20	0.92480769		0.2164

Degeneration for 28 day control and EGCG treated C57BL/6J and *mdx* mice

Analysis of Variance

Source	DF	Sum of Squares	Mean Square	F Ratio
Model	3	5.716283	1.90543	0.9066
Error	24	50.443788	2.10182	**Prob > F**
C. Total	27	56.160072		0.4525

Degeneration for 42 day control and EGCG treated C57BL/6J and *mdx* mice

Analysis of Variance

Source	DF	Sum of Squares	Mean Square	F Ratio
Model	3	0.3369768	0.112326	0.6008
Error	17	3.1781031	0.186947	**Prob > F**
C. Total	20	3.5150799		0.6232

Myotubes for 28 day control and EGCG treated C57BL/6J and *mdx* mice

Analysis of Variance

Source	DF	Sum of Squares	Mean Square	F Ratio
Model	3	101.03617	33.6787	1.1952
Error	24	676.30425	28.1793	**Prob > F**
C. Total	27	777.34042		0.3327

Myotubes for 42 day control and EGCG treated C57BL/6J and *mdx* mice

Analysis of Variance

Source	DF	Sum of Squares	Mean Square	F Ratio
Model	3	3.975670	1.32522	2.0146
Error	17	11.182893	0.65782	**Prob > F**
C. Total	20	15.158563		0.1501

Macrophage infiltration for control and EGCG treated C57BL/6J and *mdx* mice

Analysis of Variance

Source	DF	Sum of Squares	Mean Square	F Ratio
Model	3	292453.63	97484.5	9.5034
Error	44	451346.03	10257.9	**Prob > F**
C. Total	47	743799.67		<.0001*

Effect Tests

Source	Nparm	DF	Sum of Squares	F Ratio	Prob > F
Geno	1	1	187218.36	18.2512	0.0001*
Treatment	1	1	5504.08	0.5366	0.4677
Age	1	1	83905.54	8.1796	0.0065*

NF-κB staining in necrotic fibers for control and EGCG treated C57BL/6J and *mdx* mice

Analysis of Variance

Source	DF	Sum of Squares	Mean Square	F Ratio
Model	3	156.94328	52.3144	16.7692
Error	40	124.78672	3.1197	**Prob > F**
C. Total	43	281.73000		<.0001*

Effect Tests

Source	Nparm	DF	Sum of Squares	F Ratio	Prob > F
Genotype	1	1	141.48531	45.3527	<.0001*
Treatment	1	1	0.63891	0.2048	0.6533
Age	1	1	12.63500	4.0501	0.0509

NF-κB staining in regenerating fibers for control and EGCG treated C57BL/6J and *mdx* mice

Analysis of Variance

Source	DF	Sum of Squares	Mean Square	F Ratio
Model	3	1157.5476	385.849	25.3098
Error	24	365.8810	15.245	**Prob > F**
C. Total	27	1523.4286		<.0001*

Effect Tests

Source	Nparm	DF	Sum of Squares	F Ratio	Prob > F
Treatment	1	1	221.46815	14.5272	0.0008*
Age	1	1	895.14382	58.7171	<.0001*
Age*Treatment	1	1	120.27896	7.8897	0.0097*